Pavel Grigoriev

Magnetic quantum oscillations in quasi-two-dimensional metals

Ph. D. thesis
University of Konstanz

2002

Promoter:
Professor P. Wyder
Grenoble High Magnetic Fields Laboratory,
Max-Planck-Institute für Festkörperforschung
and Centre National de la Recherche Scientifique

Contents

1 INTRODUCTION **11**

1.1 3D de Haas - van Alphen effect 12

1.1.1 Physical origin of the magnetic quantum oscillations . . 13

1.1.2 Thermodynamic potential 13

1.1.3 The LK-formula for magnetization 14

1.2 Shoenberg's formula for the 2D case 17

1.3 The Shubnikov - de Haas effect in 3D metals. 20

2 2D dHvA effect (the model study) **23**

2.0.1 Comparison between 2D and 3D dHvA cases 23

2.1 Chemical potential in two-dimensional electron gas in strong magnetic field 25

2.1.1 Fermi Energy and Chemical Potential 25

2.1.2 Calculation of the chemical potential (for finite temperature and sharp LLs). 27

2.1.3 Some generalizations 31

2.2 2D magnetization oscillations at finite temperature 34

2.2.1 Thermodynamic potentials 35

2.2.2 The magnetization 37

2.2.3 The envelope of magnetization oscillations 37

2.2.4 Susceptibility 38

2.3 Finite k_z-dispersion and quasi-two-dimensional dHvA effect . . 38

3 The dHvA effect under more realistic conditions **43**

3.1 Low-temperature limit; direct summation over LLs 44

3.1.1 Magnetization at arbitrary density of states 44

3.1.2 Relation between the magnetization and the DoS function 48

3.1.3 A test of the one-particle approximation 56

3.1.4 The envelope of magnetization oscillations 58

3.2 Harmonic expansion of magnetization oscillations 64

3.2.1 General case 64
3.2.2 Influence of the reservoir DoS 67
3.3 Summary of the results on the dHvA effect 71

4 The Shubnikov-de Haas effect in quasi-2D compounds 73
4.1 Approximate analysis using the Boltzmann transport equation 75
4.1.1 Phase shift of the beats 76
4.1.2 Slow oscillations 82
4.2 Calculation using the Kubo formula 87
4.2.1 General formula for interlayer conductivity 88
4.2.2 Conductivity in the self-consistent Born approximation 91
4.2.3 Discussion of the results 95

5 Discussion and prospects 101

6 Summary 107

7 Some calculations and mathematical formulas 111
7.1 Transformation of sums over LLs to sums over harmonics . . . 111
7.1.1 The Poisson summation formula 111
7.1.2 Transformations of sums over LLs to sums over harmonics in the quasi-2D case 112
7.2 Calculation of magnetization and its envelope in the quasi-2D case at weak warping 113
7.2.1 Chemical potential 113
7.2.2 Magnetization 116
7.2.3 The magnetization envelope 118
7.3 The absence of slow oscillations in magnetization 119

List of Figures

1.1 The LLs(parabolas) and the Fermi level. 13

1.2 The logarithmic plot of temperature dependence of the amplitude of magnetization oscillations. The slope γ gives approximatly the effective mass according to eq. (1.15). 16

1.3 The logarithmic plot which allows to extract the Dingle temperature. The slope β is connected to T_D according to eq. 1.16. 17

2.1 The Fermi surface and Landau levels in the three- and two-dimensional cases. 23

2.2 The energy of the 2D electron gas as a function of magnetic field. Solid line correspondes to constant electron density (formula 2.1) while the dashed line correspondes to constant chemical potential. 25

2.3 The schematic view of the dHvA oscillations in the 3D (upper graph) and 2D (lower graph) cases in the limit of weak harmonic damping (ignoring temperature and scattering damping factors). While the 3D magnetization oscillations are quite smooth, the 2D dHvA signal has a saw-tooth form. 26

2.4 A comparison of the magnetic field dependence of the ideal 2D magnetization oscillations and the quantum Hall effect. . . 27

2.5 The schematic picture of sharp LLs in 2D DoS in magnetic field and the position of the chemical potential. It is almost all the time trapped by the highest occupied Landau level. . . 28

2.6 The 2D electron DoS with broadened Landau levels. The Landau levels just below and just above the Fermi energy dominate the magnetic field dependence of the chemical potential. 29

2.7 Chemical potential oscillations in the 2D electron gas at low temperature. The chemical potential is always pinned to one of the LLs exept in the narrow regions near $B = B^*$. 30

2.8 The inclusion of the electron spin leads to splitting of each LL by $g\beta H$. 31
2.9 The magnetic field dependence of the chemical potential with spin-splitting at zero temperature. 32
2.10 A schematic view of the density of electron states in magnetic field with reservoir states (a) and in the case of a finite LL broadening (b). 32
2.11 Chemical potential (a) and magnetization (b) as functions of magnetic field at finite DoS between LLs and zero temperature. The dotted lines give chemical potential and magnetization at zero electron reservoir while the solid lines give them as functions of magnetic field at finite D_{loc}. 33
2.12 (a) The effect of LL broadening on chemical potential and (b) magnetization oscillations. The dotted lines give the chemical potential (in (a)) and the magnetization (in (b)) for sharp LLs while the solid lines correspond to rectangular-broadened LLs. 34
2.13 The magnetization of 2D electron gas at finite temperature without spin-splitting and with sharp LLs. 37
2.14 The susceptibility of an ideal 2D electron gas at zero temperature 39
2.15 A quasi-two-dimensional Fermi surface has the shape of warped cylinder. 40
2.16 Three envelopes of magnetization oscillations obtained using: (a) formula (2.19) with finite k_z dispersion; (b) the ideal 2D formula (eq. 2.20); and (c) the L-K formula (1.13). 41

3.1 The magnetization (dashed curve) and its derivative (solid curve) from the dHvA measurements on α-(BEDT-TTF)$_2$KHg(SCN)$_4$ (see the text) 51
3.2 The normalized magnetization (solid curve) and its derivative transformed according to eq. 3.19 (dashed curve) on one dHvA period. 53
3.3 The temperature-smeared DoS distribution on one LL at $B \approx 28T$. 54
3.4 The shape of a Landau level that intersects the Fermi surface at $B \approx 24T$. 55
3.5 Temperature dependence of harmonic amplitudes. The solid lines are the numerical results (at $n_R = 1$, $m^* = 2m_0$, $T_D = 0.2K$ and $W = 1K$; see text) and the dashed lines represent the Lifshitz-Kosevich prediction for the same parameters. Their strong deviations are clearly seen, especially for higher harmonics. 70

4.1 a - DoS (solid line) near the Fermi level and its first harmonic (dashed line) according to Eq.(4.3), at $4t/\hbar\omega_c = 2.25$; b - same at $4t/\hbar\omega_c = 1.8$; c - the quantity $I(\epsilon)$ (solid line) and its first harmonic (dashed line) according to Eq.(7) at $4t/\hbar\omega_c = 2.25$; c - same at $4t/\hbar\omega_c = 1.8$. In all four panels: the dotted lines are the contributions from individual Landau levels. 78
4.2 dHvA (left scale) and SdH (right scale) oscillations in β-(BEDT-TTF)$_2$IBr$_2$ at $\theta \approx 14.8°$. Insets: corresponding FFT spectra. . 80
4.3 The positions of the nodes in the oscillating magnetization (filled symbols) and resistance (open symbols) versus inverse field. The straight line is the linear fit to the magnetization data. 81
4.4 Tangent of the phase shift between node positions in the SdH and dHvA signals taken from the data on Fig. 3 as a function of magnetic field. The dashed line is a linear fit according to Eq.(4.10) [78]. 82
4.5 Conductivity as a function of magnetic field at two different temperatures. One can see that the frequency of the slow oscillations is twice as large as the beat frequency of Shubnikov oscillations. While the fast Shubnikov oscillations are seen to be damped very strongly by temperature, the amplitude of slow oscillations is almost temperature-independent. 87
4.6 Comparison of angular dependences of the frequency of slow oscillations (filled circles connected by dashed lines) with those of resistance (solid line) and of conductivity (dotted line). . . . 88
4.7 The Dyson equation for the irreducible self-energy in self-consistent Born approximation. The double solid line symbolizes the exact electron Green's function. 91
4.8 Interlayer conductivity given by formula (4.33) (Fig. 2a) and by the standard L-K formula (Fig. 2b) at the same parameters. The difference between the L-K formula and the new formula is very pronounced. The parameters are taken to be relevant to the SdH effect in β-(BEDT-TTF)$_2$IBr$_2$ in tilted magnetic field. The parameters are T_D =0.4K, T_D^{tot}=1.0K, T=1.2K, F_b=10T that corresponds to the tilt angle $\theta \approx 26°$ or $-12°$. 96
4.9 A comparison of the results of different theoretical models with the experimental data on the field dependence of the phase shift of beats. The standard 3D theory gives $\phi_b = 0$. The dash line is the prediction of the Boltzmann transport equation while the solid line is the result of the present theory (see text). 97

Acknowledgment

This work has been done at the joint Grenoble High Magnetic Fields Laboratory of the Max-Planck-Institut für Festkörperforschung and Centre National de la Recherche Scientifique in collaboration with L.D. Landau Institute for Theoretical Physics. Here I would like to express my gratitude to all the people who have added to this work by advice, help, discussion or friendship:

- to Prof. Peter Wyder for a nice opportunity to work in his laboratory and for accepting me as his PhD student. His enthusiasm and encouragement were of a great importance for writing this Ph.D. thesis.

- to Prof. Dehnen und Prof. Schatz for being my opponents on the defence.

- to Prof. Israel Vagner for guidance through the different scientific topics I have worked on since I arrived to Grenoble, for many useful discussions and for practical help.

- to Prof. A. Dyugaev for very many useful and interesting discussions, for numerous advises, for the encouragements and support.

- to Dr. M. Kartsovnik and Dr. W. Biberacher for kind cooperation and help.

- to Prof. V.P. Mineev and Prof. E. Kats, Dr. A. Lebed, Prof. S.V. Iordanskii and Prof. Yu.N. Bychkov from L.D. Landau Institute for Theretical Physics for many useful discussions.

- to David Plantier with whom I have had the pleasure of sharing an office.

- to Brigitte Indigo, Uschi Laitenberger and Gislaine Meneroud for help with administrative problems.

- to all my friends and colleagues who surrounded me in Grenoble, especially to Yury Pershin, Masha and Vladimir Gvozdikov, Vladimir Pashenko, Sergey Shevchenko, Roland Schleser, Cornelius Ströhm for a nice time spent together, for interesting discussions, tea-breaks, sport games, etc.

- to Christian de Looze, Jeane van Dyk et Tatyana Zabarina pour les bonnes soirèes et les discussions.

- to Sebastian Buisson for his help with computer problems.

- to my friends G. Loukova, Lew and Nastya Dunin-Barkovsy and Olya Kouznetsova for friendship and warmth.

- to my University friends V. Ruban, A. Maltsev, D. Podolsky, A. Kovalchuk, K. Fomenko for friendship and nice discussions.

- to my parents and my brother for their support and understanding during all these years.

Chapter 1

INTRODUCTION

The magnetic quantum oscillations (MQO) are the oscillations of different thermodynamic and transport properties of metals in strong magnetic field in response to changes in magnetic field. These phenomena arise due to the quantization of the electron energy spectrum in magnetic field[1],[8] which leads to the oscillations of the electron density of states at the Fermi level. This results in the oscillations of magnetization, conductivity, sound absorption etc. The magnetic quantum oscillations play a very important role in the investigation of the electronic properties of metals since these phenomena give information about the Fermi surface, the cyclotron mass of electrons, their relaxation time and spin splitting.

The theory of magnetic quantum oscillations in 3D metals has been constructed in the 1960s. It has been verified by many experiments and have been widely used to analyze the experimental data. We shall describe it later. Recently much interest was caused by the strongly anisotropic compounds. The present work is mainly aimed at studying magnetic quantum oscillations in two- or quasi-two-dimensional (quasi-2D) metals that consist of stack of 2D layers with a small electron hopping probability between the layers. This structure takes place in heterostructures, organic metals, intercalated graphites etc. and the magnetic quantum oscillations is one of the main tools to study their electronic properties. The standard 3D theory of the MQO is often not valid in these compounds and a modified theory is of great importance.

In this introduction chapter we shall describe the main existing approaches to the theory of de Haas-van Alphen (dHvA) effect. In Sec. 1.1 we shall outline this theory in 3D metals with its applications to processing of experimental data. Then (in section 1.2) we represent the Shoenberg's formula (designed for 2D metals) and describe its limitations. In Sec. 1.3 a theory of the Shubnikov - de Haas effect in 3D metals is sketched. Chapter 2 is de-

voted to a study of 2D dHvA effect in model approximations that shows the difference between 3D and 2D cases in detail. In chapter 3 the dHvA effect is studied for more general and realistic conditions. In chapter 4 quantum oscillations of conductivity are considered.

1.1 3D de Haas - van Alphen effect

The de Haas-van Alphen (dHvA) effect consists in oscillations of the magnetization in response to magnetic field changes. This phenomenon is very important for investigating the properties of metals, since it provides information about the Fermi surface and cyclotron mass of electrons in different compounds. This effect has been suggested in 1930 by L.D.Landau [2] and has first been measured by de Haas and van Alphen in the same year [3].

The calculation of magnetization as a function of magnetic field and temperature for arbitrary electronic spectrum in 3-dimensional metals has been carried out in 1955 by Lifshitz and Kosevich [4]. This theory is based on the quasi-classical study of the electron motion along the Fermi surface and is well described in the book of Abrikosov[8]. We shall give the main points of this theory.

Let us consider a set of independent electrons (or electron-type quasi-particles) that fill the states inside the Fermi surface. For arbitrary dispersion relation $\epsilon(\vec{p})$ the energy levels of these quasi-particles in magnetic field $\vec{B} \approx \vec{H}$ parallel to the z-axis are given by the Onsager relation [9]:

$$A\left(\epsilon, k_z\right) = (n+\gamma) 2\pi\hbar \frac{eB}{c} \tag{1.1}$$

where k_z is the wave number along the z-axis ($\vec{k} = \vec{p}/\hbar$), $A(\epsilon, k_z)$ is the area of the Fermi surface cross-section at a given k_z, the index $n = 0, 1, 2, ..$ is the number of a Landau level (LL) and γ is approximately constant. For a parabolic isotropic band ($\epsilon(\vec{p}) = \vec{p}^2/2m^*$, where m^* is the effective electron mass) one has $\gamma = 1/2$, the cross section $A(\epsilon, k_z) = \pi(p_x^2 + p_y^2) = \pi\left(2m^*\epsilon - p_z^2\right)$ and the electron energy levels in magnetic field are given by

$$\epsilon_{n,k_z,\sigma} = \hbar\omega_c \left(n + \frac{1}{2}\right) + \frac{k_z^2}{2m} + \sigma\mu_e B \tag{1.2}$$

where $\omega_c = eB/m^*c$ is the cyclotron frequency. The last term is due to the electron spin; $\sigma = \pm 1$ is the spin orientation and $\mu_e = e\hbar/2mc$ is the Bohr magneton.

1.1.1 Physical origin of the magnetic quantum oscillations

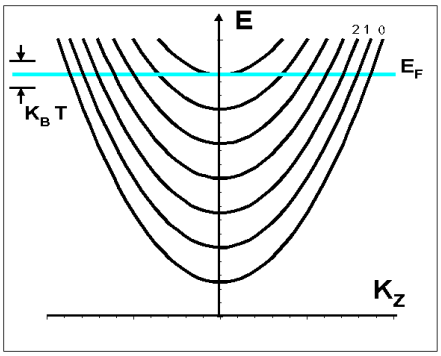

Figure 1.1: The LLs(parabolas) and the Fermi level.

Consider the Landau tube of largest area inside the FS, Fig. 1.1. Its occupied length will shrink as B increases and vanishes rapidly when the tube just touches the extreme cross-section of the Fermi surface (FS) The density of electronic states at the Fermi level is maximal when the Landau level's minima (see Fig. 1.1) just cross the Fermi energy E_F. When the magnetic field is swept this happens periodically in $1/B$. The period is defined by (see Onsager relation 1.1)

$$\Delta\left(\frac{1}{H}\right) = \frac{2\pi e}{\hbar A}$$

where A is the area of the extreme cross-section of the FS, perpendicular to B. This results in the oscillatory behavior of the free energy and the magnetization in $1/B$.

The Fermi energy in a three-dimensional system is practically field independent because all the occupied Landau levels cross the FS. In calculating the thermodynamic properties, like magnetization for 3dEG, one therefore should keep the chemical potential μ constant.

1.1.2 Thermodynamic potential

According to its definition the three-dimensional thermodynamic potential with a given energy spectrum is given by

$$\Omega = -k_B T \sum_n \sum_{k_y} \sum_{k_z} \sum_\sigma \ln\left[1 + \exp\left(\frac{\mu - \epsilon\left(n, k_z, \sigma\right)}{k_B T}\right)\right] \qquad (1.3)$$

In writing this we disregard the electron-electron interaction on the Fermi surface. According to the Fermi liquid theory this is a good approximation if the dispersion relation of the electron-type quasi-particles on the Fermi surface is specified. Usually, the renormalization of the electron effective mass tensor is sufficient to take into account the crystalline potential and the electron-electron interactions. Then formula (1.3) can be applied.

For $B = 0$ the number of electron states (bearing in mind that there are two spin states for each k state) is $\left(2V/\left(2\pi\hbar\right)^3\right)\int d^3p$ where V is the volume of a metal. In the presence of a magnetic field, the permitted states are on the Landau tubes, and the area between neighboring Landau levels in k-space is (using 1.1)

$$\Delta A = \frac{B}{\phi_o}(2\pi)^2 \tag{1.4}$$

where $\phi_0 = 2\pi\hbar c/e$ is the magnetic flux quantum. Eq.(1.4) defines the degeneracy of a Landau level. The number D of states on a tube lying between k_z and $k_z + dk_z$ is:

$$D = \Delta A \Delta k_z \frac{V}{4\pi^3} = \frac{eHV dk_z}{2\pi^2 c\hbar}\,. \tag{1.5}$$

Since D is independent of the form of $\epsilon(k)$, Eq.(1.5) is valid for arbitrary dispersion $\epsilon(k)$. Formula (1.3) now can be written as

$$\begin{aligned}\Omega &= -k_B T \sum_{\sigma=\pm 1}\int_{-\infty}^{+\infty} dk_z \left(\frac{eHV}{(2\pi)^2 c\hbar}\right) \\ &\quad \sum_n \ln\left[1+\exp\left(\mu - \epsilon\left(n,k_z,\sigma\right)/k_B T\right)\right]\,.\end{aligned} \tag{1.6}$$

1.1.3 The LK-formula for magnetization

In the three-dimensional dHvA case the magnetization is a smooth function of magnetic field, and the Poisson summation formula (Appendix A, Eq. 7.1) can be used to turn the sums over n in Eq.(1.6) into an integral. Performing then the k_z summation and differentiating with respect to $B \approx H$, one arrives at the Lifshitz-Kosevich (LK) formula [6]:

$$\begin{aligned}M \propto \frac{eFk_B TV}{\sqrt{2\pi H A"}} \sum_{p=1}^{\infty} p^{\frac{-3}{2}} R_T(p)\, R_D(p)\, R_s(p) \times \\ \times \sin\left[2\pi p\left(\frac{F}{H} - \frac{1}{2}\right) \pm \frac{\pi}{4}\right]\end{aligned} \tag{1.7}$$

where

$$A" = \left|\frac{\partial^2 A}{\partial k_z^2}\right|_{k_z = k_{extr}}$$

The notation k_{extr} indicates that only extreme cross sections of the Fermi surface must be considered in formula (1.7). The factor R_T describes the effect of a finite temperature,

$$R_T(p) = \frac{\pi\kappa}{\sinh \pi\kappa} = \frac{2\pi^2 p k_B T/\beta^* H}{\sinh\left(2\pi^2 p k_B T/\beta^* H\right)} \tag{1.8}$$

where β^* is the effective Bohr magneton; $\beta^* H = \hbar\omega_c$. The factor R_D describes the effect of finite relaxation time τ of the electrons:

$$R_D(p) = \exp\left(\frac{-2\pi^2 p k_B T_D}{\beta^* H}\right) \tag{1.9}$$

where T_D is the *Dingle temperature* which can be introduced when the broadening of the Landau levels can be described by a Lorentzian distribution function. It is then connected to the electron relaxation time τ by the relation

$$T_D = \frac{\hbar}{2\pi k_B \tau}\,. \tag{1.10}$$

The effect of electron spin is described by the factor R_s, defined as:

$$R_S(p) = \cos\left(\frac{1}{2} p\pi g \frac{m}{m_o}\right)\,.$$

The *dHvA frequency* F is defined as:

$$F = \frac{c\hbar A_{extr}}{2\pi e} \tag{1.11}$$

where A_{extr} is one of the extreme cross sections of the Fermi surface under study. Applying magnetic field at different angles and using the last relation for F one can find all extreme cross sections of the FS and thus reconstruct the total FS. This procedure has been used to find the geometry of the FS of very many metals.

But one can extract not only the geometry of the Fermi surface but also the effective electron mass and the information about the scattering rate of an electron in a compound under investigation.

Because of the smooth form of magnetic oscillations in 3D, only the first harmonics in the sum over p in (1.7) need be kept, and the LK-formula takes a very simple form often used for analyzing the experimental data on dHvA:

$$M \propto \frac{-eFk_BTV}{\sqrt{2\pi HA"}} R_T\, R_D\, R_s \times \sin\left[2\pi\frac{F}{H} \pm \frac{\pi}{4}\right]\,. \tag{1.12}$$

It follows from Eq.(1.12) that the amplitude of the oscillations is proportional to:

$$R_T\, R_D = \frac{\lambda}{\sinh(\lambda)} \exp\left(-\lambda \frac{T_D}{T}\right) \tag{1.13}$$

where

$$\lambda \equiv \frac{2\pi^2 k_B T}{\hbar \omega_c}\,. \tag{1.14}$$

Plotting the logarithm of the amplitude of magnetization oscillations as a function of either temperature or inverse magnetic field (Figs. 1.2 and 1.3), one gets information on the effective mass and the Dingle temperature from the slopes γ and β of the curves according to the equations

$$\tan\gamma \approx \lambda/T = \frac{2\pi^2 k_B m^* c}{e\hbar B} \tag{1.15}$$

and

$$\tan\beta = \frac{2\pi^2 k_B T_D}{e\hbar/m^* c}. \tag{1.16}$$

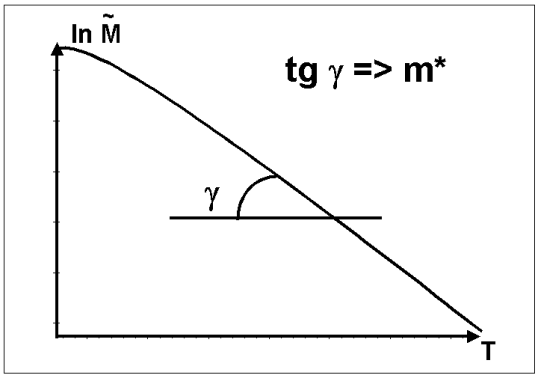

Figure 1.2: The logarithmic plot of temperature dependence of the amplitude of magnetization oscillations. The slope γ gives approximatly the effective mass according to eq. (1.15).

The effective mass m^* is important since it enters many thermodynamic and transport properties, while the Dingle temperature describes the purity of a sample as given by (1.10).

The above analysis is well applicable to the 3D magnetization oscillations but it explicitly uses the 3D electron dispersion relation. How should it be modified to describe two-dimensional magnetization oscillations ? This question was first systematically studied by Shoenberg[16]. We present his results and discuss their reliability in the next subsection.

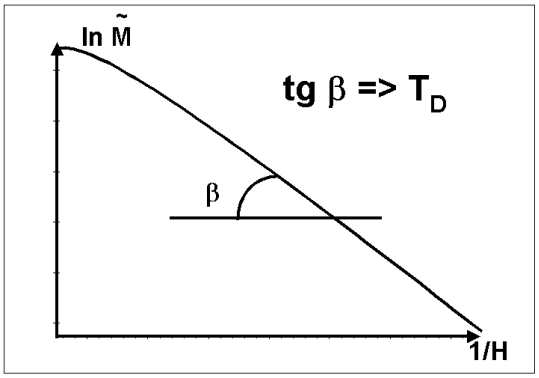

Figure 1.3: The logarithmic plot which allows to extract the Dingle temperature. The slope β is connected to T_D according to eq. 1.16.

1.2 Shoenberg's formula for the 2D case

Assuming the chemical potential to be constant the magnetization in two-dimensional case can be expressed as a harmonic series by the formula similar to the L-K in 3D case. The derivation of this formula is somewhat different from that used to derive the L-K formula because no integration over k_z should be performed. This formula was first derived by Shoenberg [1] using the phase smearing arguments. We shall derive it by a more rigorous method.

The density of states (DoS) in the 2D case consists of the set of Landau levels (LLs),

$$\rho(\varepsilon, B) = g(B) \sum_{n=0}^{\infty} D(\varepsilon - \hbar\omega_c(n + \frac{1}{2})) \ , \tag{1.17}$$

where the LL degeneracy $g(B) = 2B/\Phi_0$; $\Phi_0 = 2\pi\hbar c/e$ and the function $D(\varepsilon)$ determines the shape of the LLs. One can take this function to be the same for all LLs since only a few LLs near the FS are important. The formula (1.17) can be rewritten as a harmonic series

$$\rho(E, B) = \frac{g}{\hbar\omega_c} \sum_{k=-\infty}^{\infty} \exp\left[2\pi i \left(\frac{E}{\hbar\omega_c} - \frac{1}{2}\right) k\right] R_D(k) \frac{1 + \mathrm{sign}(E)}{2} \tag{1.18}$$

where we introduced the Fourier transform of the DoS distribution on each LL

$$R_D(k) = \int_{-\frac{\hbar\omega_c}{2}}^{\frac{\hbar\omega_c}{2}} D(E') \exp\left(2\pi i \frac{E'k}{\hbar\omega_c}\right) \mathrm{d}E' \tag{1.19}$$

(for the Lorentzian shape of LLs coincides with the usual Dingle factor 1.9). The factor $(1+\mathrm{sign}(E))/2$ indicates that no electron states exist for $E<0$. One can omit the term with $k=0$ since it does not affect magnetic oscillations.

To calculate the magnetization one calculates first the thermodynamic potential $\Omega(\mu,B)$. By definition in one particle approximation

$$\Omega=-k_BT\int d\varepsilon\rho(\varepsilon,B)\ln\left(1+\exp\frac{\mu-\varepsilon}{k_BT}\right)\ , \tag{1.20}$$

Substituting (1.18) into (1.20) and integrating by parts twice we get

$$\tilde{\Omega}=-\frac{g}{\hbar\omega_c}\int \mathrm{d}E\frac{\partial f}{\partial E}\sum_{k\neq 0}\frac{\hbar^2\omega_c^2}{(2\pi k)^2}\exp\left[2\pi i\left(\frac{E}{\hbar\omega_c}-\frac{1}{2}\right)k\right]R_D(k) \tag{1.21}$$

Since $\frac{\partial f}{\partial E}\neq 0$ only in a small region near the FS, the factor $(1+\mathrm{sign}(E))/2$ has been omitted.

Introducing the Furrier transform of $\partial f/\partial E$

$$R_T(k)\equiv\int \mathrm{d}E\left(-\frac{\partial f}{\partial E}\right)\exp\left(2\pi i\frac{(E-\mu)k}{\hbar\omega_c}\right)=\frac{2\pi^2Tk/\hbar\omega_c}{\sinh(2\pi^2Tk/\hbar\omega_c)}\equiv\frac{k\lambda}{\sinh k\lambda} \tag{1.22}$$

we get

$$\tilde{\Omega}=\frac{g\hbar\omega_c}{2\pi^2}\sum_{k=1}^{\infty}\frac{(-1)^k}{k^2}\cos\left(\frac{\mu}{\hbar\omega_c}2\pi k\right)R_D(k)\ R_T(k) \tag{1.23}$$

Differentiating (1.23) we obtain the harmonic expansion of the oscillating part of the magnetization oscillations

$$\tilde{M}=-\frac{\partial\tilde{\Omega}}{\partial B}\mid_{\mu=const}=\frac{g\mu}{\pi B}\sum_{k=1}^{\infty}\frac{(-1)^{k+1}}{k}\sin\left(\frac{\mu}{\hbar\omega_c}2\pi k\right)A(k)\ F_T(k) \tag{1.24}$$

This coincides with Shoenberg's formula[1].

Let us now discuss this formula. It assumes the same physical input as the Lifshitz-Kosevich formula; only integration over k_z was removed. Nevertheless, the change from 3D to 2D case leads to many new effects.

First, both the L-K and Shoenberg's formula assume the chemical potential to be constant, that is a very good approximation in the 3-dimensional case but is not valid for two dimensions. This difference occurs because in three dimensions the spectrum of electrons is continuous (due to the z-component of momentum) and the Fermi surface is intersected by many

Landau levels. Therefore the chemical potential is approximately equal to the Fermi energy and does not oscillate with varying magnetic field. In the two-dimensional (2D) system the electron spectrum has gaps(between LLs) and the chemical potential (which is the minimal energy of a particle to be added to the system) is pinned to the highest occupied Landau level. As the magnetic field is reduced this LL becomes completely filled and the chemical potential jumps to the next LL. These jumps have been clearly detected by the magnetization measurement in several single-layer high-mobility 2D electron gas AlGaAs-GaAs heterostructures [23]. This indicates that the electron density rather than the chemical potential is fixed in the heterostructures. Schematically the oscillations of the chemical potential in the pure 2D limit are shown in fig. 2.7. Hence the chemical potential in two dimensions oscillates strongly as the magnetic field varies and must not be considered as a constant. This fact greatly changes the amplitude and the shape of the magnetization oscillations.

Another difficulty in the theoretical description of the 2D dHvA effect arises when the electron scattering on impurities is taken into account. The impurity scattering changes the electron motion and therefore affects the magnetization. In three-dimensional case the point-like impurity scattering leads to the Dingle factor [49][50] in the harmonic expansion of the magnetization oscillations. This means that the oscillations of the density of electron states are damped by the same factor due to impurity scattering. This may be incorrect in the 2D case. The impurity scattering and many-particle effects should be stronger in the 2D case because of the degeneracy of the LLs. The problem of the density of quasiparticle states in 2D metals is not solved yet and will be discussed in chapter 3. One should note that this problem is much more complicated than the effect of oscillations of the chemical potential. This is because the magnetization is a thermodynamic quantity and can in principle be calculated (expressed via some integrals and algebraic equations) if the density of quasi-particle states $\rho(E)$ is given (formulas (1.20) and (2.11)). But to find the function $\rho(E)$ one should solve some microscopic model.

Third, Shoenberg's formula does not take into account the finite k_z dispersion that exists due to interlayer electron jumps both in organic metals and in heterostructures. These are important limitations that make Shoenberg's formula invalid in very many interesting cases. A more reliable theory will be proposed in chapter 3.

1.3 The Shubnikov - de Haas effect in 3D metals.

The quantization of the electron energy spectrum in magnetic field leads to the quantum oscillations not only of the magnetization but almost of all electronic properties [[1], chap. 4]. The conductivity also reveals quantum oscillations as magnetic field is swept. This effect was discovered by Shubnikov and de Haas [1] even several months earlier than the dHvA effect. The standard 3D theory of the Shubnikov - de Haas effect (SdH) [[10], for a review see [8], chap. 11] is based on the same quasi-classical consideration of the electron motion along the Fermi surface as the dHvA theory is. From the Onsager quantization rule one determines the electron spectrum and the density of states $\rho(E)$. The oscillations of the density of states at the Fermi level make the main contribution to the conductivity because they lead to the oscillations of the electron relaxation time τ to which the conductivity is proportional. The scattering rate $1/\tau$ on the point-like impurities in Born approximation is proportional to the density of electron states at the Fermi level $\rho(\mu)$. The DoS can be found as

$$\rho(E) = \sum_{n} \sum_{k_y} \sum_{k_z} \sum_{\sigma} \delta\left(E - \epsilon\left(n, k_z, \sigma\right)\right) \tag{1.25}$$

where $\delta(x)$ is the Dirac delta function. The summations in (1.25) are similar to those in (1.3). Applying the same mathematical tricks as in Sec. 1.1 one finds that the oscillating part $\tilde{\sigma}(B)$ of conductivity is proportional to the derivative of magnetization [[8], chap. 11]:

$$\tilde{\sigma}(B) \sim \frac{1}{\sqrt{A"}} \sum_{p=1}^{\infty} p^{-1/2} R_T(p)\, R_D(p)\, R_s(p) \times \cos\left[2\pi p \left(\frac{F}{B} - \frac{1}{2}\right) \pm \frac{\pi}{4}\right] \sim \frac{\partial M}{\partial B}. \tag{1.26}$$

Even more than in the case of magnetization, the 3D theory of the Shubnikov - de Haas effect fails to describe the 2D or quasi-2D magnetotransport in strong fields. The problem of the 2D magnetotransport is known to differ completely from the 3D case. The quantum Hall effect (Q.H.E.) certainly can not be described by the 3D magnetotransport theory. But even when the electron dispersion in the third dimension is larger than the cyclotron energy, the new qualitative effects appear that can not be explained in the framework of the 3D theory. Namely, these are the slow oscillations of conductivity or the phase shift of the beats of conductivity oscillations. These effects were observed, for example, in strongly anisotropic organic metals. We shall discuss these problems and their solutions in detail in chapter 4 of this thesis.

In chapter 2 we shall emphasize the difference between the 3D and 2D cases and illustrate the physics by many pictures. There we shall study the 2D chemical potential oscillations and their effect on magnetization oscillations in the simplest case of sharp Landau levels and low temperature. Practically, chapter 2 is also introductory (although it contains some new results) and the main results are given in chapters 3 and 4. In the third chapter we shall consider the dHvA effect under more general conditions including also the LL broadening, finite k_z dispersion and chemical potential oscillations at arbitrary electron reservoir. This chapter requires more mathematics, but we shall invariably indicate the physics of the phenomena. The fourth chapter is devoted to magnetoresistance oscillations where the theory of the quasi-two-dimensional Shubnikov-de Haas effect is developed. Actually, this theory still uses many approximations. These limitations and the further perspectives of the development of the theories are then discussed.

Chapter 2

2D dHvA effect (the model study)

2.0.1 Comparison between 2D and 3D dHvA cases

From the general point of view, oscillations in the two-dimensional (2D) case are much sharper and even stronger than in the 3D case. This is because the k_z dispersion smears out the effect of the quantization of Landau levels. As a result (see chapter 1) only the extreme cross sections of the Fermi surface effectively contribute to the magnetic quantum oscillations. In the 2D case the Fermi surface is a cylinder that goes along the LLs (see Fig. 2.1). Hence, in the 2D case the entire FS is extreme.

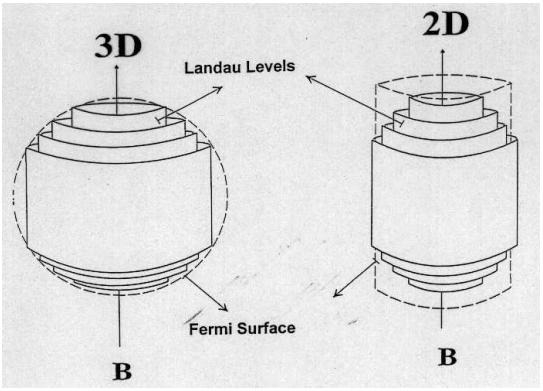

Figure 2.1: The Fermi surface and Landau levels in the three- and two-dimensional cases.

The area of the extreme parts of the FS in the 3D case is about $\sqrt{\hbar\omega_c/E_F}$ times smaller than the total Fermi surface area. Hence, at the same electron concentration the magnetic quantum oscillations in the 2D case are

$\sim \sqrt{E_F/\hbar\omega_c}$ times larger than in the 3D case. The smearing from the k_z dispersion leads also to a much stronger harmonic damping of the oscillations. Comparison of the 2D Shoenberg formula (1.24) with the Lifshitz-Kosevich formula (1.7) gives that the coefficient before the k-th harmonics in the 3D case has an additional $k^{-1/2}$ power of the harmonic number. This leads to a different shape of oscillations in the weak harmonic damping limit (at low temperature and in pure compounds; see Fig. 2.3). Magnetization oscillations in the 2D case without any smearing have the saw-tooth shape (Fig. 2.3 b or Fig. 2.4 b). This can be easily derived. At zero temperature the magnetization $M(B)$ is given by the derivative of the total electron energy $E(B)$ as a function of magnetic field:

$$M(B) = -dE(B)/dB.$$

The electron energy is calculated as a sum over all Landau levels at a constant electron density N. Assume the electrons to be spinless and the LLs to be sharp. The last occupied LL with a number n_F has $N - n_F g$ electrons where $g = B/\Phi_0$ is the degeneracy of LLs and $\Phi_0 = 2\pi\hbar c/e$. The total electron energy becomes

$$\begin{aligned} E(B) &= g\sum_{n=0}^{n_F-1} \hbar\omega_c(n+1/2) + (N - n_F g(B))\,\hbar\omega_c(n_F + \frac{1}{2}) = \\ &= \frac{n_F^2}{2} g\hbar\omega_c + (N - n_F g(B))\,\hbar\omega_c(n_F + \frac{1}{2}) = \\ &= -\frac{n_F^2}{2} g\hbar\omega_c + N\hbar\omega_c(n_F + \frac{1}{2}) - n_F g(B)\hbar\omega_c/2. \end{aligned} \tag{2.1}$$

It has a quadratic dependence on the magnetic field on each dHvA period (see Fig. 2.2).

The magnetization is

$$\begin{aligned} M(B) &= -\frac{dE(B)}{dB} = \frac{n_F^2}{B} g\hbar\omega_c - \frac{N\hbar\omega_c}{B}(n_F + \frac{1}{2}) + n_F g(B)\hbar\omega_c/B = \\ &= \frac{\hbar\omega_c n_F}{B}(n_F g - N) + (n_F g - N/2)\,\hbar\omega_c/B \end{aligned} \tag{2.2}$$

When many LLs are occupied ($n_F \gg 1$) the first term in (2.2) gives the main contribution to magnetization. The magnetization is always linear in B except at points where an integer number of LLs is occupied and the number of the highest occupied LL n_F jumps by unity. The magnetization at these points jumps by $\approx E_F/\Phi_0$. This dependence is plotted on the graphs 2.3b and 2.4b. Such magnetization behavior has a relation to the

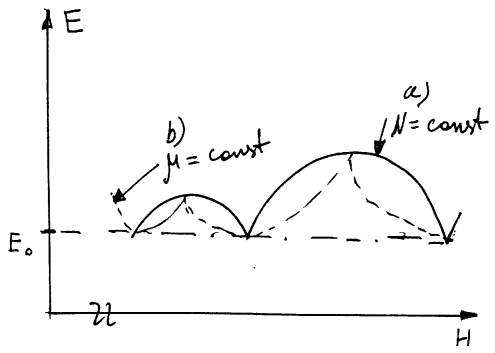

Figure 2.2: The energy of the 2D electron gas as a function of magnetic field. Solid line correspondes to constant electron density (formula 2.1) while the dashed line correspondes to constant chemical potential.

integer quantum Hall effect that is illustrated on Fig. 2.4. Since $n_F = Int[E_F/\hbar\omega_c]$ the magnetization has a periodicity as a function of $1/B$ and the slope $dM/dB \sim 1/B^2$.

Of course, this is only a model picture because to describe the real experiments one has to take into account finite temperature, LL broadening, spin-splitting and, probably, other factors. In this chapter we shall study the characteristic features of the 2D magnetic quantum oscillations in detail, successively considering different complicating factors.

2.1 Chemical potential in two-dimensional electron gas in strong magnetic field

2.1.1 Fermi Energy and Chemical Potential

The significant point for the understanding of statistics and thermodynamics of the two-dimensional electron gases in quantizing magnetic fields is the magnetic filed dependence of the chemical potential $\mu(B)$. Huge degeneracy of the energy levels and large energy gaps between them result in sharp magnetic oscillations of chemical potential in these systems.

One should be alert to the difference between the notions of the **Fermi energy** and of the **chemical potential** in the following sense.

Using a simple definition of the chemical potential as the *minimal energy needed to add a particle to a statistical system* it is straightforward to see that at $T = 0$ the chemical potential will be "trapped" by a partially occupied Landau level during almost a whole dHvA period and will cross the Landau

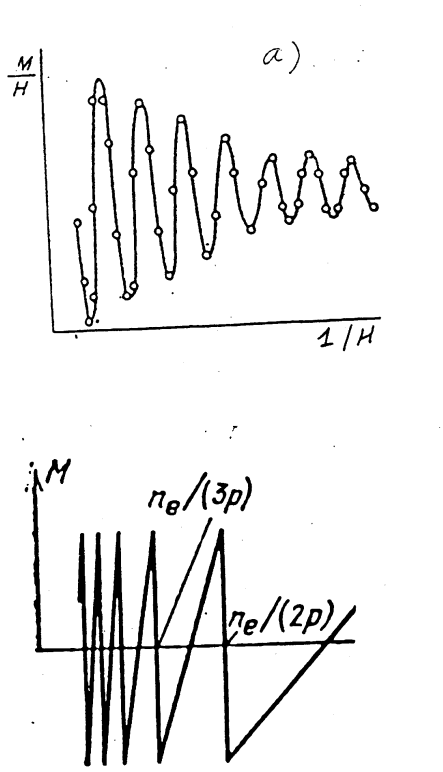

Figure 2.3: The schematic view of the dHvA oscillations in the 3D (upper graph) and 2D (lower graph) cases in the limit of weak harmonic damping (ignoring temperature and scattering damping factors). While the 3D magnetization oscillations are quite smooth, the 2D dHvA signal has a saw-tooth form.

gap in infinitesimally narrow region around B^* , (Eq. 2.6). This is visualized by the "Landau fan", Fig. 2.5, and in more details in Fig. 2.6. The magnetic field dependence of the chemical potential is shown in Fig. 2.7.

The Fermi energy E_F is *the maximal occupied energy level in an electronic system at zero temperature and in the absence of external magnetic field.* Hence, the Fermi energy is independent of the magnetic field. In a 2D electron gas in magnetic field (2DEG + H) it is useful to take E_F as the *point of reference for energy.* The chemical potential $\mu(H)$ and the Fermi energy E_F coincide, therefore, at $T = 0, H = 0$: $\mu(B = 0; T = 0) \equiv E_F$.

One should distinguish between three possible situations:

a) The total number of electrons on the LLs is field-independent, while the chemical potential is oscillating with an amplitude equal to the distance

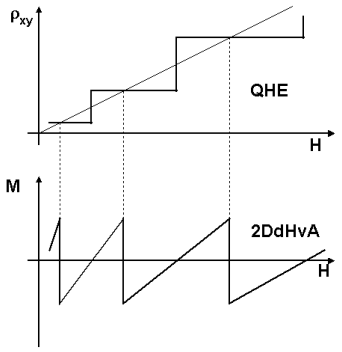

Figure 2.4: A comparison of the magnetic field dependence of the ideal 2D magnetization oscillations and the quantum Hall effect.

between the adjacent LLs. (N=const(B); $\mu = \mu(B)$)

b) The chemical potential is field-independent, while the number of electrons on the LLs is oscillating with field. (μ=const(B); N=N(B)).

c) Both the chemical potential and the number of electrons on the LLs are allowed to vary corresponding to the external conditions.

In this chapter we shall concentrate on the case **a).** The case **b)** can be described with sufficient accuracy by Shoenberg's formula (1.24) while the more general case **c)** will be considered in the next chapter.

2.1.2 Calculation of the chemical potential (for finite temperature and sharp LLs).

As we have briefly outlined in the introduction, the magnetic field dependence of the magnetization in the 2D case has much more sharp form (or even the saw-tooth shape in the ideal case ignoring temperature and electron scattering damping factors; see Fig. 2.3). Such a different magnetic field dependence of magnetization dictates, obviously, a different mathematical approach to the problem: the Poisson summation formula (a Fourier transform of a smooth function), operative when all but the first harmonics have negligible amplitudes, will not be useful in the two-dimensional case, where the magnetic field dependence of magnetization is saw-tooth and the number of Fourier harmonics is, therefore, expected to be relatively large.

The Poisson summation formula, used in the L-K theory to change the summation over Landau levels into an integral, is very convenient in the 3D case because very many LLs intersect the FS. In the two-dimensional case both the Fermi surface and the LL are cylinders in momentum space.

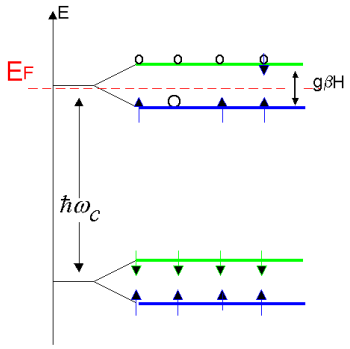

Figure 2.5: The schematic picture of sharp LLs in 2D DoS in magnetic field and the position of the chemical potential. It is almost all the time trapped by the highest occupied Landau level.

Hence, at low temperature only two LLs just above and below the Fermi level make important contribution to the thermodynamic quantities (such as magnetization) because only these two Landau levels are partially full. The standard log M versus either T or $1/H$ plots may be inapplicable in the 2D case because of strong oscillations of the chemical potential. Some formulas appropriate for this case will be given in this chapter.

Sharp Landau levels at finite temperature

Consider sharp (δ - functions) Landau levels (Fig. 2.5) at finite temperature. The equation, governing the magnetic field dependence of chemical potential at T $\simeq 0$ reads

$$g(B)\Sigma_{n=0}^{\infty} f_n(n) = N \tag{2.3}$$

where

$$f_n(n) = \frac{1}{1 + exp\left(\frac{\hbar\omega_c(n+\frac{1}{2})-\mu(B)}{k_B T}\right)} \tag{2.4}$$

is the Fermi distribution, $g(B) \equiv \frac{BS}{\Phi_o}$ is the degeneracy of the Landau levels, S is the sample area and N is the total number of particles.

Let n_F be the highest occupied Landau level, so that $\hbar\omega_c(n_F - 1/2) < \mu < \hbar\omega_c(n_F + 1/2)$. At typical experimental conditions on inversion layers or on heterostructures one has $T \simeq 1K$, $H \simeq 10$T and the effective electron mass $m^* \simeq 0.1m_0$, so that $\alpha \equiv \hbar\omega_c/2k_BT \simeq 80$. Therefore all terms in the sum of Eq.(2.3) up to $n = n_F - 2$ could be replaced by unity with an exponential accuracy: $e^{-\alpha} << 1$, and the field dependence of the chemical potential is

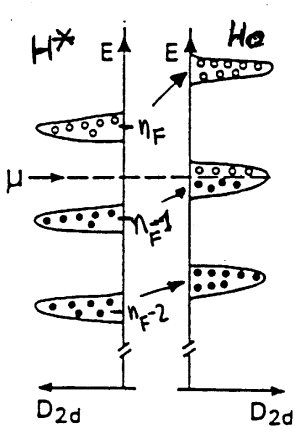

Figure 2.6: The 2D electron DoS with broadened Landau levels. The Landau levels just below and just above the Fermi energy dominate the magnetic field dependence of the chemical potential.

defined by the distribution of electrons on the levels $n_F - 1$ and n_F. Hence, Eq. (2.3) can be cast in a form containing only sum over two uppermost LLs:

$$\frac{1}{1 + exp[x_{nF} - \alpha]} + \frac{1}{1 + exp[x_{nF} + \alpha]} = \frac{n_s}{g} - (n_F - 1) = 1 + \tilde{n} \tag{2.5}$$

where $x_n \equiv (n\hbar\omega_c - \mu)/k_B T$.

Eq. (2.5) yields an algebraic quadratic equation for y$\equiv e^{x_{nF}}$ which can be solved to give the following field and temperature dependence of chemical potential in the 2D electron gas in magnetic field:

$$\mu(B,T) = \hbar\omega_c n_F - k_B T ln\left[\frac{-\tilde{n} cosh\alpha + \sqrt{1 + \tilde{n}^2 sinh^2\alpha}}{1 + \tilde{n}}\right]. \tag{2.6}$$

Here $\tilde{n} \equiv N_0/g - n_F = (B^* - B)F/B^2$ is the amount of electrons on the highest occupied Landau level (divided by the LL degeneracy); B^* is the magnetic field at which the integer number of LLs is filled.

Eq.(2.6) shows that $\mu \approx \hbar\omega_c(n_F + 1/2)$ at $T \ll \hbar\omega_c$ for all values of magnetic induction except in very narrow regions where $|\tilde{n}| \lesssim \exp(-\alpha)$ near a discrete set $B = B^*$. In these regions assuming $|\tilde{n}| \exp^{\alpha} < 1$ and making the expansion on $\tilde{n} \exp^{\alpha}$ and $\tilde{n}$ in (2.6) one finds that the chemical potential is,

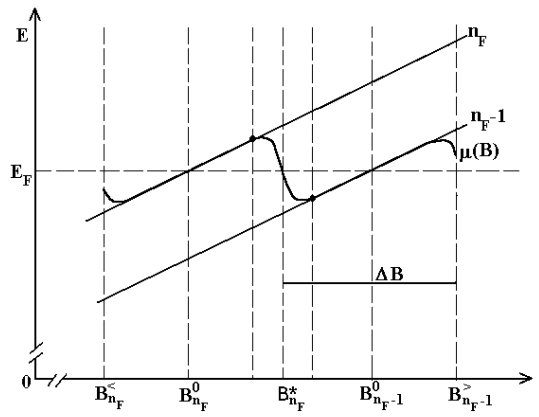

Figure 2.7: Chemical potential oscillations in the 2D electron gas at low temperature. The chemical potential is always pinned to one of the LLs exept in the narrow regions near $B = B^*$.

approximately:

$$\mu(B) \simeq \hbar\omega_c^* n_F + k_B T \frac{\tilde{n} e^{\alpha}}{2}. \tag{2.7}$$

Therefore, at $B = B^*$ the chemical potential is in the middle of the energy gap between the n_F-th and $(n_F + 1)$th LLs, see Fig. 2.5. According to Eq. 2.7 in the vicinity of B^* the derivative of the chemical potential with respect to B is exponentially large :

$$\frac{\partial \mu}{\partial B} \simeq \frac{k_B T}{2} e^{\alpha} \frac{F}{B^2}.$$

This reflects the zero-temperature behavior of the chemical potential. At these field values the highest occupied LL becomes completely filled and the chemical potential jumps to the next Landau level. Such exponentially sharp dependence is a consequence of the "model approximation" of extremely sharp Landau levels and zero density of electron states between the LLs. In Sec. 2.1.3 we shall show how this jump is smeared by a finite DoS between LLs.

At $|\tilde{n}|e^{\alpha} \gg 1$ (or $|B - B^*| > e^{-\alpha} B^2/F$) the expansion of Eq. 2.6 gives

$$\mu = \hbar\omega_c (n_F + 1/2) + k_B T \ln\left(\frac{\tilde{n}}{1 - \tilde{n}}\right).$$

At $k_B T \ll \hbar\omega_c$ the second term is small and the chemical potential is pinned to a Landau level over almost the entire dHvA period.

2.1.3 Some generalizations

INCLUSION OF SPIN

The spin splitting in one-particle approximation leads to doubling the number of energy levels (Fig. 2.8). The chemical potential μ is defined now by a normalization condition

$$\sum_{\sigma=\pm\frac{1}{2},n=0}^{\infty} f_{\sigma,n} = N_o,$$

where

$$f_{\sigma,n} = \frac{1}{1+\exp\left\{\frac{\hbar\omega_c(n+1/2)+\sigma\beta gH-\mu}{T}\right\}} \equiv \frac{1}{e^{(x_n\pm s)}}.$$

If the temperature is low ($T \ll g\beta H, \hbar\omega_c$) one can again keep only the

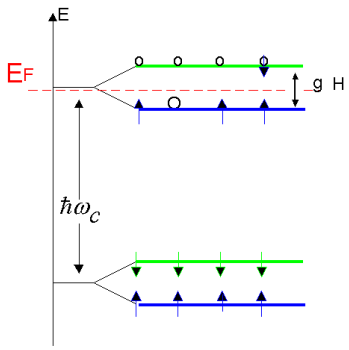

Figure 2.8: The inclusion of the electron spin leads to splitting of each LL by $g\beta H$.

nearest two LLs just above and below the chemical potential and make the calculations similar to that of the previous section. These two nearest LLs are now changed twice during one dHvA period as chemical potential passes through the spin-split LLs. We shall not give this calculation here but depict the behavior of the chemical potential at zero temperature (Fig. 2.9). Later we shall consider even a more general case.

FINITE DOS BETWEEN LANDAU LEVELS

Let us first study the influence of finite density of electron states between LLs on the chemical potential oscillations at zero temperature. A model DoS is shown on Fig. 2.10 (a). We denote the DoS between LLs per one layer and unit area by D_{loc}, and the average DoS on LLs by D_{LL}. The latter is

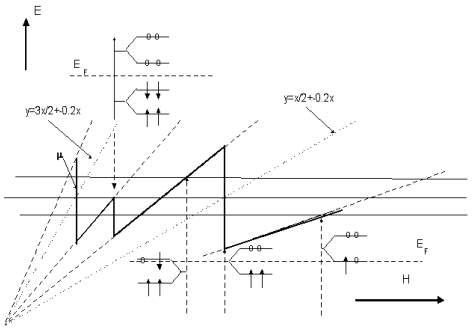

Figure 2.9: The magnetic field dependence of the chemical potential with spin-splitting at zero temperature.

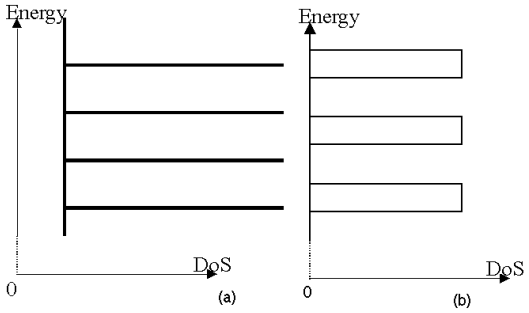

Figure 2.10: A schematic view of the density of electron states in magnetic field with reservoir states (a) and in the case of a finite LL broadening (b).

equal to the LL degeneracy (per unit area) divided by the LL separation: $D_{LL} = g(B)/\hbar\omega_c = m^*/2\pi\hbar^2$. There are no more jumps of the chemical potential when the highest occupied LL becomes completely filled. The chemical potential moves instead though the distance between LLs with a finite velocity that is determined by the ratio D_{LL}/D_{loc}. This slope $\mu(B)$ can be easily obtained from the equation of the constant total electron density:

$$N_e = n_F\, g(B) + D^*_{loc}\mu(B),\ \Rightarrow$$

$$\frac{d\mu}{dB} = -\frac{n_F g(B)}{D_{loc}B} = -\frac{m^* n_F}{2\pi\hbar^2}\frac{D_{LL}}{D_{loc}}.$$

At zero density of localized states $D_{loc} = 0$ one gets $d\mu/dB = -\infty$ that corresponds to the jumps in chemical potential discussed above. The resultant change of the chemical potential and the magnetization oscillations due to localized states is shown on fig. 2.11.

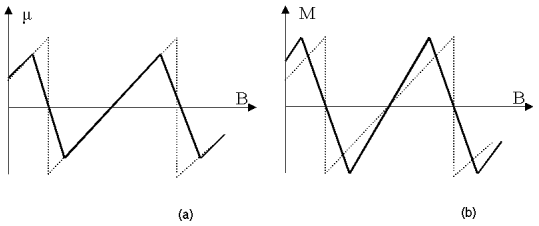

Figure 2.11: Chemical potential (a) and magnetization (b) as functions of magnetic field at finite DoS between LLs and zero temperature. The dotted lines give chemical potential and magnetization at zero electron reservoir while the solid lines give them as functions of magnetic field at finite D_{loc}.

Analytical calculation

We have seen that the presence of localized electronic states within the magnetic energy gap such as, for example, impurity states or edge states, may lead to a significant slowing down in the variation of the chemical potential with respect to B, or even to pinning of μ (a Q.H.E. situation).

Assume, for the sake of simplicity, a given localized state density $D_{loc}(E)$ within the magnetic energy gap. The chemical potential of the system is now determined by the equation

$$N = g\left(n_F - 1\right) + \frac{g}{1 + exp[\frac{E_{nF-1}-\mu}{k_B T}]} +$$

$$\frac{g}{1 + exp[\frac{E_{nF}-\mu}{k_B T}]} + \int_0^\infty D_{loc} \frac{E}{1 + exp[\frac{(E-\mu)}{k_B T}]} dE \approx$$

$$\approx g\left[n_F - \exp\left(\frac{E_{nF-1} - \mu}{k_B T}\right) + \exp\left(\frac{\mu - E_{nF}}{k_B T}\right)\right] + \mu D_{loc}.$$

Introducing $x \equiv \left(\mu - \hbar\omega_c n_F\right)/k_B T$ and $\alpha \equiv \hbar\omega_c / 2k_B T$ this equation can be rewritten as

$$N = g n_F + g \exp\left(-\alpha\right) 2 \sinh\left(x\right) + \mu D_{loc}. \tag{2.8}$$

Differentiating Eq. (2.8) with respect to B and assuming $D_{loc}(E)$ to be a slowly varying function of E around the middle of the magnetic energy gap, one gets:

$$\frac{\partial \mu}{\partial B} \simeq \frac{-n_F g/B + 2ge^{-\alpha} \cosh\left(x\right) \left(\hbar\omega_c n_F / B k_B T\right)}{2ge^{-\alpha} \cosh\left(x\right)/k_B T + D_{loc}(\mu)}.$$

In the middle of the Landau gap this gives

$$\frac{\partial \mu}{\partial B}|_{B=B^*} \simeq \frac{-n_F k_B T/B}{2e^{-\alpha} + D_{loc}(\mu^*) k_B T/g}.$$

The condition under which $\frac{\partial \mu}{\partial B}$ retains its intrinsic behavior (i.e. $\propto \frac{e^{\alpha}}{\alpha}$) is that the density of localized states within the magnetic energy gap should be exponentially small with respect to the density of states of the 2D free electron gas:

$$D_{loc}(E) < 4\alpha e^{-\alpha} D_{2d}^{free}$$

LANDAU LEVEL BROADENING

The LL broadening leads to a reduction of the amplitude of magnetization and chemical potential oscillations. If one replaces δ-type LLs by the rectangles of the finite width Γ (Fig. 2.10 (b)), the chemical potential and magnetization at zero temperature change as is shown in Fig. 2.12. In this case both the chemical potential and the magnetization oscillations are damped by a factor $\sim (1 - \Gamma/\hbar\omega_c)$.

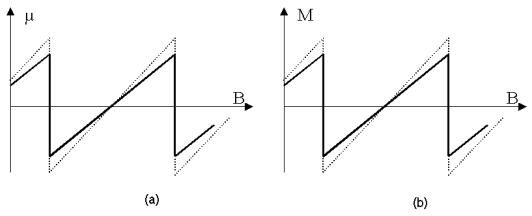

Figure 2.12: (a) The effect of LL broadening on chemical potential and (b) magnetization oscillations. The dotted lines give the chemical potential (in (a)) and the magnetization (in (b)) for sharp LLs while the solid lines correspond to rectangular-broadened LLs.

2.2 2D magnetization oscillations at finite temperature

The magnetization at zero temperature is given by formula (2.2) and is plotted in figs. 2.11 (b) and 2.12 (b). In this section we shall calculate finite-temperature magnetization. The chemical potential at finite temperature has already been calculated in Sec. 2.1.2. In this section we use a similar calculation procedure. The magnetization is a thermodynamic quantity and, hence, can be found from the thermodynamic potential.

2.2.1 Thermodynamic potentials

Here we remind the definitions of a number of thermodynamic potentials, [1, 20] which will be used in following sections:

The Helmholtz free energy is

$$F = U - TS,$$

where U is the internal energy,

$$dU = TdS + \mu dN - MdB,$$

T is temperature, S is the entropy of a system and μ is the chemical potential. The differential relationship reads

$$\begin{aligned} dF &= \mu dN - MdB - \delta dT \\ &\Rightarrow \quad M = -\left(\frac{\partial F}{\partial B}\right)_{V,T,N}. \end{aligned} \tag{2.9}$$

The Gibbs thermodynamic potential Ω is connected with the Helmholz free energy F by the relation

$$\Omega = F - N\mu,$$

and in differential form

$$\begin{aligned} d\Omega &= -MdB - SdT - Nd\mu \\ &\Rightarrow \quad M = -\left(\frac{\partial \Omega}{\partial B}\right)_{V,T,\mu}. \end{aligned} \tag{2.10}$$

Although formulas (2.9) and (2.10) determine the magnetization only at constant electron density and at fixed chemical potential, respectively, each of these formulas can be used to determine the magnetization in both these limits. For example, to obtain the magnetization at a constant particle density from formula (2.10) one should substitute the explicit dependence of chemical potential on magnetic field $\mu(B,N)$ into the final expression for magnetization after differentiating over B in (2.10). This can be easily verified. The magnetization oscillations at constant electron density $N = const$ are given by

$$\begin{aligned} M &= -\left(\frac{\partial F(B,N)}{\partial B}\right)_{N=const} = -\frac{d(\Omega(\mu(B,N),B) + N\mu(B,N))}{dB} \mid_{N=const} = \\ &= -\frac{\partial \Omega(\mu,B)}{\partial B} \mid_{\mu=const} - \left(\frac{\partial \Omega(\mu,B)}{\partial \mu} + N\right)\frac{d\mu(B,N)}{dB} \mid_{N=const} = \end{aligned}$$

$$= -\frac{\partial\,\Omega(\mu,B)}{\partial B}\mid_{\mu,N=const}\,. \tag{2.11}$$

For small magnetization M(B) values, the difference between magnetic field intensity H and induction B, given by

$$B = H + 4\pi M(B)$$

is negligible, and we will use H instead of B in all cases when this will not lead to a qualitative difference. Only when the magnetization oscillations become very strong ($dM/dB > 1/4\pi$) the difference between H and B may result in spontaneous symmetry breaking and the formation of Condon domains [48].

In what follows we develop a calculational scheme (based on the reference [15]) for the determination of magnetic field and temperature dependence of chemical potential in 2D electron gas in quantizing magnetic field.

In the case of sharp (δ - function) Landau levels the thermodynamical potential $\Omega(B)$ can be written in the form

$$\Omega(B) = k_B T g(B) \sum_{n=0}^{\infty} \ln(1 - f_n) \tag{2.12}$$

where

$$f_n = \frac{1}{1 + exp\left(\frac{\hbar\omega_c(n+\frac{1}{2})-\mu(B)}{k_B T}\right)} \tag{2.13}$$

is the Fermi distribution and $g(B)\equiv B/\Phi_o$ is the degeneracy of the Landau level.

For the calculation of $\Omega(B)$ we employ here the approximation, similar to the one used previously for the calculation of magnetic field and temperature dependence of chemical potential.

Let n_F be the highest occupied Landau level, so that $\hbar\omega_c(n_F - 1/2) < \mu < \hbar\omega_c(n_F + 1/2)$. The Fermi distribution f_n in all the terms of the sum in Eq.(2.12), up to $n = n_F - 2$, can be replaced by unity with an exponential accuracy: $e^{-\alpha} << 1$. In this approximation we arrive at the following expression for the thermodynamic potential:

$$\begin{aligned}\Omega(B) \;\simeq\; & -g(B)[\mu(B)n_F - \hbar\omega_c\frac{n_F^2+1}{2} \\ & +k_B T \ln\left(2\cosh x_{nF} + 2\cosh\alpha\right)],\end{aligned} \tag{2.14}$$

where $x_n = \left(n\hbar\omega_c - \mu\right)/k_B T$.

2.2.2 The magnetization

Differentiating the thermodynamic potential, Eq. (2.14), with respect to magnetic field and substituting the obtained expression for $\mu(B)$, we get an analytical expression for the magnetization of 2DEG+B at finite temperature [15]

$$\begin{aligned} M(B) &= -\frac{\partial F(B)}{\partial B} = \frac{2}{\phi_0}[n_F\mu(B) + \\ &\quad +\hbar\omega_c\left[n_F + \frac{sinh\alpha}{2sinh(x_F)}\right] - \hbar\omega_c(n_F^2+1) + \\ &+ \quad k_BTln[2cosh(x_F) + 2cosh\alpha]] \end{aligned} \tag{2.15}$$

This function is plotted in Fig. 2.13.

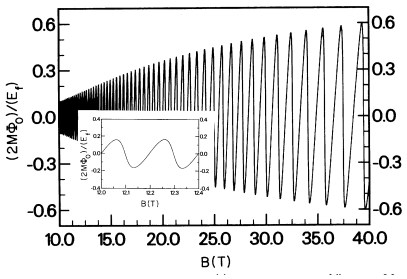

Figure 2.13: The magnetization of 2D electron gas at finite temperature without spin-splitting and with sharp LLs.

2.2.3 The envelope of magnetization oscillations

In order to guide an experimental study of dHvA effect in 2DEG, one should obtain an analytical expression for the envelope of magnetization oscillations, i.e. the 2D analog of the LK formula.

The maxima (minima) of magnetization, can be obtained from the Eq.(2.15) by equating to zero the derivative

$$\frac{\partial M}{\partial B}\Big|_{B_{extr}} = 0. \tag{2.16}$$

This equation gives

$$B_{extr} = B^*\left[1 \mp \frac{1}{2\alpha^*\left(n_F \pm 1\right)}\right]. \tag{2.17}$$

Keeping in mind that

$$\frac{1}{2\alpha^* (n_F \pm 1)} \ll 1$$

we substitute B_{extr} , defined by Eq.(2.17), into Eq.(2.15) and obtain the analytical behavior of the magnetization amplitude [17]:

$$M_{extr} \simeq \pm \frac{E_F}{\phi_o} \left[1 - \frac{1}{\alpha^*} \ln (2\alpha^*) - \frac{1}{\alpha^*} \right]. \tag{2.18}$$

This function is plotted in Fig. 2.16 (graph (b)) where it is compared with the Lifshitz-Kosevich amplitude and the quasi-2D formula (see next section).

2.2.4 Susceptibility

The saw tooth form of magnetization of the two-dimensional electron gas in a magnetic field (see Sec. 2.0.1) results in a constant (between the adjacent values B^*) orbital susceptibility: $\chi_{orb} = dM(B)/dB$. Between the two adjacent Landau levels the susceptibility at $T = 0$ should take infinite negative values, Fig. 2.14. Differentiating (2.2) with respect to magnetic field we find that at zero temperature and sharp LLs the susceptibility is

$$\chi_{orb} = \frac{\hbar\omega_c n_F (n_F + 1)}{B\Phi_0}, \;\; B \neq B^*.$$

Since $n_F = Int[E_F/\hbar\omega_c]$, the step values of susceptibility decrease with increasing magnetic field as $\sim 1/B^2$. At $B = B^*$, $\chi_{orb} = -\infty$ (Fig.2.14). Finite temperature smooths out this unphysical "jumps" and results in exponentially ($exp\frac{\hbar\omega_c}{k_B T}$) sharp spikes, [15].

2.3 Finite k_z-dispersion and quasi-two-dimensional dHvA effect

In many layered compounds, such as heterostructures and organic metals, electrons have a small probability to jump from one layer to another. This results in a finite k_z dispersion of electrons that in the tight binding approximation is given by the formula $E_z(k_z) = 2t \cos(k_z d)$ where $t \ll \epsilon_F$ is the interlayer transfer integral. The Fermi surface of the electron gas with this dispersion relation is a warped cylinder (see Fig. 2.15). If this k_z dispersion is quite large, $2t \gg \hbar\omega_c$, the system changes to nearly three-dimensional. Then the Lifshitz-Kosevich formula can be applied. We have two extreme cross sections of the Fermi surface in this case that lead to the two close

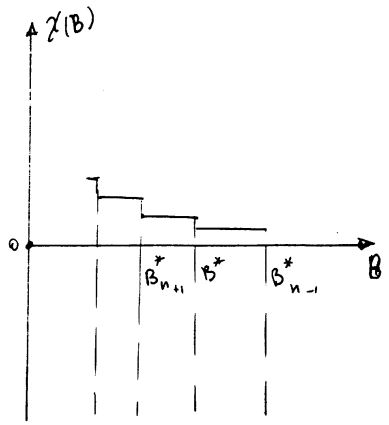

Figure 2.14: The susceptibility of an ideal 2D electron gas at zero temperature

fundamental frequencies in the dHvA oscillations: F and $F + \Delta F$, where $\Delta F = (c\hbar/2\pi e)(A_{\max} - A_{\min}) = F\,(4t/\epsilon_F)$. Since

$$\sin\left(2\pi\frac{F}{B}\right) + \sin\left(2\pi\frac{F+\Delta F}{B}\right) \equiv 2\sin\left(2\pi\frac{F}{B}\right)\cos\left(2\pi\frac{\Delta F}{2B}\right)$$

the two close frequencies lead to beats of magnetic quantum oscillations (see, e.g. Fig. 4.2). From the beat frequency one can readily evaluate the warping of the Fermi surface and the interlayer transfer integral.

In this section we consider the opposite limit of $2t < \hbar\omega_c$ (the intermediate limit will be considered in the next chapter). If one assumes that the magnetic field does not alter such k_z dispersion (at least for the magnetic field normal to layers), then one can perform an analytical calculation of the magnetization envelope in the limit of weak warping $W \equiv 4t < \hbar\omega_c$. This calculation was performed by Grigoriev and Vagner [35]. As any other generalization, this one requires some more calculations. These calculations follow the algorithm presented above (in Sec. 2.1.2 and 2.2) to calculate magnetization at finite temperature and sharp LLs in pure 2D case. These calculations are placed in Appendix C. The reader who does not want to follow these calculations but only wants to understand the physics may jump directly to the final result (formulas (2.19) and (2.21)) and its discussion, fig. 2.16.

The calculation (Appendix C) gives the following answer for the envelope

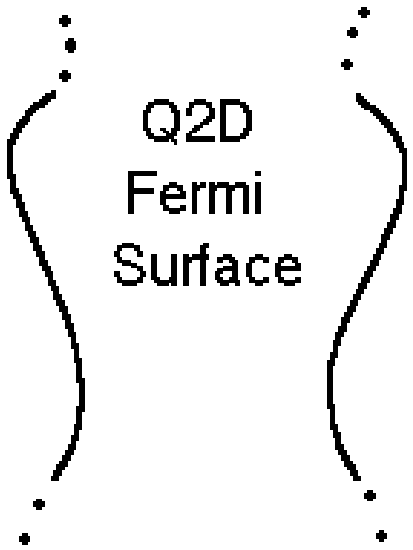

Figure 2.15: A quasi-two-dimensional Fermi surface has the shape of warped cylinder.

of magnetization oscillations:

$$M_{\pm} = \pm \frac{SE_F}{\Phi_0} \left\{ \frac{1}{\alpha} \mathrm{arsh} \left(\frac{e^{\alpha}}{4\alpha I_0(\frac{W}{2kT})} \frac{n_F}{n_F + 3/2} \right) - \frac{1}{\alpha} \frac{n_F + 1}{n_F + 3/2} \right\}. \qquad (2.19)$$

In the limit of very small warping ($W/2kT \ll 1$) and $n_F \gg 1$ this formula coincides with the previous one obtained for the ideal two-dimensional case [17],

$$M_{\pm} = \pm \frac{SE_F}{\Phi_0} \left[1 - \frac{1}{\alpha} \ln(2\alpha) - \frac{1}{\alpha} \right] , \qquad (2.20)$$

which is valid when the number n_F of filled LLs is large.

In the inverse case of large warping ($W/2kT \gg 1$) formula (7.22) becomes:

$$M_{\pm} = \pm \frac{SE_F}{\Phi_0} \left[1 - \frac{W}{\hbar\omega_c} + \frac{1}{\alpha} \ln \left(\frac{\sqrt{kT \cdot \pi W}}{\hbar\omega_c} \right) - \frac{1}{\alpha} \right]. \qquad (2.21)$$

This formula differs substantially from the ideal-2D one, (Eq. 2.20). The three envelopes of magnetization oscillations obtained using the L-K formula (1.13), the ideal 2D formula (Eq. 2.20) and the new formula (2.19) are shown in fig. 2.16. The L-K formula is valid only at $\hbar\omega_c < W$ and is plotted on the

graph only within this interval. One can see that the 2D formula (2.20) does not fit in the L-K formula as the cyclotron energy $\hbar\omega_c$ becomes comparable to the warping W of the Fermi surface while the new formula (2.19) obtained at finite warping W describes this crossover properly.

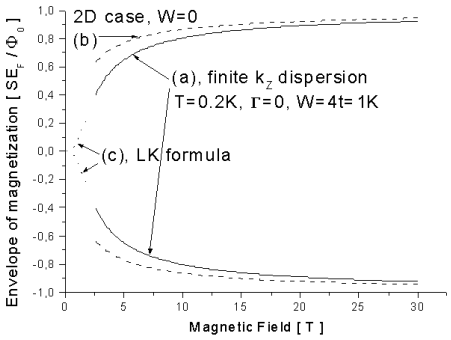

Figure 2.16: Three envelopes of magnetization oscillations obtained using: (a) formula (2.19) with finite k_z dispersion; (b) the ideal 2D formula (eq. 2.20); and (c) the L-K formula (1.13).

Chapter 3

The dHvA effect under more realistic conditions

In this chapter we shall consider the dHvA effect under more general conditions closer to those of real experiments. We will use two different methods – direct summation over LLs that works well when temperature is low ($T \ll \hbar\omega_c$) and the harmonic expansion that is applicable at arbitrary temperatures. Using the first method (Sec.3.1) we shall find the explicit relation between the shape of LLs and the magnetization oscillations that allows us to extract the DoS distribution from the low-temperature experimental data on the dHvA effect and to test the one-particle approximation. Then the envelopes of the magnetization oscillations at finite LL broadening and finite temperature are calculated for two different shapes of LLs. The envelopes of magnetization oscillations are shown to be strongly dependent on the shape of the LLs. The second method (Sec. 3.2) gives a good quantitative description of the magnetization and chemical potential oscillations under general conditions. The results of this section are more useful to describe the dHvA effect in different quasi-2D compounds because the formula for magnetization oscillations derived in this section is simpler and more general for the practical purpose of processing of the experimental data. Thus, this formula is valid at arbitrary temperature and LL width, arbitrary value of warping of the Fermi surface and spin splitting. Moreover, it takes into account the chemical potential oscillations at arbitrary electron reservoir existing in strongly anisotropic organic metals due to open sheets of the Fermi surface. Nevertheless, the results of the section 3.1 are also interesting because they raise important general questions such as the shape of the Landau levels and the role of the electron-electron interactions.

3.1 Low-temperature limit; direct summation over LLs

In this section we derive general formulas that describe magnetization oscillations provided the DoS distribution $\rho(E)$ is given. We consider the most common case of constant electron density. Any finite electron reservoirs (like those in the organic metals due to open sheets of Fermi surface) are included in the function $\rho(E)$. The electron density will not be constant only as a result of the giant magnetostriction that was observed in some materials [31] with high electron density and huge magnetization oscillations. It takes place when an increase in the sample volume is more favorable energy-wise than the corresponding changes of the chemical potential. In organic metals or in heterostructures this giant magnetostriction does not occur because electron density is not large enough. As any generalization, this chapter contains more mathematics than the previous almost introductory chapter. However, we invariably focus on the physics of the phenomena.

3.1.1 Magnetization at arbitrary density of states

In this section we derive formulas for magnetization without specifying the shape of LLs. We assume the one-particle approximation to be valid; this means that the system consists of a set of independent electron-type quasiparticles with concentration equal to the concentration of real electrons. Then the total density of electron states in magnetic field may be written in the form

$$\rho(\varepsilon, B) = \frac{2B}{\Phi_0} \sum_{n=0}^{\infty} D_n(\varepsilon - \hbar\omega_c(n + 1/2)) + \rho_R(\varepsilon) \tag{3.1}$$

where $\Phi_0 = 2\pi\hbar c/e$ is the flux quantum. The function $D_n(\varepsilon)$ is normalized to unity and gives the shape of the n -th LL with some spin-splitting and possible k_z-dispersion.

We shall consider the limit where the Fermi energy ϵ_F is much greater than the LL separation $\hbar\omega_c$. Then the number of occupied LLs $n_F \equiv [\epsilon_F/\hbar\omega_c] \gg 1$ (square brackets here mean the integer part of a number). As the LL number n_F at the FS is changed by unity, the function $D_{n_F}(E)$ does not change substantially (the change has the smallness $\sim \hbar\omega_c/\epsilon_F$). We shall study the behavior of magnetization on one dHvA period. Hence, in the lowest order on $\hbar\omega_c/\epsilon_F$ one can neglect the changes of $D_{n_F}(E)$ as well as the change of the reservoir DoS $\rho_R(\mu)$ where μ is the chemical potential which oscillates with the amplitude $|\tilde{\mu}| < \hbar\omega_c/2$ as the magnetic field is swept. Then the DoS

takes the form

$$\rho(\varepsilon, B) = g(B) \sum_{n=0}^{\infty} D_1 \left(\varepsilon - \hbar\omega_c (n + \frac{1}{2}) \right) \tag{3.2}$$

where the LL degeneracy $g(B) = 2B/\Phi_0 + n_R \cdot \hbar\omega_c$ includes two spin polarizations and constant reservoir density of states $n_R = const$. We take the same $g(B)$ for all LLs since only a few LLs near FS are important for the dHvA effect in quasi-2D metals. For the dHvA effect the DoS only near FS is important. It can be written as

$$\rho(\varepsilon, B) = g(B) D \left(\varepsilon - \hbar\omega_c (n_F + \frac{1}{2}) \right) \ , \tag{3.3}$$

where the DoS function $D(E)$ is periodic, $D(E + \hbar\omega_c) = D(E)$, and normalized to unity

$$\int_{-\hbar\omega_c/2}^{\hbar\omega_c/2} D(E) dE = 1 \tag{3.4}$$

Writing formula (3.1) we assumed that the LL broadening due to impurities and finite k_z dispersion is of the order of $\hbar\omega$ and much less than the Fermi energy. For the dHvA effect only the DoS near FS is important. Hence, without less of generality one can extend formula (3.1) on the interval $\varepsilon \in [0, \infty)$.

To calculate magnetization we need first to calculate chemical potential. It is given by the equation

$$N = \int \frac{\rho(\varepsilon, B) d\varepsilon}{1 + \exp\left(\frac{\varepsilon - \mu}{T}\right)}. \tag{3.5}$$

It is convenient to measure energy and chemical potential off the last occupied LL:

$$\delta\mu \equiv \mu - \hbar\omega_c (n_F + 1/2) \ ; \ E \equiv \varepsilon - \hbar\omega_c (n_F + 1/2) \tag{3.6}$$

where $n_F \equiv \text{Int}[N/g] = \text{Int}[E_F/\hbar\omega_c]$ is the number of completely filled LLs; n_F is an integer and jumps by unity once on each dHvA period.

Now we apply the direct summation over the LLs. At $T \ll \hbar\omega_c$ only three LLs near FS produce the temperature-dependent contribution to the oscillations because the contribution from other LLs is smaller by a factor $\exp^n(-\hbar\omega_c/T)$. The equation (3.5) then simplifies to

$$\tilde{n} + 1 = \int_{-3\hbar\omega_c/2}^{3\hbar\omega_c/2} \frac{D(E) \ dE}{1 + \exp\left(\frac{E - \delta\mu}{T}\right)} \tag{3.7}$$

where $\tilde{n} \equiv N/g - n_F = F/B - n_F$ is the filling factor of the last occupied LL, N is the area electron density, $F = const$ is the dHvA frequency. $\tilde{n}(B)$ is an oscillating function of the magnetic field. On each dHvA period it monotonically decreases from 1 to 0 with increasing magnetic field.

Now we have to calculate thermodynamic potential. By definition, in one particle approximation it is given by (1.20)

$$\Omega(\mu, B) = -k_B T \int d\varepsilon \rho(\varepsilon, B) \ln \left(1 + \exp \frac{\mu - \varepsilon}{k_B T}\right) ,$$

where the density of states is given by (3.1). As in the derivation of (3.7) we calculate the temperature-dependent contribution only from three LLs near FS. Actually one can retain only one LL because the function $D(E)$ is periodic, but now the derivation is more general. The expression for the thermodynamic potential becomes

$$\Omega = -Tg \sum_{n=0}^{n_F-2} \frac{\mu - \hbar\omega_c(n+1/2)}{T} -$$

$$-Tg \int_{-3\hbar\omega_c/2}^{3\hbar\omega_c/2} dE D(E) \ln \left(1 + \exp \frac{\delta\mu - E}{T}\right) .$$

The summation in the first term is easy and gives

$$\Omega(\mu, B) = \frac{g\hbar\omega_c(n_F - 1)^2}{2} - g\mu(n_F - 1) -$$

$$-Tg \int_{-3\hbar\omega_c/2}^{3\hbar\omega_c/2} dE D(E) \ln \left(1 + \exp \frac{\delta\mu - E}{T}\right) . \qquad (3.8)$$

As has been shown previously (see (2.11)) the magnetization can be found as a derivative $M = -\partial\,\Omega(\mu, B)/\partial B \mid_{\mu, N=const}$. To calculate it one should differentiate all the magnetic field-dependent quantities in this expression. As a result, one obtains a quite huge formula which is useless for the analytical calculations. The formulas greatly simplify in the limit $n_F \gg 1$ (many LLs are occupied); this always takes place in organic metals (where $n_F \sim 300$) and usually in heterostructures. Then one can differentiate only the very large or rapidly oscillating quantities in (3.8) since they give additional factor n_F. We take the function $D(E)$ to be independent of the position of the chemical potential; this is true if the *e*-*e* interactions are neglected. Then in the last line of (3.8) only $\delta\mu \equiv \mu - \hbar\omega_c(n_F + 1/2)$ should be differentiated with respect to B. The procedure of differentiation is straightforward but requires

vigilance. We have

$$M(B) = -\frac{g}{B}\Bigg\{ \left[\hbar\omega_c(n_F-1)-\mu(B)\right](n_F-1)+ \\ +\hbar\omega_c(n_F+1/2)\int_{-3\hbar\omega_c/2}^{3\hbar\omega_c/2}\frac{dED(E)}{1+\exp\frac{E-\delta\mu}{T}}\Bigg\}.$$

Neglecting the difference between n_F-1 and $n_F+1/2$ (it is of the next order on $1/n_F$) and substituting (3.7) we get

$$M(B)=\frac{g}{B}\left[\mu(B)-E_F\right] \tag{3.9}$$

where the Fermi energy is related to the total electron number by the relation $E_F=(N/g)\hbar\omega_c$. Magnetization in the limit $n_F\gg 1$ is thus proportional to the oscillating part of the chemical potential. Using the definitions (3.6) the formula (3.9) may be rewritten as

$$M=-\frac{dF}{dB}\approx C\left[\frac{1}{2}-\tilde{n}+\frac{\delta\mu}{\hbar\omega_c}\right] \tag{3.10}$$

where $\delta\mu$ is the solution of (3.7) and the prefactor is

$$C\equiv\frac{g}{B}\hbar\omega_c n_F\approx\frac{g}{B}E_F=const. \tag{3.11}$$

The first two terms in square brackets in (3.10) give the saw-tooth form of magnetization, and the last term $\delta\mu/\hbar\omega_c$ determines the damping of the oscillations due to finite temperature and LL broadening.

To recapitulate, in this section we have derived equation (3.7) for chemical potential and formulas (3.9) or (3.10) for magnetization at finite temperature and arbitrary DoS distribution. This DoS includes reservoir states, warping of the Fermi surface and impurity scattering. In the next sections we derive the explicit results for magnetization using these formulas.

These results have been obtained in the one-particle approximation because in the thermodynamic potential (1.20) there is no quasi-particle interaction term. All existing theories of the dHvA effect are also based on the one-particle approximation. In the next two sections we use these formulas to obtain more concrete results that allow us to check this approximation from the dHvA measurement on a particular compound. If this approximation works, the obtained formulas are quite useful for the analysis of the dHvA effect. If this approximation turns out to be unapplicable to some compound it would be nice to check this fact.

3.1.2 Relation between the magnetization and the DoS function

Now we derive the relation between the wave form of magnetization $M(B)$ and the DoS distribution $D(E)$, which allows a direct measurement of the function $D(E)$ at different magnetic field and spin-splitting values, provided the temperature smearing is much less than LL broadening. Then a real procedure of extracting of the DoS distribution from the magnetization oscillation is described. Although mathematically this procedure is correct, its physical realization encounters many problems. For example, if the oscillations of chemical potential are very small, the accuracy of obtained value of the nonoscillating part of the DoS (compared to the oscillating part) is very low. This is a consequence of the fact that at constant chemical potential the nonoscillating part of the DoS does not contribute to magnetization oscillations. Another difficulty that the procedure proposed below does not take into account is the giant magnetostriction that takes place at high electron density and reduces the chemical potential oscillations. Hence, this method can be applied only in nearly 2D compounds with not very high electron density. Examples of such a type of compounds where the proposed procedure may be applicable are heterostructures. This procedure may also be applicable to intercalated graphites and to strongly anisotropic (almost 2D) organic metals. Another difficulty concerned with the electron-electron interactions is discussed in the next subsection.

We assume $T \ll \Gamma$, where $\Gamma \sim D(E)/D'(E)$ is the width of LLs. Since we need the function $M(B)$ on one particular dHvA period ($0 < \tilde{n} < 1$), it is convenient to consider magnetization as a function of $\tilde{n} \approx n_F(B_0 - B)/B_0$, such that $\tilde{n}(B_0) = 0$ on this period. Differentiating (3.10) we obtain

$$\frac{dM}{d\tilde{n}} = C\left[-1 + \frac{1}{\hbar\omega_c}\frac{d\delta\mu}{d\tilde{n}}\right]. \tag{3.12}$$

Differentiating equation (3.7) with respect to $\delta\mu$ we get

$$\frac{d\tilde{n}}{d\delta\mu} = \int_{-3\hbar\omega_c/2}^{3\hbar\omega_c/2} \frac{D(E)\ dE}{4T\cosh^2\left(\frac{E-\delta\mu}{2T}\right)}. \tag{3.13}$$

At $T \ll \Gamma$ the important region of integration is $|E - \delta\mu| \sim T$ and the function $D(E)$ can be expanded in Tailor series near this point:

$$\frac{d\tilde{n}}{d\delta\mu} = \int_{-\frac{3\hbar\omega_c}{2}}^{\frac{3\hbar\omega_c}{2}} \frac{D(\delta\mu) + D''(\delta\mu)\frac{(E-\delta\mu)^2}{2} + ..}{4T\cosh^2\left(\frac{E-\delta\mu}{2T}\right)}\, dE. \tag{3.14}$$

All odd terms drop out because the integrand should be a symmetric function of $(E-\delta\mu)$. We shall keep only the T^2 term. The integration can be extended to infinity. After the integration we get

$$\frac{d\tilde{n}}{d\delta\mu} = D(\delta\mu) + T^2 D''(\delta\mu)\frac{\pi^2}{6} + O\left(\left(\frac{T}{\Gamma}\right)^4 \frac{1}{\hbar\omega_c}\right). \tag{3.15}$$

Substituting this into (3.12) we obtain

$$\frac{dM}{d\tilde{n}} = C\left[-1 + \frac{1}{\hbar\omega_c\left(D(\delta\mu) + T^2 D''(\delta\mu)\frac{\pi^2}{6} + O(T^4)\right)}\right]. \tag{3.16}$$

The temperature-dependent terms in (3.16) are small and can be separated by taking measurements at several low temperatures and extrapolating to $T = 0$. One can thus measure the function

$$\frac{dM_{T=0}(\tilde{n})}{d\tilde{n}} = C\left[-1 + \frac{1}{\hbar\omega_c D(\delta\mu)}\right]. \tag{3.17}$$

On the experiment it is very difficult to obtain the proportionality coefficient between the measured signal and magnetization. For this reason we shall look at the constant C as on an unknown factor. We later describe how to obtain it. Now suppose one can measure the ratio

$$R(\tilde{n}) \equiv \frac{M_{T=0}(\tilde{n})}{C} \approx \left[\frac{1}{2} - \tilde{n} + \frac{\delta\mu}{\hbar\omega_c}\right]. \tag{3.18}$$

With this function one can rewrite equation (3.17) as

$$D(\delta\mu(\tilde{n})) = \frac{1}{\hbar\omega_c\left(\frac{dR(\tilde{n})}{d\tilde{n}} + 1\right)} \tag{3.19}$$

The function $D(\delta\mu(\tilde{n}))$ is not $D(\delta\mu) = D(E)$. The dependence $\delta\mu(\tilde{n})$ is simply related to the function $R(\tilde{n})$ since the formula (3.18) can be recast to

$$\delta\mu(\tilde{n}) = \hbar\omega_c\left[\tilde{n} - \frac{1}{2} + R(\tilde{n})\right] \tag{3.20}$$

The DoS distribution $D(E)$ is just the plot of $D(\tilde{n})$ (3.19) as a function of $\delta\mu(\tilde{n})$ (3.20).

Now we need to say how to obtain the constant C by which to divide the measured torque to get the function $R(\tilde{n})$ (3.18). The normalization condition (3.4) does not give this constant since at any C the described

procedure automatically gives normalized DoS distribution. The constant C determines the strength of magnetization and, hence, of the DoS oscillations. The smaller the constant C is taken in (3.18), the larger the resulting oscillations of the DoS function are. There is some critical value C_0 such that if we assume $C < C_0$, we get a singularity in the DoS calculated from (3.19). At $C = C_0$ this singularity is in the middle of a LL. The peak value $D(0)$ of the DoS is indeed large compared with the average DoS $\bar{D} = 1/\hbar\omega_c$ for small LL broadening $\Gamma \ll \hbar\omega_c$. The correct value of the constant C is then close to C_0 which always gives the function $D(E)$ accurately except in the vicinity of the peaks of LLs. We shall use this singularity to obtain a more accurate value of the constant C.

The derivative (3.17) has a sequence of the periodically situated minima that occur on each dHvA period when the chemical potential crosses the position in the middle of a LL ($\delta\mu = 0$). Since $n_F \gg 1$ and magnetization is measured on many dHvA periods, these minima form a smooth function of magnetic field,

$$M'_{min}(B) = C\left[-1 + \frac{1}{\hbar\omega_c D(0)}\right].$$

This function monotonically decreases to some finite limit since $\hbar\omega_c D(0)$ increases with increasing magnetic field. This is because $\hbar\omega_c \sim B$ while the peak value of the DoS $D(0)$ depends very slowly on magnetic field. In the vicinity of the peaks the DoS distribution may be given by only two parameters: the LL width Γ and the peak value $D(0) = 1/\alpha\Gamma$. The width Γ is determined mainly by impurity scattering which is approximately independent of magnetic field. The parameter $\alpha \sim 1$ depends on the DoS distribution but is also almost independent of magnetic field. For Lorentzian shape of LLs, $\alpha = \pi$.

Hence, one can assume $D(0) = 1/\alpha\Gamma = const$ and from the curve of the minimum values of

$$M'_{min}(B) = C\left[-1 + \frac{\alpha\Gamma}{\hbar\omega_c}\right] \tag{3.21}$$

one can easily obtain two unknown constants: $\alpha\Gamma$ and C. This value of the constant C is accurate enough for the calculation of the density of states distribution $D(E)$ (using formulas (3.19) and (3.20)) even in the vicinity of its maxima.

Now we shall see how all this works on practice. We shall analyze the experimental data on the quantum magnetization oscillations in quasi-2D organic compound α-(BEDT-TTF)$_2$KHg(SCN)$_4$ using the method described above. The experiment has been performed by M. Kartsovnik and W. Biberacher (unpublished) at a temperature of $0.4K$. The dHvA frequency in

α-(BEDT-TTF)$_2$KHg(SCN)$_4$ is $F_0 \approx 700T$ but the measurements were performed at a substantial tilt angle of $\theta = 53^\circ$ between the magnetic field and the normal to the conducting planes so that the effective dHvA frequency was $F = 1160T$. Such a big tilt angle of magnetic field may lead to a strong torque interaction that reduces the accuracy of the measurements. We use these results merely to illustrate how the proposed method of extracting of the DoS from the dHvA measurement works in practice.

The measured magnetization curve plotted as a function of the quantity $x \equiv F/B$ is shown in fig. 3.1 (solid line). The experimental data are available only in a narrow region of magnetic field from $22.5T$ to $28T$ because at a field $B \approx 22.5$T some kind of phase transition occurs and the range above $28T$ was not accessible for the experimental equipment. Usually the dHvA measurements in such a small range of magnetic field cannot give much information about the compound. However, we will be able to process these data. The next step is to find the derivative dM/dx which can be easily done (Fig. 3.1, dashed line).

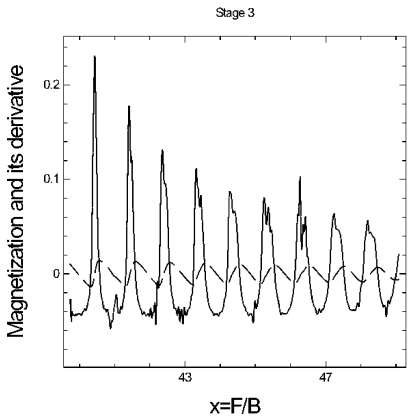

Figure 3.1: The magnetization (dashed curve) and its derivative (solid curve) from the dHvA measurements on α-(BEDT-TTF)$_2$KHg(SCN)$_4$ (see the text)

From this graph one can estimate C using formula (3.21). The minima of

the derivative $M'(x)$ form a curve close to linear which is best approximated by the line $y(x) = 8.9 \cdot 10^{-4}x - 0.079$. The extrapolation of this line to $x = 0$ gives the value $C \approx 0.08$ ($\pm 20\%$). This estimate is not very accurate. Its accuracy is limited mainly by the assumption that the linear fit (3.21) is valid and by the measurement errors. The determination of the constant C seems to be the most delicate point in the proposed method. Fortunately, the final result of the DoS distribution is not extremely sensitive to these errors. Another way to determine the value of the constant C is to calculate it from the formula (3.11). One measures the torque $F_T(B) = (V/d)\, MB \sin\theta$, where V is the volume of a sample, d is the interlayer distance, $M(B)$ is the magnetization given by formula (3.10) and θ is the tilt angle of the magnetic field B. Hence,

$$F_T(B) = C^* \sin\theta \left[\frac{1}{2} - \tilde{n} + \frac{\delta\mu}{\hbar\omega_c}\right]$$

where

$$C^* \approx \frac{2VB}{d\Phi_0} E_F = \frac{2VF_{dHvA}}{d\Phi_0}\hbar\omega_c = \frac{VF_{dHvA}e^2B}{\pi\, d\, m^* c^2},$$

F_{dHvA} is the dHvA frequency and m^* is the effective electron mass that can be obtained from the temperature dependence of harmonic amplitude. The only problem is to estimate the volume of the sample and to obtain the value of amplitude of the torque oscillations. This method of determining the constant C, although possible, also has some difficulties.

One could also obtain the value of C from the temperature dependence of magnetization. But we shall reserve this dependence for checking the one-particle approximation discussed in the next section. The one-particle approximation means also that the DoS function $D(E)$ is independent of the position of the chemical potential $\delta\mu$ and, hence, $D(E)$ does not oscillate as a function of magnetic field.

The next step is to normalize the magnetization and its derivative dividing them by the obtained constant C (formula 3.18). Then we choose one dHvA period on which we want to determine the LL shape and plot the algebraic function (3.19) of the derivative. It is shown in Fig. 3.2. The dashed curve on this figure is already very close to the DoS distribution curve which we will obtain. To finish the procedure one should only rescale the abscissa axis according to Eq. (3.20). If the chemical potential oscillations are negligible compared to $\hbar\omega_c$ this operation is not necessary. The resulting DoS is shown in fig. 3.3. The energy on the x-axis is plotted in units of $\hbar\omega_c$; the graph gives the shape of one LL. On this graph one can see two maxima. These two maxima could appear due to a finite k_z dispersion; their separation then gives the warping W of the Fermi surface which is related to the interlayer transfer integral $t = W/4$. This method to determine the transfer integral

is very useful if $W < \hbar\omega_c$ and the warping W cannot be determined from the beats of the quantum oscillations. According to fig. 3.3 we have an estimate $W \approx 0.25\hbar\omega_c \approx 2K$ which twice exceeds the theoretical estimate for W at this tilt angle. In our case these two maxima on the DoS curve (fig. 3.3) are most probably due to experimental errors that can be cancelled out by averaging of the DoS on different dHvA periods. At a lower value of magnetic field, the DoS over a different dHvA period does not manifest these two maxima (see fig. 3.4). However, the DoS maximum on fig. 3.4 slopes off quite gently that could result from the two maxima smeared out by temperature or Dingle temperature.

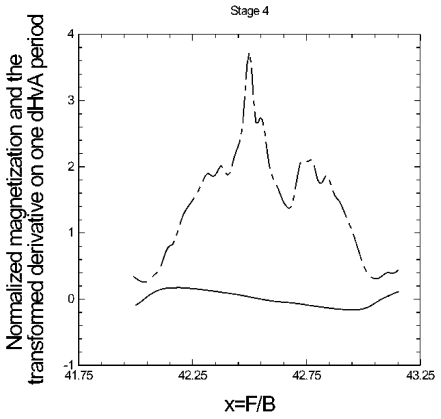

Figure 3.2: The normalized magnetization (solid curve) and its derivative transformed according to eq. 3.19 (dashed curve) on one dHvA period.

The small sharp spikes on the top are, probably, caused by experimental errors that were enhanced in this region by the calculation procedure. The proposed procedure enhances the errors at the top of the maximum of the DoS while reduces them on the tails of the DoS distribution. The width of the maximum is about $2\Gamma \approx 0.3\hbar\omega_c$ that at a given magnetic field of $24T$ and the effective electron mass $m^* \approx 3m_e$ is about $2\Gamma \approx 2.5K$. Actually the DoS on the graphs is additionally smoothed around about $0.4K$ because

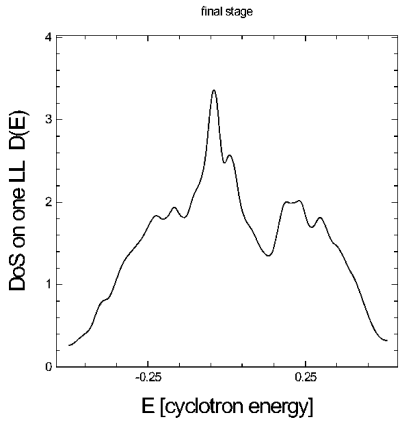

Figure 3.3: The temperature-smeared DoS distribution on one LL at $B \approx 28T$.

we chose the magnetization curve at temperature $T = 0.4K$ and made no extrapolation to $T = 0$. An extrapolation to $T = 0$ may not be warranted by the accuracy of our calculation and of the experimental data. Such an extrapolation would consume additional time and, more importantly, could lead to additional errors. Indeed, our analysis is intended to illustrate how the procedure works and to show what information about the compound can be extracted from the final result. The obtained Landau level width is a result of the combined effect of warping of the FS, impurity scattering, temperature smearing and spin-splitting (the latter also gives two maxima).

To summarize, the suggested procedure of extracting of the DoS distribution from the oscillations of magnetization consists of two steps. The first is to obtain the constant C (that normalizes the measured signal) and the second is to plot $D(E)$ itself. To do this one should measure the torque as a function of $x = F/B$ where $F = const$ and x changes by unity on each dHvA period; then $x = n_F + \tilde{n}$. This function $M(x)$ should be measured at several low temperatures and extrapolated to $T = 0$. As a result one gets an oscillating function $M_0(x)$ with period equal to unity. We also need

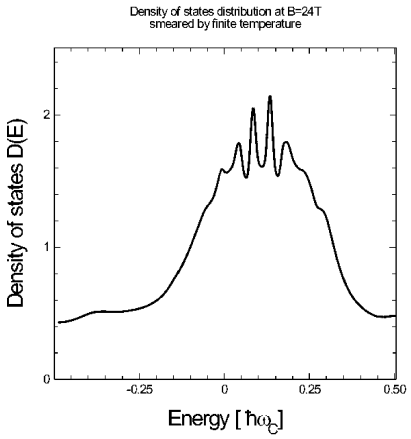

Figure 3.4: The shape of a Landau level that intersects the Fermi surface at $B \approx 24T$.

its derivative $M_0'(x) = dM_0(x)/dx$ which is also an oscillating function. The minima of $M_0'(x)$ form a smooth monotonic function $M_{min}(x)$. Extrapolating this function to $x = 0$ one gets the constant

$$C = \lim_{x \to 0} M_{min}(x)$$

Or one can use formula (3.21) and obtain the constant C from $M_{min}(x)$ more accurately. Substituting the functions $R(x) = M_0(x)/C$ and $R'(x) = M_0'(x)/C$ into (3.19) and (3.20) one can plot (3.19) as a function of (3.20) on one period of oscillations. This plot is the desired DoS distribution at the magnetic field corresponding to the chosen dHvA period.

The described procedure allows one to measure the DoS distribution at the Fermi level for different magnetic field values (because one can obtain $D(E)$ on each dHvA period) and for different spin-splitting energy (because one can tilt the magnetic field with respect to the conducting plane of a sample). This information about the DoS distribution is very important to study the role of different scattering mechanisms in the electron motion at different external parameters. Such information cannot be obtained using the

previous methods of processing the data of dHvA measurements where one assumed some particular shape $D(E)$ and then numerically calculated the magnetization. The results of the calculation (usually only of the envelope) were compared with the measured signal and if the agreement was good enough the chosen function $D(E)$ was taken as a result. Our method is simpler and more accurate.

3.1.3 A test of the one-particle approximation

The procedure described above gives the DoS at the position of the chemical potential while the magnetic field and the chemical potential are varied. In general, this is not the same as fixing the magnetic field and the chemical potential while varying the energy itself because the e-e interactions may create a dimple or a hump at the Fermi level. In our previous analysis we disregarded the quasi-particle interactions and, hence, the dependence of $D(E)$ on the position of the chemical potential. This approximation works when the DoS distribution is determined by one-electron processes. These are the electron scattering on lattice imperfections and inhomogeneities, the finite probability of the interlayer jumping and so on. When many particle effects play an important role (for example, change of the magnetic field drives a sequence of phase transitions as in fractional quantum Hall effect), our previous results are not applicable since we neglected nontrivial many-body effects at the beginning when we wrote formulas (3.5) and (1.20) assuming that the system may be described by the distribution of single fermion states (3.1). Probably, this has a wide application region because usually subtle many-particle effects are damped by impurities, finite k_Z dispersion and other factors, especially when many LLs are occupied. Nevertheless, this assumption has to be checked. This can be done by using the low temperature dependence of the magnetization.

The DoS distribution can thus be described by formulas (3.1) or (3.1) only if the e-e interaction does not play an important role. Otherwise, a hump or a dimple at the Fermi level may appear. Can one detect such a corrugation of the DoS distribution at the position of the chemical potential from the magnetization curve? The answer is yes. This information can be extracted from the temperature-dependent term of the quantity (3.19). At law temperature this temperature-dependent term is approximately equal to $T^2 D''(\delta\mu)\frac{\pi^2}{6}$, which gives the second derivative of the DoS function. If no corrugation of the DoS at the Fermi level takes place and the DoS is given by (3.1), the integral of $D''(\delta\mu)$ over the interval $[0, \hbar\omega_c]$ is zero:

$$\int_{-\hbar\omega_c/2}^{\hbar\omega_c/2} D''(\delta\mu)d\delta\mu = D'(\hbar\omega_c/2) - D'(-\hbar\omega_c/2) = 0. \qquad (3.22)$$

If this integral has a substantial nonzero value, this means that the DoS on the Fermi surface changes due to many-particle effects. If the oscillations of the chemical potential are not very strong the integration over $\delta\mu$ can be replaced by the integral over $\tilde{n}$:

$$\hbar\omega_c \int_0^1 D''(\delta\mu(\tilde{n}))d\tilde{n} = 0. \tag{3.23}$$

At finite temperature equation (3.19) becomes:

$$D(\delta\mu(\tilde{n})) + T^2 D''(\delta\mu)\frac{\pi^2}{6} + O\left(T^4 D^{(\mathrm{IV})}(\delta\mu)\right) = \frac{1}{\hbar\omega_c\left(\frac{dR(\tilde{n})}{d\tilde{n}} + 1\right)} \tag{3.24}$$

where the right-hand part can be measured. Separating the temperature-dependent part (denoted by $[..]_{Tem}$) of (3.24) and substituting it into (3.23) we find that the electron-electron interaction can be neglected only if the dimensionless quantity

$$\int_0^1 \left[\left(\frac{dR(\tilde{n})}{d\tilde{n}} + 1\right)^{-1}\right]_{Tem} d\tilde{n} \approx 0 \tag{3.25}$$

within the experimental accuracy. If this quantity is of the order of unity, the e-e interaction is quite strong and should not be neglected in the calculations of magnetic quantum oscillations.

If the oscillations of chemical potential are strong, formula (3.22) instead of (3.23) must be used. Differentiating formula (3.18) we find

$$\frac{d\mu(\tilde{n})}{d\tilde{n}} = \hbar\omega_c\left(\frac{dR(\tilde{n})}{d\tilde{n}} + 1\right).$$

Substituting this into (3.22) we obtain that in the case of strong chemical potential oscillations the condition (3.25) should be modified as

$$\int_0^1 \left[\left(\frac{dR(\tilde{n})}{d\tilde{n}} + 1\right)^{-1}\right]_{Tem} \left(\frac{dR(\tilde{n})}{d\tilde{n}} + 1\right) d\tilde{n} \approx 0. \tag{3.26}$$

If chemical potential oscillations are small, the term $R'(\tilde{n}) \ll 1$ and, hence, formula (3.26) coincides with (3.25), and the modification (3.26) is not needed.

Direct experimental data about the role of e-e interactions in 2D compounds in magnetic field could answer many theoretical question and verify (or disprove) different theories on this subject. Hence, the proposed method of the test of the role of many-particle interactions in 2D or quasi-2D electron gas using the dHvA method is important not only for the processing

of experimental data but also for the theoretical study of different electronic properties of 2D compounds. This procedure requires a careful separation of the temperature-dependent component of the magnetization at temperature $T \ll \hbar\omega_c$ as a function of magnetic field. This is possible but requires time and accuracy.

3.1.4 The envelope of magnetization oscillations

We can also calculate the envelope of magnetization oscillations for several simple DoS distributions in the limit $\hbar\omega_c \gg \Gamma \gg T$. At low temperature the envelope turns out to depend strongly on the shape of LLs while the additional constant contribution to the DoS from other parts of the FS leaves the envelope almost unchanged. The envelope of magnetization oscillations does not give as much information about the electronic structure of the compounds as the DoS distribution does. Nevertheless it is still useful for the analysis of the dHvA effect and is quite easy for measurement.

To calculate the envelope of magnetization oscillations, we take the total density of states function in the form

$$D(E) = (1-\kappa)\frac{D_0\left(E/\Gamma\right)}{\Gamma} + \frac{\kappa}{\hbar\omega_c} \tag{3.27}$$

where Γ is the width of LLs, $\kappa < 0$ is a number that determines the constant part of the DoS and

$$\int_{-\hbar\omega_c/2}^{\hbar\omega_c/2} D_0\left(\frac{E}{\Gamma}\right)\frac{dE}{\Gamma} = 1$$

converges rapidly. Then the function $D(E)$ is normalized to unity. The degeneracy $g(B)$ of LLs should be renormalized to include all additional parts of the FS.

How does the envelope of magnetization depend on κ? The answer is that in the limit $n_F \gg 1$ the constant part of DoS affects the shape of magnetization oscillations only but not their envelope. This is different from the case of $\mu = const$ where the constant part of DoS does not change either the envelope or the shape of the oscillations.

To show this we first substitute (3.27) into (3.7). The LLs just above and just below the last occupied LL contribute only when $|\delta\mu| \approx \hbar\omega_c/2$. As we shall see, if $T, \Gamma \ll \hbar\omega_c$, the extrema of magnetization take place when $|\delta\mu| \ll \hbar\omega_c/2$. Hence, the regions where $(\hbar\omega_c/2 - |\delta\mu|) \sim T \ll \hbar\omega_c/2$ are not important for the envelope of magnetization, and the T- and Γ-dependent

contribution is given by only one LL. Then equation (3.7) becomes

$$\tilde{n} = \int_{-\hbar\omega_c/2}^{\hbar\omega_c/2} \frac{D(E)\ dE}{1+\exp\left(\frac{E-\delta\mu}{T}\right)}. \tag{3.28}$$

Using the integral

$$\int_{-\hbar\omega_c/2}^{\hbar\omega_c/2} \frac{dE}{1+\exp\left(\frac{E-\delta\mu}{T}\right)} \approx \frac{\hbar\omega_c}{2} + \delta\mu$$

and substituting (3.27) into equation (3.28) we get

$$\tilde{n} = \int_{-\hbar\omega_c/2}^{\hbar\omega_c/2} \frac{(1-\kappa)D_0(E)\ dE}{1+\exp\left(\frac{E-\delta\mu}{T}\right)} + \kappa\left(\frac{1}{2} + \frac{\delta\mu}{\hbar\omega_c}\right). \tag{3.29}$$

Substituting this into expression (3.10) for the magnetization we obtain

$$M = \frac{g*}{B}\hbar\omega_c n_F\left[\frac{1}{2} + \frac{\delta\mu}{\hbar\omega_c} - \tilde{n}_0\right] \tag{3.30}$$

where $g* = (1-\kappa)g$ is the LL degeneracy of only the oscillating part of the DoS and

$$\tilde{n}_0(\delta\mu) = \int_{-\hbar\omega_c/2}^{\hbar\omega_c/2} \frac{D_0(E)\ dE}{1+\exp\left(\frac{E-\delta\mu}{T}\right)}. \tag{3.31}$$

So, if one adds a constant reservoir density of states to a 2D electron system, this influences the magnetization oscillations via only the change of $\delta\mu(B)$ in formula (3.30).

The magnetization on each dHvA period may be considered as a function of $\delta\mu:\ M(B) = M(\delta\mu)$. The envelope of magnetization oscillations is then given by

$$M_{\pm}(B) = M(\delta\mu_{ex}(B)) = C^*\left[\frac{1}{2} + \frac{\delta\mu_{ex}}{\hbar\omega_c} - \tilde{n}_0(\delta\mu_{ex})\right] \tag{3.32}$$

where $C^* = g^*\hbar\omega_c n_F/B$ and the extremum values $\delta\mu_{ex}(B)$ at which the magnetization has maxima or minima are given by the equation

$$\frac{dM}{dB} = 0 \Leftrightarrow \frac{dM(\delta\mu)}{d\delta\mu} = C^*\left(\frac{1}{\hbar\omega_c} - \frac{d\tilde{n}}{d\delta\mu}\right) = 0. \tag{3.33}$$

After accounting for (3.29) this equation becomes

$$\frac{d\tilde{n}}{d\delta\mu} = \int_{-\hbar\omega_c/2}^{\hbar\omega_c/2} \frac{(1-\kappa)D_0(E)\ dE}{4T\cosh^2\left(\frac{E-\delta\mu_{ex}}{2T}\right)} + \frac{\kappa}{\hbar\omega_c} = \frac{1}{\hbar\omega_c} \Rightarrow$$

$$\int_{-\hbar\omega_c/2}^{\hbar\omega_c/2} \frac{D_0(E)\ dE}{4T\cosh^2\left(\frac{E-\delta\mu_{ex}}{2T}\right)} = \frac{1}{\hbar\omega_c}. \tag{3.34}$$

Equation (3.34) for $\delta\mu_{ex}$ is independent of κ and so is the envelope of magnetization given by (3.32).

The function $\delta\mu(B)$ is monotonic on each dHvA period and different on different dHvA periods. Moreover, if $D(E)$ is a symmetric function then $\delta\mu$ is an antisymmetric function of $(\tilde{n} - 1/2)$ that can be obtained from (3.7) using the identity

$$\frac{1}{1+\exp\frac{E-\delta\mu}{T}} = \frac{1}{2} - \frac{1}{2}\frac{\sinh\frac{E}{T} - \sinh\frac{\delta\mu}{T}}{\cosh\frac{E}{T} + \cosh\frac{\delta\mu}{T}}.$$

Magnetization (3.10) is then also an antisymmetric function of $(\tilde{n} - 1/2)$.

In the limit $T \ll \Gamma$ the function $D_0(E)$ may be expanded in the Taylor series as has been done in (3.14). If we retain only $\sim T^2$ terms the equation (3.34) becomes

$$D_0(\delta\mu_{ex}) + T^2 D_0''(\delta\mu_{ex})\frac{\pi^2}{6} = \frac{1}{\hbar\omega_c}. \tag{3.35}$$

Formula(3.31) can also be simplified. Integrating by parts and expanding up to the terms $\sim T^2$ we get

$$\tilde{n}_0 = G_0(\delta\mu) + T^2 D_0'(\delta\mu)\frac{\pi^2}{6} \tag{3.36}$$

where we have introduced the function

$$G_0(E) = \int_{-\hbar\omega_c/2}^{E} D_0(E')dE'. \tag{3.37}$$

The function $G_0(E)$ is dimensionless and changes in the range $[0; 1]$. From the equation (3.34) one can immediately say that if $D_0(x)$ has the exponentially falling tails, then $\delta\mu_{ex} \sim \pm\Gamma\ln(\hbar\omega_c/\Gamma)$. If $D_0(x)$ falls off as $x^{-\gamma}$, then $\delta\mu_{ex} \sim \Gamma(\hbar\omega_c/\Gamma)^{1/\gamma}$. This determines the behavior of the envelope (3.32). Now we shall consider in detail two different functions $D_0(x)$.

Exponentially decaying $D(x)$

There are many symmetric exponentially decaying functions that are eligible to be a density of states function $D_0(E)$. They all lead to the expressions for the envelope of magnetization oscillations. For example, we take

$$D_0(E) = \frac{1}{4\Gamma\cosh^2\left(\frac{E}{2\Gamma}\right)}. \tag{3.38}$$

Now equation (3.34) possesses the symmetry $T \leftrightarrow \Gamma$ if T or $\Gamma \ll \hbar\omega_c$ (the last condition is needed for the limits of integration in (3.34) can be extended to infinity) and one can easily obtain the limit $\Gamma \ll T$ from the limit $T \ll \Gamma$.

Equation (3.35) can be solved by the iteration procedure with a small parameter T^2/Γ^2. In zeroth approximation

$$D_0(\delta\mu_{ex}^0) = \frac{1}{4\Gamma\cosh^2\left(\frac{\delta\mu_{ex}^0}{2\Gamma}\right)} = \frac{1}{\hbar\omega_c}.$$

Since the magnetization (3.10) is an antisymmetric function of $\delta\mu$ we shall consider only one (negative) root of this equation

$$\delta\mu_{ex}^0 = -2\Gamma arccosh\sqrt{\frac{\hbar\omega_c}{4\Gamma}} \approx -\Gamma\ln\left(\frac{\hbar\omega_c}{\Gamma}\right). \tag{3.39}$$

From equation (3.36) we get

$$\tilde{n}_0(\delta\mu_{ex}^0) \approx \frac{1}{1+\frac{\hbar\omega_c}{\Gamma}}. \tag{3.40}$$

Substituting (3.39) and (3.40) into (3.32) we get the envelope in zeroth approximation

$$M_{\pm}^0 = \pm C^*\left[\frac{1}{2} - \frac{\Gamma}{\hbar\omega_c}\ln\left(\frac{\hbar\omega_c}{\Gamma}\right) - \frac{\Gamma}{\hbar\omega_c}\right]. \tag{3.41}$$

If one makes the replacement $\Gamma \to T$, this result coincides with the result of Vagner et al. [17] obtained for the case of $\Gamma = 0$ and finite temperature. It is not surprising because of the mentioned above symmetry $\Gamma \leftrightarrow T$.

One can easily obtain the first temperature correction to the envelope (3.41). In the first approximation equation (3.35) becomes

$$D_0(\delta\mu_{ex}) + T^2 D_0''(\delta\mu_{ex}^0)\frac{\pi^2}{6} = \frac{1}{\hbar\omega_c}. \tag{3.42}$$

The correction to the chemical potential is

$$\Delta_T\mu_{ex} \equiv \delta\mu_{ex}^1 - \delta\mu_{ex}^0 = \frac{T^2 D_0''(\delta\mu_{ex}^0)\frac{\pi^2}{6}}{D_0'(\delta\mu_{ex}^0)}. \tag{3.43}$$

This correction $\Delta_T\mu$ is proportional to T^2. The first correction to the magnetization $\Delta M_+ \sim (\Delta_T\mu)^2$ because according to equation (3.33) $M'(\delta\mu_{ex}) = 0$ and the correction to the envelope of magnetization is

$$\Delta M_+ = M(\delta\mu_{ex}^1) - M(\delta\mu_{ex}^0) = M'(\delta\mu_{ex}^0)\,\Delta_T\mu_{ex} + \frac{d^2M(\delta\mu_{ex}^0)}{d(\delta\mu_{ex}^0)^2}\frac{(\Delta_T\mu_{ex})^2}{2} =$$

$$= -\frac{d^2M(\delta\mu_{ex}^0)}{d(\delta\mu_{ex}^0)^2}\frac{(\Delta_T\mu_{ex})^2}{2} = C^*\frac{d^2\tilde{n}_0(\delta\mu_{ex}^0)}{d(\delta\mu_{ex}^0)^2}\frac{(\Delta_T\mu_{ex})^2}{2}. \tag{3.44}$$

In writing this we used $M'(\delta\mu_{ex}^0) = M'(\delta\mu_{ex}) - M''(\delta\mu_{ex}^0)\Delta_T\mu_{ex}$. From (3.36) we have

$$\tilde{n}_0''(\delta\mu_{ex}^0) \approx D_0'(\delta\mu_{ex}^0). \tag{3.45}$$

In our case (3.38)

$$D_0'(\delta\mu_{ex}^0) = -\frac{\sinh\left(\frac{\delta\mu_{ex}^0}{2\Gamma}\right)}{4\Gamma^2\cosh\left(\frac{\delta\mu_{ex}^0}{2\Gamma}\right)} \approx \frac{1}{\Gamma\hbar\omega_c}\ ,$$

$$D_0''(\delta\mu_{ex}^0) \approx \frac{3}{2\Gamma^2\hbar\omega_c} \quad \text{and} \quad \Delta_T\mu_{ex} = -\frac{T^2}{\Gamma}\frac{\pi^2}{4}.$$

Substituting this into (3.44) and (3.45) and using (3.41) we obtain the envelope in the first approximation:

$$M_\pm^1 = C^*\left[\frac{1}{2} - \frac{\Gamma}{\hbar\omega_c}\ln\left(\frac{\hbar\omega_c}{\Gamma}\right) - \frac{\Gamma}{\hbar\omega_c} - \frac{\Gamma}{\hbar\omega_c}\frac{1}{2}\left(\frac{\pi^2}{4}\right)^2\left(\frac{T}{\Gamma}\right)^4\right]. \tag{3.46}$$

Lorentzian shape of LLs

For the Lorentzian shape of LLs,

$$D_0(E) = \frac{1/\pi\Gamma}{1+(E/\Gamma)^2}, \tag{3.47}$$

we shall do the same steps as for the exponentially decaying $D(E)$. From equation (3.35) in zeroth approximation we obtain

$$\delta\mu_{ex}^0 = \Gamma\sqrt{\frac{\hbar\omega_c}{\pi\Gamma} - 1} \approx \sqrt{\Gamma\hbar\omega_c/\pi} \tag{3.48}$$

and

$$\tilde{n}_0(\delta\mu_{ex}^0) = \frac{1}{\pi}\arctan\left(\frac{\delta\mu_{ex}^0}{\Gamma}\right) + \frac{1}{2}. \tag{3.49}$$

Substituting this into the expression for magnetization (3.32) we get

$$M_\pm^0 = \pm C^*\left[\frac{1}{2} - 2\sqrt{\frac{\Gamma}{\pi\hbar\omega_c}}\right]. \tag{3.50}$$

This is different from (3.41). The envelope is therefore different for different shapes of LLs. The temperature correction is also different.

To obtain the first temperature correction we need

$$D_0'(\delta\mu_{ex}^0) \approx \frac{2}{\hbar\omega_c}\sqrt{\frac{\pi}{\Gamma\hbar\omega_c}} \text{ and } D_0''(\delta\mu_{ex}^0) \approx \frac{6\pi}{\Gamma(\hbar\omega_c)^2}$$

$$\Rightarrow \Delta_T\mu_{ex} = -\frac{\pi^{5/2}T^2}{2\sqrt{\Gamma\hbar\omega_c}}.$$

Substituting this into (3.44) and (3.45) and using (3.50) we get

$$M_\pm^1 = C^* \left[\frac{1}{2} - 2\sqrt{\frac{\Gamma}{\pi\hbar\omega_c}} - 2\sqrt{\frac{\Gamma}{\pi\hbar\omega_c}}\frac{\pi^6T^4}{8\Gamma^2(\hbar\omega_c)^2}\right]. \tag{3.51}$$

Formulas (3.46) and (3.51) have been derived for very special DoS functions (3.38) and (3.47). Hence, these formulas may be not very precise to describe real experiments even at low temperature, because the oscillating part of the real DoS distribution function depends not only on one parameter, namely the width Γ, but also on the LL separation $\hbar\omega_c$ and hence on the magnetic field. Hence, the approximate DoS functions (3.38) and (3.47) may be far from reality. The Lorentzian shape of LLs takes place in 3D metals and corresponds to finite electron scattering time which adds an imaginary part to the electron self-energy. In the two-dimensional case these arguments may not hold. Nevertheless, the Lorentzian shape of LLs even in the 2D case remains interesting. The exponentially decaying $D_0(E)$ does not have such an evident justification but is also possible in 2D compounds. The envelope of magnetization oscillations is very sensitive to the tails of the DoS function $D(E)$ at low temperatures and one should use more realistic (probably magnetic field-dependent) functions $D(E)$ for accurate calculations.

Nevertheless, formulas (3.46) and (3.51) can be used to indicate the qualitative features. They predict, for example, that the first temperature correction to the envelope is proportional to T^4 and that this envelope depends strongly on the shape of LLs at low temperatures.

We can now say also at what conditions the previous results are valid. At $N = const$ and a finite temperature the only results[17], [35] for magnetization and its envelope have been obtained for sharp LLs ($D(E) = \delta(E)$). These formulas have been derived also in the limit $T \ll \hbar\omega_c$. If we assume the shape of LLs to be Lorentzian, these result are valid as long as $\hbar\omega_c \gg T \gg \sqrt{\Gamma\hbar\omega_c}$. This narrow region may not exist at all, which explains why many experimental data cannot be described by these formulas.

3.2 Harmonic expansion of magnetization oscillations

3.2.1 General case

As has been explained before, in two- or quasi-two-dimensional compounds the deviations from the Lifshitz-Kosevich (L-K) formula (1.7) are possible for three reasons: harmonic damping in 2D case is different, impurity scattering may not be described by the usual Dingle law and the chemical potential becomes also an oscillating function of magnetic field. The first problem is important only when the harmonic damping is weak and can be easily solved by using the 2D harmonic expansion (1.24). The second problem concerns an accurate calculation of the density of states (DoS) with electron-electron interactions and impurity scattering. The electron-electron interactions are not very important when many Landau levels are occupied (we consider the case when the Fermi energy ϵ_F is much greater than the Landau level separation and temperature). The impurity scattering in 3D case adds an imaginary part $i\Gamma(B)$ to the electron spectrum which means that an electron may leave its quantum state with probability $w = \Gamma(B)/\pi\hbar$ per second. If one assumes this width $\Gamma(B)$ of energy levels to be independent of magnetic field B he gets the Dingle law of harmonic damping[49]

$$A_l \sim \exp\left(-2\pi l\Gamma/\hbar\omega_c\right)$$

where A_l is the amplitude of the harmonic number l and $\omega_c = eB/m^*c$ is the cyclotron frequency. This Dingle law was proved in many experiments on 3D metals. In 2D case this law may be incorrect and the problem of the DoS distribution in 2D metals has not been solved yet, although much theoretical work was devoted to this subject (see, for example, [51],[52],[53]). The problem is complicated because even an exact calculation of point-like impurity scattering is not enough since long-range impurities (and, probably, electron-electron interactions) are also important in the 2D case[54]. A procedure of extracting the DoS distribution from the dHvA measurements was proposed in Sec. 3.1.2 [55]. In the present section we focus on the third question, and so assume the Dingle law to be valid. In this approximation we consider the influence of the chemical potential oscillations on the harmonic amplitudes of the dHvA oscillations. Since we study the quasi-2D case, the Dingle law is not a bad approximation. We shall show that the oscillations of the chemical potential change substantially the temperature and the Dingle temperature dependence of the harmonic amplitudes even in the limit of strong harmonic damping. Hence, the estimate of the effective electron mass based on the L-K

formula may lead to errors up to 30% . This can be an explanation of the difference between the effective electron masses obtained from the dHvA effect and those obtained from cyclotron resonance measurements (for example, in [56] and [57]). This problem was examined numerically by Harrison et al. [58] at zero warping W of the Fermi surface. In this paper we derive the explicit formulas that describe quantum magnetization oscillations at arbitrary parameters. The electron reservoir is also taken into account. An analytical study of this result is made in some limiting cases. It shows the importance of the oscillations of chemical potential for the harmonic amplitudes.

The energy spectrum of the quasi-two-dimensional electron gas is

$$E_{n,k_z,\sigma} = \hbar\omega_c\,(n+\frac{1}{2}) + \frac{W}{2}\cos(k_z d) + \sigma\mu_e B \tag{3.52}$$

where W is the warping of a quasi-cylindrical Fermi surface. The DoS distribution with impurity scattering may be written as

$$\rho(E,B) = \rho_0(E,B) + \tilde{\rho}(E,B)$$

where the oscillating part of the DoS at $E \gg \hbar\omega_c$ is [37]

$$\tilde{\rho}(E,B) = \frac{4g}{\hbar\omega_c}\sum_{l=1}^{+\infty}(-1)^l \cos\left(\frac{2\pi l E}{\hbar\omega_c}\right) J_0\left(\frac{\pi l W}{\hbar\omega_c}\right) R_S(l) R_D(l). \tag{3.53}$$

In this formula $g = B/\Phi_0$ is the Landau level degeneracy and the factor $J_0\,(\pi l W/\hbar\omega_c)$ comes from the finite warping W of quasi-cylindrical Fermi surface. $J_0(x)$ is the Bessel function of zeroth order. The factor $R_S(l) = \cos\,(2\pi l \mu_e B/\hbar\omega_c) \approx \cos\,(2\pi l m^*/m)$ is due to spin-splitting, m^* and m_0 are the effective and bare electron masses, respectively. The last factor $R_D(l) = \exp\,(-2\pi l\,\Gamma/\hbar\omega_c)$ in (3.53) is the usual Dingle factor. Generally, the Dingle factor $R_D(l)$ may differ from $\exp\,(-2\pi l\,\Gamma/\hbar\omega_c)$. Therefore, later we always write $R_D(l)$.

The non-oscillating part of the DoS is

$$\rho_0(E,B) = \frac{2g}{\hbar\omega_c}(1 + n_R(E))$$

where $n_R(E)$ is the ratio of the reservoir density of states to the average DoS on quasi-2D part of the FS. The reservoir density of states exists in quasi-2D organic metals due to open sheets of the Fermi surface. These quasi-one-dimensional states do not contribute to magnetization oscillations since they form a continuous spectrum.

If the DoS is known one can calculate the thermodynamic potential

$$\Omega(\mu,B,T)=-T\int_0^\infty \rho(E,B)\ln\left[1+\exp\left(\frac{\mu-E}{T}\right)\right]\,dE=\Omega_0(\mu,B,T)+\tilde{\Omega}(\mu,B,T) \tag{3.54}$$

where $\mu(B)$ is the chemical potential and the oscillating part of the thermodynamic potential is[37]

$$\tilde{\Omega}=2gT\sum_{l=1}^{+\infty}\frac{(-1)^l}{l}\cos\left(\frac{2\pi l\mu}{\hbar\omega_c}\right)J_0(\pi l\frac{W}{\hbar\omega_c})R_T(l)R_S(l)R_D(l)$$

where the damping temperature factor is

$$R_T(l)=\frac{\lambda l}{\sinh(\lambda l)}\ ,\ \ \lambda\equiv\frac{2\pi^2k_BT}{\hbar\omega_c}.$$

The total particle number is usually constant:

$$N=-\left(\frac{\partial\Omega(\mu,B,T)}{\partial\mu}\right)_{T,B}=\int_0^\infty\frac{\rho(E,B)}{1+\exp\left(\frac{E-\mu}{T}\right)}\,dE=const. \tag{3.55}$$

This is an equation for the chemical potential as a function of magnetic field. Separating the oscillating part of the DoS and substituting

$$N=\int_0^\infty\frac{\rho_0(E,B)}{1+\exp\left(\frac{E-\varepsilon_F}{T}\right)}\,dE$$

(ε_F is the Fermi energy at zero magnetic field) we get

$$\int_0^\infty\left(\frac{1}{1+\exp\left(\frac{E-\varepsilon_F}{T}\right)}-\frac{1}{1+\exp\left(\frac{E-\mu}{T}\right)}\right)\rho_0(E,B)\,dE=\int_0^\infty\frac{\tilde{\rho}(E,B)}{1+\exp\left(\frac{E-\mu}{T}\right)}\,dE. \tag{3.56}$$

Now we use the fact that the reservoir DoS $n_R(E)$ does not change appreciably on the scale of T or $|\mu-\varepsilon_F|<\hbar\omega_c/2$ (this is true if many LLs are occupied because $n_R(E)$ changes substantially on the scale of the Fermi energy ε_F). Then $n_R(E)\approx n_R(\varepsilon_F)=const\equiv n_R$. The left hand side of equation (3.56) now simplifies and after substitution of (3.53) we get the equation for the oscillating part $\tilde{\mu}(B)$ of the chemical potential:

$$\tilde{\mu}(B)\equiv\mu(B)-\varepsilon_F=\frac{\hbar\omega_c}{\pi(1+n_R(\varepsilon_F))}\times \tag{3.57}$$

$$\times\sum_{l=1}^{+\infty}\frac{(-1)^{l+1}}{l}\sin\left(\frac{2\pi l\,(\varepsilon_F+\tilde{\mu}(B))}{\hbar\omega_c}\right)J_0\left(\frac{\pi l\,W}{\hbar\omega_c}\right)\,R_T(l)R_S(l)R_D(l).$$

This nonlinear equation cannot be solved analytically without using any approximations but it determines the oscillations of the chemical potential at arbitrary parameters (only $\epsilon_F \gg T, \hbar\omega_c$ is assumed).

The magnetization oscillations at constant electron density $N = const$ are given by the same formula as (2.11):

$$M = -\frac{d(\Omega + N\mu)}{dB} \mid_{N=const} = -\frac{\partial \Omega}{\partial B} \mid_{\mu, N=const} -$$

$$-\left(\frac{\partial \Omega}{\partial \mu} \mid_{N,B=const} + N\right) \frac{d\mu}{dB} \mid_{N=const} = -\frac{\partial \Omega}{\partial B} \mid_{\mu, N=const} . \qquad (3.58)$$

The oscillating part of the magnetization is

$$\tilde{M}(B) = -\frac{\partial \tilde{\Omega}}{\partial B} \mid_{\mu, N=const} = \frac{2N_{LL}\varepsilon_F}{\pi B} \sum_{l=1}^{+\infty} \frac{(-1)^{l+1}}{l} R_T(l) R_S(l) R_D(l) \times \qquad (3.59)$$

$$\times \left\{ \sin\left(2\pi l \frac{\mu(B)}{\hbar\omega_c}\right) J_0\left(\frac{\pi l W}{\hbar\omega_c}\right) + \frac{W}{2\mu} \cos\left(2\pi l \frac{\mu(B)}{\hbar\omega_c}\right) J_1(\pi l \frac{W}{\hbar\omega_c}) \right\}$$

where $\mu(B)$ is given by equation (3.57) and contains the dependence on the reservoir DoS. Formulas (3.57) and (3.59) describe the magnetization oscillations at arbitrary parameters. The only approximation used in these formulas is the Dingle law of harmonic damping. In quasi-2D organic metals with warping $W > T_D$ the Dingle law is believed to be a fairly good approximation.

Formulas (3.57) and (3.59) are a good starting point for numerical calculations. From these formulas we see that in the limit $W/\mu \ll 1$ the oscillating parts of magnetization and chemical potential are connected by the simple relation

$$\tilde{M}(B) = \frac{\varepsilon_F}{B} \frac{2g}{\hbar\omega_c} (1 + n_R) \tilde{\mu}(B).$$

At zero warping this was obtained in [55].

3.2.2 Influence of the reservoir DoS

The nonlinear equation (3.57) for $\tilde{\mu}(B)$ can be solved analytically only in some simple approximations. We shall do this to illustrate the influence of the oscillations of chemical potential on the temperature and Dingle temperature dependence of harmonic amplitudes. So we consider zero warping, zero spin-splitting and zero temperature. Then the sum in the right-hand side of equation (3.57) can be calculated and we get

$$\frac{x}{2} = \frac{1}{(1 + n_R)} \arctan\left(\frac{\sin(y + x)}{\cos(y + x) + e^b}\right) \qquad (3.60)$$

where $x \equiv 2\pi\tilde{\mu}(B)/\hbar\omega_c$, $y \equiv 2\pi\varepsilon_F/\hbar\omega_c$ and $b \equiv 2\pi\Gamma/\hbar\omega_c$.

At very large electron reservoir ($n_R = \infty$) we get $x = 0$ that is the limit of fixed chemical potential. In this case magnetization is given by [37]

$$\tilde{M}(B) = \frac{2g\,\varepsilon_F}{\pi B}\arctan\left(\frac{\sin(y)}{e^b + \cos(y)}\right). \tag{3.61}$$

It is also possible to solve equation (3.60) analytically at $n_R = 0$ and $n_R = 1$. At zero electron reservoir $n_R = 0$ the solution of this equation is

$$\frac{x}{2} = \pi\frac{\tilde{\mu}(B)}{\hbar\omega_c} = \arctan\left(\frac{\sin(y)}{e^b - \cos(y)}\right).$$

It gives the oscillations of the chemical potential. The magnetization at zero electron reservoir is

$$\tilde{M}(B) = \frac{2g\,\varepsilon_F}{\pi B}\arctan\left(\frac{\sin(y)}{e^b - \cos(y)}\right). \tag{3.62}$$

It coincides with (3.61) after the phase shift $y \to y + \pi$ and the sign reversal $\tilde{M} \to -\tilde{M}$. This means that the harmonic damping law

$$A_l \sim (1/l)\cdot\exp\left(-l\cdot b\right) \tag{3.63}$$

does not change, and only the sign of all even harmonics is reversed. This symmetry between the cases of fixed chemical potential $\mu = const$ and constant particle density $N = const$ is a feature of the special exponential law of harmonic damping. Any finite temperature and nonzero density of electron reservoir breaks this symmetry.

Let us consider now the intermediate case $n_R = 1$. Equation (3.60) then becomes

$$\frac{\sin x}{\cos x} = \frac{\sin(y+x)}{\cos(y+x) + e^b}. \tag{3.64}$$

It gives

$$x = \arcsin\left(e^{-b}\sin y\right)$$

and magnetization becomes

$$\tilde{M}(y) = \frac{g\,\varepsilon_F}{\pi B}\arcsin\left(e^{-b}\sin y\right). \tag{3.65}$$

To say how the harmonic damping has changed we have to calculate the amplitudes of several first harmonics of this expression. The amplitude of the first harmonic is

$$A_1(b) = \frac{1}{\pi}\int_{-\pi}^{\pi}\arcsin\left(e^{-b}\sin y\right)\sin y\,dy.$$

After integration by parts we get

$$A_1(b) = \frac{4}{\pi}\int_0^{\pi/2} \frac{\cos^2 y\, e^{-b}\, dy}{\sqrt{1 - e^{-2b}\sin^2 y}}.$$

This is the superposition of two elliptic integrals:

$$A_1(b) = \frac{4}{\pi}\left[e^b E(e^{-b}) - 2\sinh b\, K(e^{-b})\right] \tag{3.66}$$

At $b \gg 1$ the deviations of $A_1(b)$ from the L-K formula are small:

$$A_1(b) = e^{-b} + e^{-3b}/8 + \ldots$$

In the opposite limit $b \ll 1$ we obtain

$$A_1(b) = \frac{4}{\pi}\left\{1 - b\left(\ln\frac{4}{\sqrt{2b}} - \frac{1}{2}\right) + O(b^2)\right\}. \tag{3.67}$$

This is substantially different from the L-K dependence $A_1(b) = \exp(-b) \approx 1 - b$. For example, the value $A_1(0)$ is $4/\pi$ times larger than the L-K prediction.

The amplitudes of the next harmonics reveal stronger deviation from the L-K formula (3.63). All even harmonics disappear since the expression (3.65) has the symmetries $\tilde{M}(\pi - y) = \tilde{M}(y)$ and $\tilde{M}(-y) = \tilde{M}(y)$.

The amplitude of the third harmonic can also be calculated. At $b \gg 1$, $e^{-b} \ll 1$,

$$A_3(b) = -e^{-3b}/12 + O(e^{-5b}).$$

This result is in contrast to the cases of $n_R = 0$ or $n_R = \infty$ where we had $A_3(b) = e^{-3b}/3$. It is not surprising since in the symmetric case of $n_R = 1$ the oscillations should be much smoother and more sinusoidal. Hence one should have an increase of the first harmonic and a decrease of higher harmonics. At $b = 0$

$$A_3(0) = \frac{4}{3\pi}\int_0^{\pi/2} \frac{\cos 3y\, \cos y\, dy}{\cos y} = -\frac{4}{9\pi} \tag{3.68}$$

which is ~ 2.35 times less than the Lifshitz-Kosevich prediction $A_3(0) = 1/3$ and has the opposite sign. So in the case $n_R = 1$ the first harmonic is increased while other harmonics are strongly decreased in amplitude compared to the cases of zero and infinite electron reservoir. The deviation from the L-K formula reduces as the warping of the FS increases. The above analysis shows also that the harmonic ratios at low temperature and low Dingle temperature can give a quantitative estimate of the electron reservoir density which is

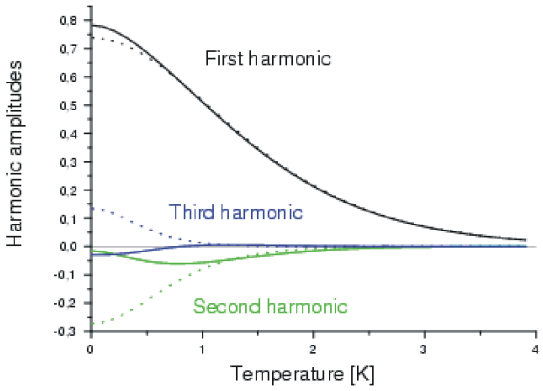

Figure 3.5: Temperature dependence of harmonic amplitudes. The solid lines are the numerical results (at $n_R = 1$, $m^* = 2m_0$, $T_D = 0.2K$ and $W = 1K$; see text) and the dashed lines represent the Lifshitz-Kosevich prediction for the same parameters. Their strong deviations are clearly seen, especially for higher harmonics.

much more precise than just a note about the slope of the magnetization curve.

To include correct temperature dependence, warping and spin-splitting and consider arbitrary reservoir density, one can perform the numerical calculations, based on the solution of equation (3.57) for the chemical potential and substitution of this solution into formula (3.59) for magnetization. This can be done for arbitrary parameters, feasible in the experiment. The temperature dependence of the first three harmonic amplitudes is given in fig.1 for the following set of parameters close to those of the real experiments on α-$(BEDT-TTF)_2KHg(SCN)_4$: reservoir density $n_R = 1$, dHvA frequency $F = 700$ Tesla, effective electron mass $m^* = 2m_0$, Dingle temperature $T_D = 0.2K$ and warping $W = 1K$. We see substantial deviation from the Lifshitz-Kosevich dependence. The obtained amplitude of the first harmonic at $T \to 0$ is about 1.1 times larger than the Lifshitz-Kosevich prediction. If we put also $T_D \to 0$ and $W \to 0$, then the ratio of the amplitudes of the first harmonic and its L-K prediction becomes $4/\pi = 1.27$ in agreement with the analytical result (3.67). The second harmonic amplitude is close to zero at $T = 0$. The amplitude of the third harmonic changes the sign at $T \approx 0.8K$ and deviates very strongly from the L-K formula. It is damped much stronger than the L-K predictions. At $T = 0$ and $W = 0$ it also coincides with the prediction (3.68).

To conclude, it was shown both analytically and numerically that the oscillations of the chemical potential are essential for the temperature dependence of harmonic amplitudes of dHvA oscillations in quasi-two-dimensional

compounds. An accurate determination of the effective electron mass from the dHvA effect should take this effect into account. This can be done by a simple numerical calculation based on formulas (3.57) and (3.59). The oscillations of the chemical potential depend on the reservoir density of states according to formula (3.57). This fact may be used to estimate the reservoir density of states in organic metals.

3.3 Summary of the results on the dHvA effect

Comparing with the previous chapter, where we have given a more detailed introduction into the 2D dHvA effect, in this chapter we have generalized the formulas on the quantum magnetization oscillations in 2D and quasi-2D compounds that makes them applicable to a description of real dHvA measurements.

In section 3.1 we followed the procedure of direct summation over LLs. This allowed us to consider an arbitrary shape of LLs at a finite temperature and to obtain explicit relation between the DoS distribution and the magnetization curve. This relation allows one to extract directly the DoS distribution in a compound in hand from the magnetization curve obtained in experiment. Any method of direct extracting of the density of electron states distribution from experiment is of essential use because the problem of the shape of LLs both in heterostructures and in strongly anisotropic organic metals is still open. In sec. 3.1.3 we proposed a possible method of testing the one-particle approximation. This approximation consists in disregarding the many-particle interaction and is typically used to describe magnetic quantum oscillations. However, no proof exists of this approximation for the compounds studied. Then we calculated the envelopes (amplitudes as functions of magnetic field) of the magnetization oscillations. These envelopes are easy for measurements and can also give some information about the shape of the Landau levels, because, as is shown, they depend strongly on this shape.

In section 3.2 we applied the harmonic expansion and obtained general formulas for magnetization oscillations that take into account oscillations of the chemical potential at arbitrary electron reservoir (arising from the open sheets of the Fermi surface in many organic metals), arbitrary spin-splitting and warping of the Fermi surface, arbitrary temperature and LL broadening (provided the LL shape is known). Without any simplifications, these formulas are a good starting point only for numerical calculation of magnetization. Explicit analytical results can be obtained in different limiting cases. For

example, at zero temperature and warping of the Fermi surface one can solve the equations for the chemical potential and, hence, write down simple explicit formulas for magnetization at different values of the electron reservoir that may be important for the analytical study of different effects.

The results obtained are thus interesting for studying both experimental and theoretical aspects of magnetic quantum oscillations and can be used for processing real experimental data.

Chapter 4

The Shubnikov-de Haas effect in quasi-2D compounds

Magnetic quantum oscillations were discovered long ago and were frequently used as a powerful tool of studying the geometry of Fermi surfaces and other electronic properties of various metals (see the introductory chapter).

In recent years, quasi-two-dimensional (quasi-2D) organic metals [59] attract great interest because many new unconventional effects are very pronounced in these compounds. These effects are high-T_c superconductivity, spin and charge density waves, strong anisotropic magnetic quantum oscillations etc. Much work was devoted to studying magnetic quantum oscillations in these compounds (for a review see e.g. [60]). The quantum oscillations of magnetization are a thermodynamic effect that is completely determined by the density-of-states distribution. Any exact calculation of the density of states is a very complicated problem but a semi-phenomenological description of magnetization oscillations in quasi-2D compounds was recently provided in a number of theoretical papers [32, 33, 34, 35, 36, 37, 38, 39] (see chapters 2, 3). The chemical potential oscillations and the arbitrary electron reservoir due to the open sheets of the Fermi surface create no principal difficulties[38]. Of course, if the e-e interaction drastically changes the ground state (like the FQHE effect) the problem becomes much more complicated. But when the number of occupied LLs is very large ($n_F > 100$ as in most quasi-2D organic metals) the effect of the e-e interaction is reduced (as in the Fermi liquid) and can be taken into account via the renormalization of the effective mass. Another open question in the theory of the quasi-2D dHvA effect is the exact shape of the Landau levels. It depends on the particular type of compound (on the type of impurities, their distribution, the interlayer transfer integral etc.). However, differences in LL shape lead to only limited quantitative differences in magnetization curves (e.g. see sec. 3.1.4), yielding no quali-

tatively new effects. On the qualitative level, therefore, the dHvA effect in quasi-2D normal metals is believed to be well understood.

Attempts of theoretical description of the quasi-2D quantum conductivity oscillations were not as successful although some work on this subject appeared in recent years [34, 63, 64, 65, 66, 67]. There are still some open qualitative questions. One of these open questions is the origin of the phase shift in the beats of the resistivity oscillations with respect to those in the magnetization. The beat behavior of the oscillations in quasi-2D metals is known reliably to originate from a slight warping of their Fermi surfaces in the direction normal to the 2D plane. The superposition of the contributions from the maximum and minimum cyclotron orbits leads to an amplitude modulation of the k-th harmonic by the factor $\cos(2\pi k\Delta F/2B - \pi/4)$, where B is the magnetic field and $\Delta F = (c\hbar/2\pi e)(A_{\max} - A_{\min})$ is the difference between the oscillation frequencies caused by the extreme orbits with the k -space areas $A_{\max}$ and $A_{\min}$, respectively [1]. From the beat frequency one can readily evaluate the warping of the Fermi surface and hence the interlayer transfer integral $4t \approx \epsilon_F \Delta F/F$ (see e.g. [76, 68]). The situation becomes less clear when the warping is so weak that less than one half of the beat period can be observed experimentally. In principle, an observation of one single node would already be quite informative [69], provided the phase offset (i.e. the phase of the beat at $1/B \to 0$) is known. In the standard LK theory this phase offset is strictly determined by geometrical reasons and is equal to $-\pi/4$ for both the dHvA and SdH effects [1].

However recent experiments on layered organic metals κ-(BEDT-TTF)$_2$ Cu[N(CN)$_2$]Br [69] and (BEDT-TTF)$_4$[Ni(dto)$_2$] [70] revealed a significant difference in the node positions of the beats of dHvA and SdH signals. The phase shift in the latter compound was estimated to be as big as $\pi/2$. Note that in both cases the oscillation spectrum was strongly dominated by the first harmonic when no substantial deviations from the standard LK theory are expected.

Another very interesting phenomenon is slow oscillations of magnetoresistance that were observed in a number of quasi-2D organic metals [60, 79, 80, 81, 82, 83, 84]. The behavior of slow oscillations resembles that of the SdH effect that lead to a suggestion of additional, very small Fermi surface pockets in these materials. However, band structure calculations (basically giving a good description of the electron band structure and of the Fermi surface topology in organic metals) show no evidence of such small pockets in any of these compounds. Moreover, while slow oscillations are often very pronounced in magnetoresistance, sometimes even dominating the oscillation spectrum, thus far no analogous observation in oscillating magnetization (dHvA effect) was reported. Certainly, slow oscillations carry useful infor-

mation about the compounds but one needs some theoretical explanation and, desirably, a quantitative description of the phenomenon to extract this information.

In what follows we develop a theory of the Shubnikov - de Haas effect in quasi-2D metals. This theory explains both of these two phenomena.

In section 4.1 we calculate conductivity from the Boltzmann transport equation. This calculation is quite simple and gives a good qualitative description of the phenomena mentioned above. Then we compare the obtained theoretical estimations with the experimental results. This section follows the work of P. Grigoriev et al.[66].

In Sec. 4.2 we calculate conductivity more rigorously starting from the Kubo formula and carefully handling all oscillating quantities in the expression for conductivity[75]. The proposed theory gives a certain quantitative description of the quasi-2D Shubnikov - de Haas effect. However, our analysis has some important limitations. The main of them are that the theory is only developed for the magnetic field perpendicular to the conducting layers and that impurity scattering is treated in the Born approximation. These problems are discussed in Sec. 4.3

4.1 Approximate analysis using the Boltzmann transport equation

First, we shall give an approximate analysis of the quasi-2D magnetoresistance using the Boltzmann transport equation. Rigorously speaking, this equation is not accurate. Nevertheless, it usually gives a simple and reasonable description of different transport phenomena. In our case we shall be able to explain both the phase shift of the beats and the slow oscillations of conductivity in magnetic field on the basis of the Boltzmann equation and to propose their qualitative analysis. Such a description (presented in this section) does not require introducing more mathematical methods such as Feinmann diagrams and is good for a qualitative understanding of magnetoresistance phenomena. More accurate calculation based on the Kubo formula requires an accurate calculation of the self-energy part of the electron Green's function. To do this one must have a well determined microscopic picture of the phenomena (for example, the type of scattering centers). This approach will be discussed in the next section.

4.1.1 Phase shift of the beats

We consider a quasi-2D metal in magnetic field perpendicular to the conducting layers with the energy spectrum

$$\epsilon\left(n, k_z\right) = \hbar\omega_c\left(n + 1/2\right) - 2t\cos(k_z d) \tag{4.1}$$

where t is the interlayer transfer integral, k_z is the wavevector perpendicular to the layers, d is the interlayer distance, $\omega_c = eB/m^*c$ is the cyclotron frequency. Both $\hbar\omega_c$ and t are assumed to be much smaller than the Fermi energy.

The DoS of the electron gas with this spectrum can be easily obtained by performing the summation over all quantum numbers at a fixed energy,

$$\rho(\epsilon) = \sum_{n=0}^{\infty} \frac{N_{LL}}{\sqrt{4t^2 - \left(\epsilon - \hbar\omega_c\left(n + 1/2\right)\right)^2}} \tag{4.2}$$

where N_{LL} is the Landau level degeneracy. The sum over Landau levels can be expanded in a harmonic series using the Poisson summation formula. As a result we have (see Appendix A2, formula 7.3):

$$\rho(\epsilon) \propto 1 + 2\sum_{k=1}^{\infty}(-1)^k \cos\left(\frac{2\pi k\epsilon}{\hbar\omega_c}\right) J_0\left(\frac{4\pi kt}{\hbar\omega_c}\right) \tag{4.3}$$

This formula has been first obtained by Gvozdikov [32] and written in the present form (including additional Dingle factor $R_D(k) = \exp(-2\pi k\Gamma/\hbar\omega_c)$, where Γ is the Lorentzian width of the LLs) by Champel and Mineev [37]. We shall consider the case $4\pi t > \hbar\omega_c$ in which beats can be observed. Then the zeroth order Bessel function $J_0\left(\pi k 4t/\hbar\omega_c\right)$ describing the beats of DoS oscillations can be simplified as $J_0(x) \approx \sqrt{2/\pi x}\cos(x - \pi/4)$. Further, we consider the limit of strong harmonic damping, retaining only the zeroth and first harmonics. In this limit the oscillations of the chemical potential μ can be neglected. Knowing the DoS we can now obtain the oscillating part of magnetization as [37]

$$\tilde{M} \propto \sin\left(\frac{2\pi\mu}{\hbar\omega_c}\right)\cos\left(\frac{4\pi t}{\hbar\omega_c} - \frac{\pi}{4}\right) R_T R_D \tag{4.4}$$

where R_T is the usual temperature smearing factor. This expression coincides with the result of the three-dimensional LK theory [1] and allows an evaluation of t from the beat frequency.

Contrary to magnetization, the conductivity is a transport quantity, and is not exclusively determined by the density of states. In the simplest approximation (as from the Boltzmann transport equation) the interlayer conductivity σ_{zz} is given by [[77], §7.1]

$$\sigma_{zz} = e^2 \int d\epsilon \, \left(-n'_F(\epsilon)\right) \, I(\epsilon)\tau(\epsilon) \tag{4.5}$$

where $n'_F(\epsilon) = -1/\{4T\cosh^2[(\epsilon-\mu(B))/2T]\}$ is the derivative of the Fermi distribution function, $I(\epsilon) \equiv \sum |v_z(\epsilon)|^2$ is the square of the electron velocity summed over all states at the energy ϵ, v_z is the z-component of the electron velocity and $\tau(\epsilon)$ is the momentum relaxation time at energy ϵ. In Born approximation, τ is inversely proportional to the density of states (DoS): $\tau(\epsilon) \propto \rho^{-1}(\epsilon)$ and oscillates in magnetic field according to the equation (see 4.3)

$$\tau(\epsilon) \propto \left[1 + 2\sum_{k=1}^{\infty}(-1)^k \cos\left(\frac{2\pi k\epsilon}{\hbar\omega_c}\right) J_0\left(\frac{4\pi kt}{\hbar\omega_c}\right) R_D(k)\right]^{-1}. \tag{4.6}$$

The physical reason for the proportionality $1/\tau(\epsilon) \sim \rho(\epsilon)$ is clear: electron scattering rate is proportional to the number of states to which an electron may scatter.

If the cyclotron energy is comparable to the interlayer transfer integral, the oscillations of the electron velocity summed over the states at the Fermi level (quantity $I(\epsilon)$ in formula (4.5)) also become important. To calculate this quantity one has to perform the integration over k_x :

$$I(\epsilon) \equiv \sum_{n,k_x,k_z} |v_z|^2 \, \delta\left(\epsilon(n,k_z) - \epsilon\right) = N_{LL} \sum_n 2\int_0^{\pi} \frac{d(k_z d)}{2\pi} v_z^2(k_z) \delta\left(\epsilon(n,k_z) - \epsilon\right)$$

where $N_{LL} = SB/\Phi_0$ is the LL degeneracy. Then we change the integration variable k_z to $\epsilon(n,k_z)$ and substitute the expression for the electron velocity v_z:

$$\begin{aligned} v_z(\epsilon,n) &\equiv \frac{\partial\epsilon(n,k_z)}{\hbar\partial k_z} = -\frac{2td}{\hbar}\sin(k_z d) = \\ &= \frac{d}{\hbar}\sqrt{4t^2 - \left(\epsilon - \hbar\omega_c\left(n+1/2\right)\right)^2}. \end{aligned} \tag{4.7}$$

As a result we obtain:

$$I(\epsilon) = \sum_{n=0}^{\infty} \frac{N_{LL}d^2}{2\pi\hbar}\sqrt{4t^2 - \left(\epsilon - \hbar\omega_c\left(n+1/2\right)\right)^2}.$$

This quantity can be expressed as a sum over harmonics as (see Appendix A2, formula (7.2)):

$$I(\epsilon) \sim 1 + \frac{\hbar\omega_c}{\pi t} \sum_{k=1}^{\infty} \frac{(-1)^k}{k} \cos\left(\frac{2\pi k\epsilon}{\hbar\omega_c}\right) J_1\left(\frac{4\pi kt}{\hbar\omega_c}\right) R_D(k). \qquad (4.8)$$

The first-order Bessel function $J_1(4\pi kt/\hbar\omega_c)$ entering (4.8) also describes beats but with a phase different from that of the DoS beats given by $J_0(4\pi kt/\hbar\omega_c)$ in Eq.(4.3): at large x, $J_1(x) \approx \sqrt{2/\pi x}\sin(x - \pi/4)$ is shifted by $\pi/2$ with respect to $J_0(x)$.

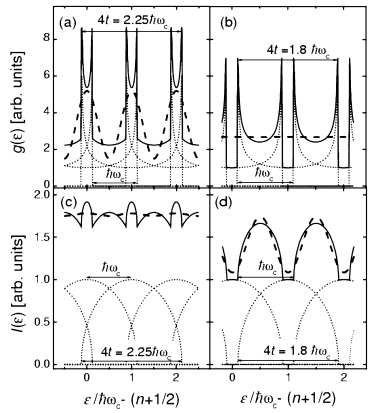

Figure 4.1: a - DoS (solid line) near the Fermi level and its first harmonic (dashed line) according to Eq.(4.3), at $4t/\hbar\omega_c = 2.25$; b - same at $4t/\hbar\omega_c = 1.8$; c - the quantity $I(\epsilon)$ (solid line) and its first harmonic (dashed line) according to Eq.(7) at $4t/\hbar\omega_c = 2.25$; c - same at $4t/\hbar\omega_c = 1.8$. In all four panels: the dotted lines are the contributions from individual Landau levels.

The phase shift in the beats of oscillations in $\rho(\epsilon)$ and $I(\epsilon)$ is illustrated in Fig. 4.1 where these quantities are plotted for two different values of the ratio $4t/\hbar\omega_c$. The DoS oscillations have a maximum amplitude of the first harmonic when $4t/\hbar\omega_c = 2.25$ (Fig. 1a). At the same value of $4t/\hbar\omega_c$ the

oscillations of $I(\epsilon)$ exhibit a nearly zero amplitude of the first harmonic as shown on Fig. 1c whilst their second harmonic (not shown in the figure) reaches maximum. By contrast, when $4t/\hbar\omega_c = 1.8$ (Fig. 1b,d), the first harmonic of the DoS is at the node whereas the first harmonic of $I(\epsilon)$ has the maximum amplitude.

The difference between the phases of the beats in oscillating $\rho(\epsilon)$ and $I(\epsilon)$ leads to a shift of the beat phase of the SdH oscillations with respect to that of the dHvA oscillations. Indeed, substituting Eqs. (4.6) and (4.8) into (4.5), applying large argument expansions of $J_0(x)$ and $J_1(x)$ and making temperature smearing (integration with $n'_F(\epsilon)$ in (4.5)), we come to the following expression for the first harmonic of the interlayer conductivity:

$$\tilde{\sigma}_{zz} \propto \cos\left(\frac{2\pi\mu}{\hbar\omega_c}\right)\cos\left(\frac{4\pi t}{\hbar\omega_c} - \frac{\pi}{4} + \phi\right) R_T \tag{4.9}$$

where

$$\phi = \arctan(a) \text{ and } a = \hbar\omega_c/2\pi t. \tag{4.10}$$

Comparing these expressions with Eq.(4.4), one can see that the beats in the SdH and dHvA oscillations can become considerably shifted with respect to each other as the cyclotron frequency approaches the value of the interlayer transfer integral.

The above evaluation is based on the semi-classical Boltzmann equation and is certainly not expected to give an exact result. Nevertheless, as will be seen below, its predictions concerning the phase shift are in good qualitative agreement with the experiment and we therefore believe that it correctly reflects the physics of the phenomenon.

Fig. 4.2 shows the oscillating parts of magnetization and interlayer magnetoresistance in the normal state of β-(BEDT-TTF)$_2$ IBr$_2$ at magnetic field tilted by $\theta \approx 14.8^\circ$ from the normal to the BEDT-TTF layers. The curves have been obtained by subtracting slowly varying backgrounds from the measured magnetic torque $\tau(B)$ and resistance $R(B)$, subsequently dividing them by B in the case of magnetization oscillations, $\tilde{M} \propto \tilde{\tau}/B$. Fast Fourier transformation (FFT) spectra shown in the insets reveal the fundamental frequency of ≈ 3930 T in agreement with previous results [73, 76]. The second harmonic contribution is about 1% of that from the fundamental harmonic at the highest field.

Clear beats with four nodes (indicated by arrows) are seen in both the dHvA and SdH curves. We made sure that the observed beats originate from the warping of the cylindrical FS by checking the angular dependence of their frequency [76]. The fact that the oscillation amplitude does not exactly vanish at the nodes was attributed to slightly different cyclotron

masses at the extreme orbits of the FS [76]. The positions of the nodes determined as midpoints of narrow field intervals at which the oscillations inverse the phase are plotted in Fig. 4.3. The straight line is a linear fit of the magnetization data revealing the beat frequency $\Delta F = 40.9$ T that, according to Eq.(4.4), corresponds to $4t/\epsilon_F = \Delta F/F = 1/96$. The error bars at the node positions do not exceed $\pm 3 \times 10^{-4}$ T^{-1} for $N = 3$ to 5 and are somewhat bigger, $\simeq \pm 10^{-3}$ T^{-1}, for $N = 6$ due to a lower signal-to-noise ratio. We note that although the angle $\theta = 14.8^\circ$ corresponds to a region in the vicinity of the maximum beat frequency ($\max\{\Delta F(\theta)\} \approx 42.0$ T for the given field rotation plane), the sensitivity of the node positions to the field orientation is still quite high: the nodes shift by $\approx 2.3 \times 10^{-3}$ T^{-1} as θ is incremented by 1°. Thus, if one has to remount the sample between the torque and resistance measurements, even a slight misalignment may cause a substantial additional error. In our experiment both quantities were measured at the same field sweep; hence, this error was eliminated.

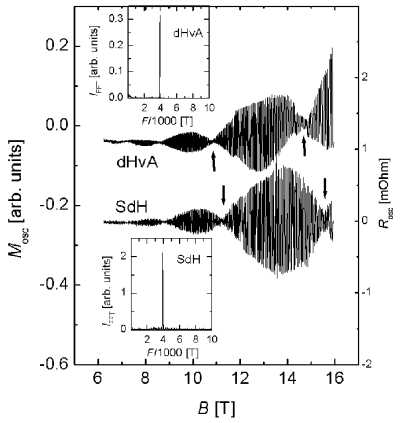

Figure 4.2: dHvA (left scale) and SdH (right scale) oscillations in β-(BEDT-TTF)$_2$IBr$_2$ at $\theta \approx 14.8^\circ$. Insets: corresponding FFT spectra.

From Figs. 2 and 3 one can see that the nodes of the SdH oscillations are considerably shifted to higher fields with respect to those of the dHvA oscil-

lations. The shift grows with increasing the field. Both these observations are fully consistent with the above theoretical prediction.

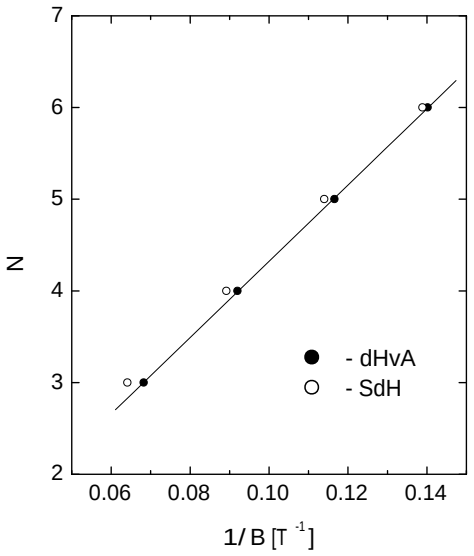

Figure 4.3: The positions of the nodes in the oscillating magnetization (filled symbols) and resistance (open symbols) versus inverse field. The straight line is the linear fit to the magnetization data.

In order to make a further comparison between experiment and theory, we plot the quantity $\tan(\phi)$ (where ϕ is the phase shift between the beats of the SdH and dHvA oscillations obtained from Fig. 4.3) as a function of magnetic field in Fig. 4.4. A linear fit to this plot (dashed line in Fig. 4.4) has a slope of 0.037 1/T [78]. A substitution of this value and the cyclotron mass $m^* = 4.2m_e$, obtained from the temperature-dependent amplitude of the fundamental harmonic, into Eq.(4.10) yields an estimate for the interlayer bandwidth $4t \simeq 0.48$ meV or the ratio $4t/\epsilon_F = \Delta F/F \simeq 1/230$. This is somewhat smaller than the value 1/96 obtained directly from the ratio between the beat and fundamental frequencies. However, taking into account an approximate character of the presented theoretical model, the difference is not surprising. Further theoretical work is needed to provide a more accurate basis for the quantitative description of the phenomenon.

Summarizing, the beats of the SdH oscillations in β-(BEDT-TTF)$_2$ IBr $_2$ are found to be shifted towards higher fields with respect to those of the dHvA signal. This phase shift arises from the oscillations of electron velocity on the FS. These oscillations produce a considerable contribution to the

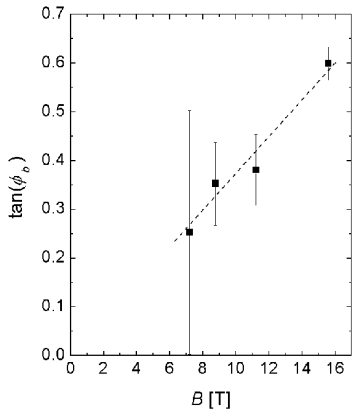

Figure 4.4: Tangent of the phase shift between node positions in the SdH and dHvA signals taken from the data on Fig. 3 as a function of magnetic field. The dashed line is a linear fit according to Eq.(4.10) [78].

magnetoresistance oscillations in strongly anisotropic organic metals, and the beats of the oscillations of electron velocity on the FS are shifted with respect to the beats of magnetization. The observed behavior appears to be a general feature of quasi-2D metals which should be taken into account whenever the cyclotron energy becomes comparable to the interlayer transfer energy. Of a particular importance is the dependence of the beat phase on the magnetic field strength which significantly affects the periodicity of the beats in the $1/B$ scale. Ignorance of this fact may lead to considerable errors in estimating FS warping from beat frequency when $2t \simeq \hbar\omega_c$.

4.1.2 Slow oscillations

Slow oscillations result from the interference of fast quantum oscillations of different quantities on which conductivity depends. These quantities are, for example, the electron relaxation time, the mean square electron velocity

(summed over all states on the FS) etc. There are many other oscillating quantities that do not enter (4.5) explicitly but are contained in the relaxation time τ. The product of any two oscillating factors gives a constant term according to the algebraic identity $(1+\tilde{\alpha}\cos x)(1+\tilde{\beta}\cos x) = 1+(\tilde{\alpha}+\tilde{\beta})\cos x + (\tilde{\alpha}\tilde{\beta}/2)\cos 2x + \tilde{\alpha}\tilde{\beta}/2$. The last term $\tilde{\alpha}\tilde{\beta}/2$ is responsible for the slow oscillations. In our case $x \equiv 2\pi\mu/\hbar\omega_c$ and the amplitudes $\tilde{\alpha}, \tilde{\beta}$ of the fast oscillations (for example, of relaxation time and mean square velocity) are themselves slowly oscillating functions of magnetic field due to the beats given by the Bessel functions in Eqs.(4.3) and (4.8). The beats are well known to originate from two close cross sections of the Fermi surface. If the transfer integral is sufficiently large, $4\pi t \gtrsim \hbar\omega_c$, one can use the large argument expansions of Bessel's functions. Then substituting (4.3) and (4.8) into (4.5) and performing the integration over energy with the Fermi distribution function we get up to the second order of the damping factors

$$\begin{aligned}\sigma_{zz} &= \sigma_0\Bigg\{1+2\sqrt{\frac{\hbar\omega_c}{2\pi^2 t}}\sqrt{1+a^2}\times \\ &\times\cos\left(\frac{2\pi\,\mu}{\hbar\omega_c}\right)\cos\left(\frac{4\pi t}{\hbar\omega_c}-\frac{\pi}{4}+\phi\right)R_D R_T + \\ &+\frac{\hbar\omega_c}{2\pi^2 t}\left[1+\sqrt{1+a^2}\cos\left(2\left[\frac{4\pi t}{\hbar\omega_c}-\frac{\pi}{4}+\frac{\phi}{2}\right]\right)\right]R_{D*}^2\Bigg\}\end{aligned} \tag{4.11}$$

where $\phi = \arctan(a)$ and $a = \hbar\omega_c/2\pi t$. The coefficient σ_0 in (4.11) can be estimated as $\sigma_0 = e^2 N_{LL} 2t^2 d^2/\pi\hbar^2\omega_c k_B T_D$ where N_{LL} is the Landau level degeneracy and $N_{LL}/\hbar\omega_c = m^*/2\pi\hbar^2$ is the DoS at the Fermi level. The second term in the curly brackets of this formula describes the Shubnikov oscillations while the last term gives slow oscillations with frequency equal to the double beat frequency. The factor $R_T = (2\pi^2 k_B T/\hbar\omega_c)\,/\sinh(2\pi^2 k_B T/\hbar\omega_c)$ is the usual temperature damping factor that comes in Shubnikov oscillations from the integration with the Fermi distribution function.

The slow oscillations in this formula do not have temperature smearing because they depend on the transfer integral t (the difference between two close cross sections of the Fermi surface) but not on the electron energy. Hence, although the amplitude of the slow oscillations contains the square of the Dingle factor, it can be larger than the amplitude of the fast SdH oscillations at $T \gtrsim T_D$. In other words, the slow oscillations depend on the electron spectrum but not on the electron distribution function. Hence, the slow oscillations do not have the temperature dependence. This fact is quite interesting and promising.

Nevertheless, our experience disagrees with the statement that the slow oscillations do not manifest any temperature dependence (and, hence, could

be seen at room temperature). Actually they do have some temperature dependence. More rigorously, the oscillating DoS itself has some temperature dependence that leads to the damping of slow oscillations if temperature is high enough. This temperature dependence of the DoS comes from the electron-phonon and electron-electron interactions. In normal 3D metals [8] the electron-electron (e-e) scattering rate $1/\tau_{ee} \sim (k_B T)^2 / \hbar\mu$ while the electron-phonon scattering rate $1/\tau_{ph} \sim (k_B T/\hbar)\,(k_B T/\hbar\omega_D)^2$. One can estimate the effect of these scattering processes on the DoS oscillations by introducing the additional damping factor

$$R_{TD} \approx \exp\left[-\pi(1/\omega_c\tau_{ee} + 1/\omega_c\tau_{ph})\right] \tag{4.12}$$

analogous to the usual Dingle factor. This factor enters squared in the amplitude of slow oscillations. The temperature at which slow oscillations become damped by this factor is much higher than the cyclotron energy. This temperature is given by $\pi(1/\omega_c\tau_{ee} + 1/\omega_c\tau_{ph}) \sim 1$ or $\pi T/\hbar\omega_c\,[T/\mu + (T/\hbar\omega_D)^2] \sim 1$. The above estimates of the temperature dependence of slow oscillations is very approximate. The rigorous calculation must be based on the exact calculation of the imaginary part of the electron self-energy due to these two types of interactions. Nevertheless, the above arguments give correct qualitative estimates. A more accurate calculation would be useful since the temperature dependence of slow oscillations at high enough temperature may give additional information about the electron-phonon and electron-electron interactions in various compounds where slow oscillations exist. In the experiment [74] the slow oscillations were damped at temperature $\approx 8K$.

Another significant feature of slow oscillations is that their Dingle factor R_{D*} is different from the factor R_D of the Shubnikov oscillations. The usual Dingle factor includes all temperature-independent mechanisms of smearing of DoS oscillations. These are not only microscopical scattering events of electrons but also macroscopic spatial inhomogeneities of the sample. These inhomogeneities lead to macroscopic spatial variations of electron energy in formula (4.5). Their effect is equivalent to a local shift of the chemical potential. The total signal is an average over the entire sample and such macroscopic inhomogeneities lead to the damping of magnetic quantum oscillations similar to that caused by temperature. Hence, the slow oscillations do not have this type of smearing. This fact can be understood in a different way: slow oscillations originate from local electron motion and are not sensitive to global variations of the position of the chemical potential with respect to the bottom of the conducting band. Hence, they are not damped out by macroscopic variations of the bottom of the conducting band. Nevertheless, this macroscopic inhomogeneity is expected to be strong in organic metals and, hence, it makes an essential contribution to the usual Dingle temperature. A

comparison between the Dingle factor of slow oscillations and the Shubnikov oscillations can give an estimate of the role of such inhomogeneities.

At low temperature when the effects of the phonon-electron and electron-electron interactions are small (as the third and second powers of temperature) and hence, can be neglected, the temperature dependence of the amplitude of slow oscillations may appear only in the next orders on the damping factors. The main contribution here comes from the chemical potential oscillations. The oscillating part of the chemical potential at arbitrary electron reservoir is given by formula (5) of [38]. In the limit of strong harmonic damping the first harmonic of this expression is:

$$\tilde{\mu}(B) \equiv \mu(B) - \varepsilon_F = \frac{\hbar\omega_c}{\pi(1+n_R)} \times \tag{4.13}$$

$$\times \sin\left(\frac{2\pi\,\varepsilon_F}{\hbar\omega_c}\right) J_0\left(\frac{4\pi t}{\hbar\omega_c}\right) R_D R_T$$

where n_R is the reservoir density due to open sheets of the Fermi surface divided by the average DoS on the 2D parts of the FS. Substituting this into (4.11) we get an additional slowly oscillating term (from the entanglement of the chemical potential oscillations with the fast Shubnikov oscillations):

$$\Delta\sigma_{zz} = \sigma_0 \frac{-\hbar\omega_c\sqrt{1+a^2}}{2\pi^2 t(1+n_R)} \cos\left[2\left(\frac{4\pi t}{\hbar\omega_c} - \frac{\pi}{4} + \frac{\phi}{2}\right)\right] R_D^2 R_T^2. \tag{4.14}$$

This term is $R_T^2/2\pi(1+n_R)$ times less than the temperature-independent term of slow oscillations and is of the order of second harmonics of the Shubnikov oscillations. At high temperature this correction to (4.11) is exponentially small and the temperature dependence of the amplitude of slow oscillations is determined by the smearing of the DoS oscillations due to phonon scattering and e-e interactions. But at low temperature these two damping mechanisms are small while the correction (4.14) is of the same order as the other contributions to slow oscillations.

At low temperature this small temperature-dependent correction can thus be measured. It is important because it gives information about the chemical potential oscillations. The problem of the chemical potential oscillations in ET-organic metals is of great interest because these oscillations are sensitive to unconventional states (such as superconducting state, spin or charge density waves etc.) and can give information about the nature of these states. More precisely, the chemical potential oscillations are strongly affected by the gap on open sheets of the FS that arises due to any transition to spin or charge density wave. The effect of this gap depends on whether the density wave is commensurate or not[105]. The chemical potential oscillations

can also give information about the nature, yet unclear, of the high magnetic field phase of the spin or charge density waves. A direct measurement of the chemical potential oscillations is problematic and the data on these oscillations based on the shape of the magnetization oscillations are very rough and, presumably, unreliable in many unconventional states (because these states also require a new theoretical description of the dHvA effect). Since the chemical potential oscillations make the main contribution to the low temperature dependence of the amplitude of the slow oscillations, the latter seems to be suitable for the experimental study of chemical potential oscillations.

It is worth noting that magnetization does not have such slow oscillating term because in the lowest order on damping factors it has only the product of $1 + a \sin x$ and $(1 + b \cos x)$ that is equal to $1 + a \sin x + (ab/2) \sin 2x$ and does not have a constant term $ab/2$. Moreover, magnetization does not have a product of oscillating quantities as conductivity (4.5) has. Hence in the same lowest order on the damping factors magnetization does not manifest slow oscillations.

Another (even stronger) reason why magnetization does not have slow oscillations is that magnetization contrary to conductivity is given by a derivative of the DoS with respect to magnetic field (3.58) and this derivative is much larger for rapidly oscillating terms.

The above theoretical analysis predicts that (i) the frequency of slow oscillations is twice as high as the beat frequency; (ii) slow oscillations do not have any temperature damping at $T \lesssim \hbar\omega_c$, and only at much higher temperatures they become damped proportionally to the square of the factor (4.12); (iii) the dependence of the frequency of slow oscillations on the tilt angle of the magnetic field with respect to the normal to the conducting planes is roughly similar to that of the interlayer transfer integral: $F^{SO}(\theta) \sim t(\theta)$. This dependence is approximately described by [89]: $t(\theta) = t(0) J_0(k_F d \tan\theta)$. These predictions can be used to verify the theory.

The temperature-independent oscillations were predicted also in [67] but their origin there is somewhat different: they originate from different chemical potential levels on two adjacent layers in heterostructures.

The agreement of the first two predictions is easily seen from fig. 4.5. Indeed, slow oscillations are not affected by temperature damping and have the frequency twice as high as the beat frequency. For the additional comparison the measurements of the tilt angle dependence of the frequency of slow oscillations have been performed again on β -(BEDT-TTF)$_2$IBr$_2$ (fig. 4.6). In this figure we also plot the constant part of the interlayer conductivity which is approximately proportional to the square of interlayer transfer integral and, hence, should have similar tilt angle dependence. As we see

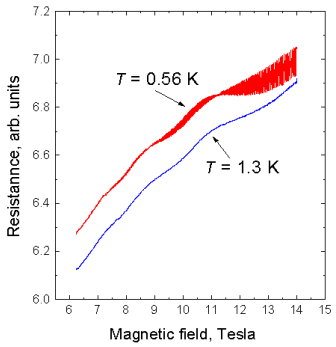

Figure 4.5: Conductivity as a function of magnetic field at two different temperatures. One can see that the frequency of the slow oscillations is twice as large as the beat frequency of Shubnikov oscillations. While the fast Shubnikov oscillations are seen to be damped very strongly by temperature, the amplitude of slow oscillations is almost temperature-independent.

from this figure, the frequency of slow oscillations indeed has very similar tilt angle dependence as the conductivity has. This fact completely proves the proposed theory.

Formula (4.11) also makes predictions about the values of the amplitude and phase of slow oscillations, but the proposed theoretical model base on the Boltzmann transport equation is very approximate and may be quantitatively inapplicable. Slow oscillations constitute a second-order effect in the limit of weak oscillations and, hence, require more accurate calculation.

The investigation outlined above is important because of a substantial interest to strongly anisotropic compounds. This interest is increased due to many unconventional properties (namely, high temperature superconductivity and density waves) that layered organic metals exhibit. Magnetic quantum oscillations are a very powerful tool for extracting information on electronic properties of these compounds.

4.2 Calculation using the Kubo formula

In this section we perform a more rigorous calculation of the interlayer conductivity in magnetic field. Since the physics of the phenomena has been described in the previous section, here we concentrate on more accurate calculations. These calculations are given in detail. In subsection 1 the general formula for the interlayer conductivity (4.23) is derived. A simple explicit formula for interlayer conductivity is obtained in the self-consistent Born ap-

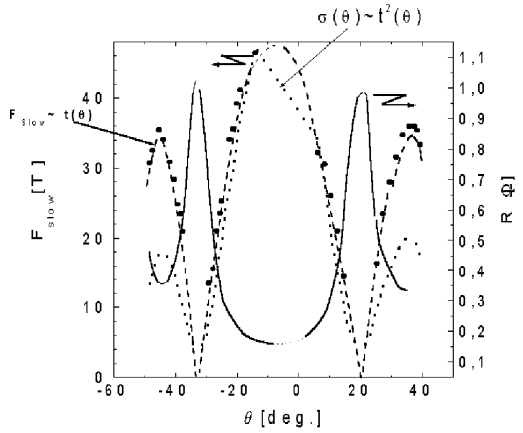

Figure 4.6: Comparison of angular dependences of the frequency of slow oscillations (filled circles connected by dashed lines) with those of resistance (solid line) and of conductivity (dotted line).

proximation in subsection 2. A discussion of the results obtained and the comparison with experimental data are given in subsection 3.

4.2.1 General formula for interlayer conductivity

We consider a quasi-2D metal in magnetic field perpendicular to the conducting layers: $\vec{B} \| \vec{z}$ (a generalization for arbitrary tilt angle of magnetic field is discussed in sec. IV). The electron spectrum of quasi-2D electron gas in magnetic field is then given by (4.1).

To calculate conductivity we use the Kubo formula [77]. The procedure is similar to that in three-dimensional metals without magnetic field ([77], § 7.1.2). In magnetic field only the new set of quantum numbers $m \equiv \{n, k_z, k_y\}$ should be used instead of momentum $\vec{p}$ and the alternative dispersion relation (4.1). We consider only the perpendicular to layers component σ_{zz} of electric conductivity since this components is simpler both for measurements and for theoretical description. The evaluation of the Kubo

formula without vertex corrections gives

$$\sigma_{zz} = \frac{e^2\hbar}{V}\sum_m v_z^2(m)\int\frac{d\epsilon}{2\pi}(2\mathrm{Im}G_R(m,\epsilon))^2\left(-n_F'(\epsilon)\right) \tag{4.15}$$

where the volume V normalizes the sum over quantum numbers m , e is the electron charge, v_z is electron velocity, the limits of the integration over ϵ are $(-\infty;\infty)$, $n_F'(\epsilon)$ is the derivative of the Fermi distribution function:

$$-n_F'(\epsilon) = 1/\{4T\cosh^2\left[(\epsilon-\mu)/2T\right]\} \tag{4.16}$$

and the electron Green's function $G_R(m,\epsilon)$ is related to the retarded self-energy part $\Sigma^R(m,\epsilon)$ by

$$\mathrm{Im}G_R(m,\epsilon) = \frac{\mathrm{Im}\Sigma^R(m,\epsilon)}{\left[\epsilon-\epsilon(m)-\mathrm{Re}\Sigma^R(m,\epsilon)\right]^2+\left[\mathrm{Im}\Sigma^R(m,\epsilon)\right]^2} \tag{4.17}$$

The self-energy part $\Sigma^R(m,\epsilon)$ arises from the electron scattering. The main contribution to the resistance comes from the short-range impurity scattering. We approximate the short-range impurities by point-like ones. We also disregard the diagrams with intersections of impurity lines in the self-energy (the contribution of these diagrams in 3D case is negligible, and if we consider the case $t \gg T_D$ this contribution is also negligibly small). Then the electron self-energy part depends only on the electron energy and not on electron quantum numbers: $\Sigma^R(m,\epsilon) = \Sigma^R(\epsilon)$. This fact greatly simplifies the calculations because the sum over the quantum numbers m in formula (4.15) can be now computed analytically.

In the real part $\mathrm{Re}\Sigma^R(\epsilon)$ of the electron self-energy one can only keep a small oscillating part $\mathrm{Re}\tilde{\Sigma}^R(\epsilon)$. The remaining weakly dependent term of $\mathrm{Re}\Sigma^R(\epsilon)$ produces only a constant shift of chemical potential. This does not influence the physical effects and, hence, is omitted in the subsequent calculations. The small oscillating part $\mathrm{Re}\tilde{\Sigma}^R(\epsilon)$ always come in the combination $\epsilon^* \equiv \epsilon - \mathrm{Re}\tilde{\Sigma}^R(\epsilon)$. The imaginary part of self-energy $\mathrm{Im}\Sigma^R(\epsilon)$ describes the momentum relaxation of electrons and, therefore, is very important for conductivity.

Performing the summation over k_y in (4.15) and changing integration over k_z by integration over energy $\epsilon' \equiv \epsilon(n,k_z)$ we get

$$\sigma_{zz} = e^2 N_{LL} d\int\frac{d\epsilon'}{\pi}\sum_n |v_z(\epsilon',n)|\int\frac{d\epsilon}{2\pi}4[\mathrm{Im}G_R(\epsilon',\epsilon)]^2\left(-n_F'(\epsilon)\right) \tag{4.18}$$

where $N_{LL} \equiv B/\Phi_0 d$ is the electron density on one Landau level, $\Phi_0 = 2\pi\hbar c/e$ is the magnetic flux quantum and the electron velocity $v_z(\epsilon,n)$ is

given by (4.7). To go further we have to transform the sum over LLs to a sum over harmonics. This can be done using the Poisson summation formula (Appendix A). Substituting (7.2) into (4.18) we obtain:

$$\sigma_{zz} = e^2 N_{LL} \sum_{k=-\infty}^{\infty} (-1)^k \frac{2td^2}{\hbar k} J_1\left(\frac{4\pi kt}{\hbar\omega_c}\right) \int \frac{d\epsilon}{2\pi} \left(-n'_F(\epsilon)\right) I_z(\epsilon, k) \qquad (4.19)$$

where one should use the expansion $J_1(kx)/k = x/2$ for the zeroth harmonic $k = 0$, and the integral $I_z(\epsilon, k)$ over ϵ' can be easily evaluated with the Green's function (4.17):

$$I_z(\epsilon, k) \equiv \int \frac{d\epsilon'}{2\pi} 4[\mathrm{Im}G_R(\epsilon', \epsilon)]^2 \exp\left(\frac{2\pi ik\epsilon'}{\hbar\omega_c}\right) = \qquad (4.20)$$

$$= \exp\left(\frac{2\pi ik\,\epsilon^*}{\hbar\omega_c}\right) \left(\frac{1}{|\mathrm{Im}\Sigma^R(\epsilon)|} + \frac{2\pi k}{\hbar\omega_c}\right) R_D(k, \epsilon) \qquad (4.21)$$

where $\epsilon^* \equiv \epsilon - \mathrm{Re}\tilde{\Sigma}^R(\epsilon)$ and

$$R_D(k, \epsilon) = \exp\left(-2\pi\,|k|\,\left|\mathrm{Im}\Sigma^R(\epsilon)\right|/\hbar\omega_c\right) \qquad (4.22)$$

has the form similar to that of the usual Dingle factor $R_D(k) = \exp\left(-2\pi^2 k\, k_B T_D/\hbar\omega_c\right)$. Collecting formulas (4.19) and (4.21) we get

$$\sigma_{zz} = e^2 N_{LL} \int \frac{d\epsilon}{2\pi} \left(-n'_F(\epsilon)\right) \sum_{k=-\infty}^{\infty} \frac{(-1)^k 2td^2}{\hbar k} J_1\left(\frac{4\pi kt}{\hbar\omega_c}\right) \times$$

$$\times \exp\left(\frac{2\pi ik\,\epsilon^*}{\hbar\omega_c}\right) \left(\frac{1}{|\mathrm{Im}\Sigma^R(\epsilon)|} + \frac{2\pi k}{\hbar\omega_c}\right) R_D(k, \epsilon). \qquad (4.23)$$

Note that this expression has an additional term $2\pi k/\hbar\omega_c$ near the standard $1/\left|\mathrm{Im}\Sigma^R(\epsilon)\right|$ term in round brackets in the second line. This term can not be obtained from the Boltzmann transport equation (compare, for example, with the results of [66] and [74]). Let us reveal the origin of this term. The function $[2\mathrm{Im}G_R(\epsilon', \epsilon)]^2 = G_A^2 + G_R^2 - 2G_A G_R$ in (4.20) has one first-order pole and one second-order pole in each complex half-plane. The first-order poles appears from the last term $-2G_A G_R$ while the second order poles come from $G_A^2 + G_R^2$. In the standard theory only the first-order poles are taken into account. In the 3D case the contribution from the second-order poles is small by a factor of $\hbar\omega_c/2t \approx \hbar\omega_c/\epsilon_F \ll 1$ and can be neglected. However, in quasi-2D case (where $\hbar\omega_c/2t \sim 1$) the contribution of second-order poles becomes important. As one can see from formula (4.32) this contribution $\sim \pi T_D/t$ and is, probably, only a first-order term in the expansion over $\pi T_D/t$. The case $\pi T_D/t > 1$ corresponds to the so-called incoherent limit [64], which we do not consider here.

To go further, we need an explicit form of the electron self-energy which enters formula (4.23). It is calculated in the next section.

4.2.2 Conductivity in the self-consistent Born approximation

We consider electron scattering only by short-range impurities because these impurities make the main contribution to the relaxation of electron momentum. To calculate the electron self-energy we use the self-consistent Born approximation. The graphical representation of the Dyson equation for the irreducible self-energy part in the self-consistent Born approximation is shown in fig. 4.7. By such an approximation we neglect the multiple scattering of an electron on one impurity (no more than two dash lines go to one impurity, denoted by a cross in fig. 4.7). The single dash line in fig. 4.7 corresponds to the first-order term which leads only to a constant shift of the chemical potential and, hence, can be omitted.

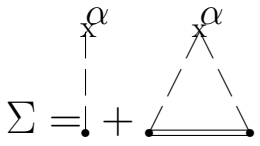

Figure 4.7: The Dyson equation for the irreducible self-energy in self-consistent Born approximation. The double solid line symbolizes the exact electron Green's function.

The corresponding analytical expression is

$$\Sigma^R(m,\epsilon) = \left\langle \sum_i U^2\, G(r_i, r_i, E) \right\rangle = C_i U^2 \int d^3 r G(r,r,E) \tag{4.24}$$

where $\sum_i$ is a sum over all impurities and the brackets $\langle .. \rangle$ denote averaging over impurity positions, C_i is the concentration of impurities which are assumed to be uniformly distributed [85]. The electron Green's function $G(r,r,E)$ in formula (4.24) contains the self-energy determined by the same formula (4.24) (this is why the approximation (4.24) is called self-consistent Born approximation). The Green's function is uniform along the conducting planes. Hence, one can write

$$G(r,r,E) = |\phi(z)|^2\, G(E), \tag{4.25}$$

where the electron wave function $\phi(z)$ along z-axis does not enter the final result because it disappears after integration over z in (4.24), and

$$G(E) = \frac{-N_{LL}}{\hbar\omega_c} \left\{ A(E) + i\pi \left[1 + 2\sum_{k=1}^{\infty} (-1)^k J_0\left(\frac{4\pi k t}{\hbar\omega_c}\right) \exp\left(2\pi i k \frac{E-\Sigma(E)}{\hbar\omega_c}\right) \right] \right\}. \tag{4.26}$$

$A(E)$ is a slowly varying function of energy which can be taken at the Fermi energy: $A(E) \approx A(E_F)$. An exact value of $A(E)$ is not important for conductivity in the Born approximation. Formulas (4.25) and (4.26) can be derived performing the summation over the electron quantum numbers $m \equiv \{n, k_z, k_x\}$ in the definition of the Green's function:

$$G(r, r, E) = \sum_{n,k_z,k_x} \frac{\Psi^*_{n,k_z,k_x}(r)\Psi_{n,k_z,k_x}(r)}{E - \epsilon(n, k_z) - \Sigma(E)} \tag{4.27}$$

The electron wave function $\Psi_{n,k_z,k_x}(r)$ in the Landau gauge is approximately given by

$$\Psi_{n,k_z,k_x}(r) = \frac{e^{i(k_x x + k_z z)}}{\sqrt{L_x L_z}} \chi_n(y - y_0)\phi(z)$$

where $y_0 = -c\hbar k_x/eB$, and the normalization condition $\int_{-\infty}^{\infty} |\chi_n(y)|^2 \, dy = 1$ should be used to perform the integration over k_x in (4.27). The further calculation of the sum in (4.27) is similar to that in (4.15).

The Born approximation (formula (4.24)) takes into account only the first term of the expansion in the small parameter $\pi U N_{LL}/\hbar\omega_c = \pi f/d$, where $N_{LL}/\hbar\omega_c$ is equal to the electron density of states at the Fermi level in unit volume, f is the scattering amplitude (which is constant at small wave vector $q \ll 1/r_0$, r_0 is the range of the impurity potential). For short-range impurities the parameter f/d is usually small.

From (4.24) one can easily see that in the self-consistent Born approximation the imaginary part of the self-energy is proportional to the density of states [86]:

$$-\mathrm{Im}\Sigma^R(\epsilon) = -C_i U^2 \, \mathrm{Im}G(\epsilon) = \pi \, C_i U^2 \times \rho(\epsilon). \tag{4.28}$$

The unknown coefficient $\pi \, C_i U^2$ in (4.28) is simply related to the average Dingle temperature T_D: $\left\langle \left| \mathrm{Im}\Sigma^R(m, \epsilon) \right| \right\rangle = \pi \, C_i U^2 \cdot \langle \rho(\epsilon) \rangle = \pi \, C_i U^2 \cdot (N_{LL}/\hbar\omega_c)\,(1 + n_R) = \pi k_B T_D$, where the triangular brackets denote the mean value of a quantity inside and $n_R \approx const$ is the density of the reservoir states that exist in many organic metals due to the open sheets of the FS.

From formulas (4.24-4.26) we get

$$\left| \mathrm{Im}\Sigma^R(m, \epsilon) \right| = \pi k_B T_D \left(1 + 2 \sum_{k=1}^{\infty} (-1)^k J_0 \left(\frac{4\pi k t}{\hbar\omega_c} \right) \cos \left(\frac{2\pi k \, \epsilon^*}{\hbar\omega_c} \right) R_D(k, \epsilon) \right). \tag{4.29}$$

Together with (4.22) this gives a nonlinear equation for $\mathrm{Im}\Sigma^R(m, \epsilon)$. We can solve it in the strong harmonic damping limit by making an expansion in the small parameter $\left(R_D \sqrt{\hbar\omega_c/2\pi^2 t} \right)$ which is an expansion in a small ratio of

oscillating part to the constant part of the density of states (or mean square electron velocity). To treat the slow oscillation accurately one also has to pick up all second-order slowly oscillating terms. We obtain

$$\left|\mathrm{Im}\Sigma^R(\epsilon)\right| \approx \pi k_B T_D \left\{ 1 - 2J_0\left(\frac{4\pi t}{\hbar\omega_c}\right)\cos\left(\frac{2\pi\,\epsilon}{\hbar\omega_c}\right) R_{0D} \right\}, \tag{4.30}$$

where $R_{0D} = \exp\left(-2\pi^2\, k_B T_D/\hbar\omega_c\right)$. There is no slowly oscillating second-order term in the self-energy in the Born approximation. At this point the real part of the electron self-energy is important because it cancels the contribution from the entanglement with the oscillations of the Dingle factor (4.22). In the second order in damping factors any combination of the form

$$\cos\left(\frac{2\pi\left(\epsilon - \mathrm{Re}\tilde{\Sigma}^R(\epsilon)\right)}{\hbar\omega_c}\right)\exp\left(\frac{-2\pi\left|\mathrm{Im}\Sigma^R(\epsilon)\right|}{\hbar\omega_c}\right) = \cos\left(\frac{2\pi\,\epsilon}{\hbar\omega_c}\right) R_{0D} \tag{4.31}$$

does not produce slowly oscillating term. This statement can be easily checked by substituting (4.24) with (4.26) into (4.31). If one neglected $\mathrm{Re}\Sigma^R(\epsilon)$ in (4.29) he would get an additional slowly oscillating term

$$\left\{ -\frac{4\pi^2\, k_B T_D}{\hbar\omega_c} J_0^2\left(\frac{4\pi t}{\hbar\omega_c}\right) R_{0D}^2 \right\}$$

in curly brackets of (4.30) which arise from the entanglement with the oscillating Dingle factor [87] and enters not only the imaginary part of the self-energy but also the density of electron states (see (4.30)). The slow oscillations of $\rho(\epsilon)$ would result in huge slow oscillations of magnetization which are increased by an additional factor $\epsilon_F/\hbar\omega_c$. Such huge slow oscillations of magnetization have not been observed on experiment that proves the absence of the second-order slowly oscillating term in (4.30).

Substituting (4.30) and (4.31) into (4.23) we obtain the following expression for the conductivity:

$$\sigma_{zz} = \sigma_0 \int d\epsilon\left(-n_F'(\epsilon)\right) \times \tag{4.32}$$

$$\times \quad \left\{ \frac{1 - \frac{\hbar\omega_c}{\pi t} J_1\left(\frac{4\pi t}{\hbar\omega_c}\right)\cos\left(\frac{2\pi\,\epsilon^*}{\hbar\omega_c}\right) R_D(\epsilon)}{\left[1 - 2J_0\left(\frac{4\pi t}{\hbar\omega_c}\right)\cos\left(\frac{2\pi\,\epsilon^*}{\hbar\omega_c}\right) R_D(\epsilon)\right]} - \right.$$
$$\left. - \frac{2\pi k_B T_D}{t} J_1\left(\frac{4\pi t}{\hbar\omega_c}\right)\cos\left(\frac{2\pi\,\epsilon^*}{\hbar\omega_c}\right) R_D(\epsilon) \right\}.$$

where the nonoscillating part of conductivity $\sigma_0 \approx (e^2 N_{LL} 2t^2 d^2)/(\hbar^2 \omega_c \pi k_B T_D)$.

If the transfer integral is large enough ($4\pi t > \hbar\omega_c$) one can use the expansions of the Bessel function at large value of argument:

$$\begin{aligned} J_0(x) &\approx \sqrt{2/\pi x}\cos\left(x - \pi/4\right)\,,\; x \gg 1 \\ J_1(x) &\approx \sqrt{2/\pi x}\sin\left(x - \pi/4\right)\,,\; x \gg 1\,. \end{aligned}$$

Then performing again an expansion in the small parameter $\left(R_D\sqrt{\hbar\omega_c/2\pi^2 t}\right)$ and making use of the standard trigonometric formulas we get

$$\begin{aligned} \sigma_{zz} = \sigma_0 \Bigg\{ & 1 + 2\sqrt{\frac{\hbar\omega_c\left(1+a^2\right)}{2\pi^2 t}}\cos\left(\frac{2\pi\,\mu}{\hbar\omega_c}\right) \times \\ & \times \cos\left(\frac{4\pi t}{\hbar\omega_c} - \frac{\pi}{4} + \phi_b\right) R_D^{tot} R_T \; + \\ & + \frac{\hbar\omega_c}{2\pi^2 t} R_D^2 \sqrt{1+a_S^2}\cos\left[2\left(\frac{4\pi t}{\hbar\omega_c} - \frac{\pi}{4} + \phi_S\right)\right] \Bigg\}, \end{aligned} \tag{4.33}$$

where the phase shift of the beats is

$$\phi_b = \arctan\left(a\right);\; a = \frac{\hbar\omega_c}{2\pi t}\left(1 + \frac{2\pi^2 k_B T_D}{\hbar\omega_c}\right), \tag{4.34}$$

and the phase of slow oscillations is

$$\phi_S = \arctan\left(a_S\right)/2 \quad \text{where} \quad a_S = \hbar\omega_c/2\pi t. \tag{4.35}$$

The temperature smearing factor is given by the usual L-K expression:

$$R_T = \frac{2\pi^2 k_B T/\hbar\omega_c}{\sinh\left(2\pi^2 k_B T/\hbar\omega_c\right)}.$$

It appear in the fast Shubnikov oscillations after the integration of a rapidly oscillating function of energy with the Fermi distribution function. The slowly oscillating term depends only on the transfer integral t and is independent of energy. Hence, it does not acquire any temperature smearing.

The superscript $''tot''$ after the Dingle-type damping factor R_D^{tot} of the fast quantum oscillations means that this damping factor comes not only from the short-range impurities but from all crystal imperfections such as macroscopic sample inhomogeneities and other long-range defects. These inhomogeneities lead to macroscopic spatial variations of the electron energy ϵ^* in formula (4.23) which is equivalent to a local shift of the background energy. The total signal is an average over the entire sample and these local shifts lead

to the damping of magnetic quantum oscillations similar to the temperature smearing. Since the slow oscillations do not have fine dependence on electron energy, they are not affected by this type of smearing and the corresponding Dingle temperature T_D of slow oscillations is determined by only short-range scatterering. One can therefore estimate the relative contributions from the macroscopic spatial inhomogeneities and long-range defects to the damping of oscillations by comparing T_D and T_D^{tot}. This role could be quite essential in organic metals. For example, in a sample of β-(BEDT-TTF)$_2$IBr$_2$ one had [74] $T_D^{tot} = (0.8 \pm 0.02)$ K while $T_D = (0.15 \pm 0.02)$ K. The relaxation of the electron momentum (leading to resistance) comes mainly from the short-range impurities.

The phase shift (4.34) obtained from the Kubo formula is larger than that of [[66], formula (9)] obtained using the Boltzmann transport equation by a factor $(1 + 2\pi^2 k_B T_D/\hbar\omega_c)$. This difference originate from the additional term $2\pi k/\hbar\omega_c$ near $1/\left|\mathrm{Im}\Sigma^R(\epsilon)\right|$ in round brackets in the second line of (4.23) that comes from the fast energy dependence of the electron mean square velocity (see discussion after formula (4.23)).

The result (4.33) and (4.35) concerning the slow oscillation does not differ from [[74], formula (4)]. However, the present derivation is much more rigorous.

4.2.3 Discussion of the results

Above we performed a detailed calculation of the interlayer magnetotransport in quasi-2D normal metals. The specific features of quasi-two-dimensionality and strong magnetic field result in several new qualitative effects. The standard formula for conductivity (derived for 3D metals but traditionally used also for quasi-2D compounds)

$$\sigma_{zz}^{3D} = \sigma_0 \left\{ 1 + 2\sqrt{\frac{\hbar\omega_c}{2\pi^2 t}} \cos\left(\frac{4\pi t}{\hbar\omega_c} - \frac{\pi}{4}\right) R_D^{tot} R_T \cos\left(\frac{2\pi\,\mu}{\hbar\omega_c}\right) \right\} \quad (4.36)$$

describes neither the phase shift of beats nor the slow oscillations.

In fig. 2 I plot the general view of conductivity as function of magnetic field using the new formula (4.33) (a) and the standard 3D formula (4.36) (b). The difference between L-K prediction and the new formula is clearly visible. For example, the outer beat node is shifted from B_{node}^{LK}=26.7T to B_{node}=53T. Practically, this means that the outer beat node (expected at 26.7T) may disappear because the field of 53T is reachable only in pulsed magnets at the present time. The parameters in fig. 2 are taken to be close to that of real experiments on β-(BEDT-TTF)$_2$IBr$_2$; in other compounds

or at higher tilt angle (where the interlayer transfer integral is less several times) figure 2 is scaled along the x-axis by the same factor. The next node at lower fields is shifted much weaker: from 11.5T to 13.5T. If one uses these two node positions to determine the beat frequency F_b according to the L-K formula (4.36), which gives:

$$B^{LK}_{node}/2F_b = 4/(4n-1), \quad n = 1, 2, 3.., \tag{4.37}$$

he obtains $F_b = 9T$ instead of the right answer $F_b = 10T$. Much larger error one gets if he tries to determine the beat frequency using only one beat node and the formula (4.37). For example, for the outer node (n=1) at $B = 53T$ one would get $F_b \approx 20T$ instead of $F_b = 10T$. The beats of magnetoresistance oscillations in layered compounds are used for estimating the interlayer transfer integral $2t = F_b(\hbar\omega_c/B)$ that determines the electronic properties of strongly anisotropic compounds. The field-dependent phase shift of beats may lead to the errors in this estimate. The modification of the formula (4.37) is

$$B_{node}/2F_b = 4/(4n-1-4\phi_b/\pi), \quad n = 1, 2, 3.. \tag{4.38}$$

where ϕ_b is given by (4.34).

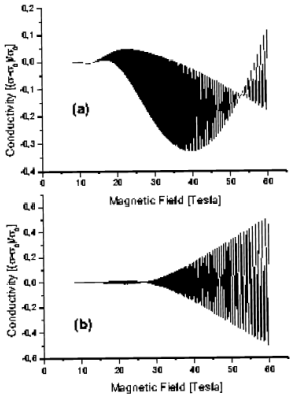

Figure 4.8: Interlayer conductivity given by formula (4.33) (Fig. 2a) and by the standard L-K formula (Fig. 2b) at the same parameters. The difference between the L-K formula and the new formula is very pronounced. The parameters are taken to be relevant to the SdH effect in β-(BEDT-TTF)$_2$IBr$_2$ in tilted magnetic field. The parameters are T_D =0.4K, T_D^{tot}=1.0K, T=1.2K, F_b=10T that corresponds to the tilt angle $\theta \approx 26^\circ$ or -12°.

The field dependence of the phase shift ϕ_b was studied experimentally in [66], and the result was compared with the prediction of the Boltzmann transport equation (fig. 4 of [66]). It was noted there that the slope of the fit line

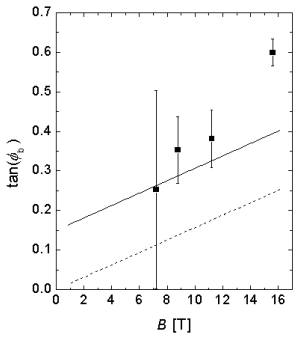

Figure 4.9: A comparison of the results of different theoretical models with the experimental data on the field dependence of the phase shift of beats. The standard 3D theory gives $\phi_b = 0$. The dash line is the prediction of the Boltzmann transport equation while the solid line is the result of the present theory (see text).

to the experimental points according to the Boltzmann equation corresponds to the value of the transfer integral $t \approx 0.48$ meV or the ratio $\Delta F/F \approx 1/230$ which is 2.3 times less than the value $\Delta F/F = 1/96$ obtained directly from the ratio between the beat and the fundamental frequencies. This discrepancy was attributed to the approximate character of the theoretical model, based on the Boltzmann transport equation. The present theoretical model is much more rigorous.

In fig. 3 a comparison of the different theoretical models with the experimental data on the field dependence of the phase shift of beats $\phi_b(B)$ is shown. The experimental points are taken from [66]). The standard 3D magnetotransport theory gives $\phi_b = 0$. The dash line is the prediction of the Boltzmann transport equation with the value of t taken from the beat frequency. This line cannot fit the experimental points properly. The solid line is the result of the present theory, based on the Kubo formula. It gives much better agreement with the experimental points. However, the last experimental point at the highest field $B = 15.7T$ is not in accord with the theoretical line. This is because at rather high magnetic field the Born approximation fails (due to a strong degeneracy of the LLs) and the result (4.34) becomes only a first-order term in the expansion over $\pi k_B T_D/t$ and $\hbar\omega_c/t$.

The slopes of the solid and the dash lines in fig. 3 are the same (they are determined by the ratio $\hbar\omega_c/2\pi t$). The phase shift in the new approach increases by a constant $\pi k_B T_D/t$. This augmentation contains T_D, which is the part of the Dingle temperature arising only from the short-range impurities.

Approximately, the same Dingle temperature enters the slow oscillations. In fig. 3 the value of $T_D \approx 0.15K$ is taken from the Dingle plot of the slow oscillations [74] (the measurements in [74] were done on the same sample as in [66]).

The present analysis is made when the magnetic field is perpendicular to the conducting layers. A finite tilt angle θ of the magnetic field with respect to the normal to the conducting planes may be approximately taken into account by rescaling the Landau level separation, $\omega_c \to \omega_c \cos\theta$, and of the warping of the Fermi surface[89], $t(\theta) = t(0)\, J_0(k_F d \tan\theta)$, where k_F is the in-plane Fermi momentum. But this is only a semiclassical approximation based on the assumption that the FS remains the same. The quantum mechanical calculation of the dispersion relation in tilted magnetic field in the first order of the transfer integral gives [90] $t(\theta)/t(0) = \exp(-g^2/4)\, L_n^0(g^2/2)$, where $g \equiv d\tan\theta/a_H$, $a_H = \sqrt{\hbar c/eB_z}$ is the magnetic length and $L_n^0(x)$ is Laguerre polynomial. This result is also approximate, but it works satisfactory at not too great tilt angles. In the limit $n \to \infty$ the above two results coincide.

In the above calculations we omit the spin splitting. Since the impurity scattering is spin-independent, one can take the spin splitting into account by the replacement in the final answer: $\sigma_{zz}(\mu) \to [\sigma_{zz}(\mu - \Delta_B) + \sigma_{zz}(\mu + \Delta_B)]/2$ where $\Delta_B = e\hbar B/m_e c$ is the shift of the Fermi level due to the spin-splitting (the conductivity given by formulas (4.15) and (4.33) already has factor 2 due to two spin orientation).

The entanglement with the oscillations of chemical potential contributes an additional temperature-dependent term to the slow oscillations of conductivity. This term can be easily obtained by substituting (3.57) into (4.33). However, this term has additional damping factors R_T^2 and $(R_D^{tot}/R_D)^2$ compared to the main slowly oscillating term. Therefore, this correction is as small as the second harmonic of Shubnikov oscillations is, and we can neglect it.

The slow oscillations do not appear in magnetization because there is no suitable entanglement of different oscillating quantities in magnetization. The magnetization being a thermodynamic quantity is completely determined by the electron density of states. However, the density of states does not have slowly oscillating terms. The mixing with the oscillations of the chemical potential, or with those of the Dingle factor and of $\mathrm{Re}\Sigma^R(\epsilon)$ does not also lead to slow oscillations of magnetization (see Appendix, section 3).

The above analysis does not take into account the vertex corrections. In our case (of point-like impurity scattering) this is right because, according to the Ward identity, the vertex $\vec{\Gamma}(m, E) = \vec{p} + m\vec{\nabla}_p \Sigma^R(m, E)$. Hence, if the retarded self-energy depends only on energy, the vertex corrections are zero. The fact that $\Sigma^R(m, \epsilon)$ is approximately a function of energy ϵ only is

a consequence of the short-range (or point-like) impurity potential. In the three-dimensional case without magnetic field the vertex corrections produce an additional factor $(1 - \cos\alpha)$ in the transport scattering relaxation time (α is the scattering angle). But the scattering probability is independent of the scattering angle in the case of point-like impurities and the additional term $\propto \cos\alpha$ vanishes after the integration over angles. Hence, the vertex corrections vanish.

In derivation of the formula (4.33) only first- and second-order terms in the small damping factors R_T and R_D were taken into account, assuming the harmonic damping to be strong. This is valid in the most experiments on quasi-2D organic metals where the amplitude of the second harmonic does not usually exceed 5% of the first harmonic. Formula (4.23) is valid at arbitrary harmonic damping.

So, the proposed theoretical description is valid in a large range of parameters which one has in real experiments on quasi-2D metals.

To summarize, in this section a quantitative theory of the Shubnikov - de Haas effect in quasi-2D metals is developed. The calculation is based on the Kubo formula that is more accurate than the calculation based on the Boltzmann transport equation, and gives much better agreement with experiment (see fig. 3). The final result is given in the analytical form, that allows a convenient comparison with any experimental data. The formulas (4.33-4.35) and (4.38) describe the general features of quasi-2D magnetoresistance and are applicable not only to the organic metals, but also to the heterostructures, intercalated compounds and other layered or quasi-2D metals. The property of the slow oscillations to remain at much higher temperatures than that of the usual quantum oscillations may be useful for studying the layered high-temperature superconductors.

Chapter 5

Discussion and prospects

Above we have summarized and extended a theory of magnetic quantum oscillations in 2D and quasi-2D compounds. These results are applicable to describing these oscillations in heterostructures, intercalated graphites, strongly anisotropic organic metals and other 2D or quasi-2D electron systems. The electronic properties of these compounds attract considerable interest and very many experiments are performed on magnetic quantum oscillations in these materials. Hence, the theory of the MQO in quasi-2D compounds is of great importance. The proposed results substantially improve and generalize the existing theories. The new results on magnetization (chapter 3) are applicable at arbitrary LL broadening, arbitrary temperature and spin-splitting, arbitrary reservoir density of states that exist, for example, in organic metals due to the additional open sheets of the Fermi surface. The theory of the Shubnikov - de Haas effect in quasi-2D metals (proposed in chapter 4) explains for the first time two very prominent qualitative deviations of the actual interlayer conductivity oscillations from the standard (and the only existing) 3D theory of this effect. It is shown that the quasi-two-dimensionality has a strong qualitative effect on magnetic quantum oscillations, especially on those of superconductivity. The comparison with the experimental data makes a strong proof of the proposed theory. Nevertheless, there are still many open questions and many effects are not considered in this thesis. Some of them are listed below.

1. Magnetic breakdown

One of these questions concerns the magnetic breakdown effects [for an introductory review see, for example, [1], Ch. 7]. The geometry of the FS of many quasi-2D ET-based organic metals implies also a magnetic breakdown, i.e. quantum tunneling of electrons from open sheets to closed orbits and vise versa. The magnetic breakdown effects have been observed in dif-

ferent ET-salts both in dHvA and in SdH measurements [e.g. [94]]. The most intriguing result of these studies is the observation of the so-called "forbidden frequencies" in the fast Fourier transform (FFT) of the dHvA and SdH oscillations, i.e. frequencies which are completely prohibited in the coupled-network model of magnetic breakdown (MB) developed by Pippard and Falikov and Stachowiak since they mean an abrupt reversion of the sense of rotation in the magnetic field. First, the forbidden frequencies were proposed to be due to oscillations of the chemical potential [95]. Then these forbidden frequencies were explained in terms of magnetic-field-dependent interaction of electronic states from the two partially occupied bands near the Fermi energy [96]. Even though some numerical calculations were done, no strict analytical study of this problem exists so far. In the LK theory, external magnetic field only fixes the cross-section of the FS. Contrary to this, the coherent magnetic breakdown changes the FS, and Landau bands appear which vary with the field. This phenomenon may be responsible for the "forbidden" frequencies both in dHvA and SdH oscillations and for many other interesting effects.

2. The interplay between the charge- or spin-density waves and the MQO

Open sheets of the FS in many organic metals can be nested which gives rise to the charge-density- (CDW)- or spin-density- waves (SDW). Both SDW and CDW drastically affect the quantum magneto oscillations (MQO) in ET-salts since they take place at the FS. In particular, opening of the Peierls gap at 1D open sheets would strongly decrease the magnetic breakdown probability of tunnelling on 2D sections of the FS, an thereby strongly affect MQO in ET-salts. Moreover, such a gap changes chemical potential oscillations. Some interesting observations of the interplay between the MQO and the density waves were reported in years. For example, the phase inversion of the Shubnikov oscillations at the point of a phase transition to density wave state or the stabilization of the chemical potential oscillations by the spin-density wave have been observed on some ET-salts. A hysteresis in magnetization [92] can probably also be attributed to this interplay. The commensurate and incommensurate DWs have different effects on chemical potential oscillations[93]. The interaction between the density waves and magnetic oscillations thus leads to new interesting effects that may be used to determine the nature of the phase transitions or to get information about the new electronic states. But there is no reliable theoretical description of these effects.

Another significant effect is the formation of magnetic field-induced charge-density-wave phases (FICDW) in quasi-2D organic compound[97]. Only very recently first experimental indications were reported[98] that unique FICDW

phenomenon is likely to exist in the pressurized a-(ET)2KHg(SCN)4. A detailed theory of this effect does not exist but it would be important for experimental observations and a study of this phenomenon.

3. Interplay of superconductivity and MQO

In many quasi-2D ET-based organic metals superconductivity can coexist with magnetic quantum oscillations. There are two kinds of problems in this context. First, what the effect of the superconductivity on the MQO is and vice versa. For more detail on this subject see, e.g. [37] and references therein.

The second even more intriguing question is the new unusual superconducting phases in quasi-2D organic superconductors. These are the "reentrant" superconductivity and the FFLO (Fulde-Ferrell-Larkin-Ovchinnikov) phase. Although they are of no immediate concern to quantum oscillations, I will make some remarks about these phases.

It is a point of a great interest that, in addition to the textbook Landau quantization of electron's energy in a magnetic field perpendicular to the conducting planes, some novel kind of quantum effects can be observed in quasi-2D (ET)-based materials in a parallel magnetic field. As was recently shown theoretically [99] quantum effects resulting from Bragg's reflections of electrons moving along open parts of the FS in a parallel magnetic field are crucial to magnetic properties of quasi-2D compounds. They result in an effective change of space dimensionality and, for example, lead to surviving of superconductivity in magnetic fields much higher than the quasi-classical upper critical field, Hc2. As was shown in the above-mentioned paper, superconducting temperature can even increase with increasing magnetic field. Recently survival of superconductivity at $H > Hc2$ was discovered in a layered Q1D $(TMTSF)_2PF_6$ superconductor [100]. All of this makes quasi-2D (ET)-based superconductors very attractive for a search for a novel high magnetic field superconducting phase surviving at $H > Hc2$.

Another unusual superconducting phase – the non-uniform FFLO state can also exist in some quasi-2D (ET)-based compounds since, as was shown in [101], since the existence of open sheets of the FS in quasi-2D compounds stabilizes the FFLO phase. Despite that the non-uniform FFLO state was predicted long time ago [102], all attempts to discover it have not been fully successful so far. The reason is that the peculiar properties of the LOFF phases are not well understood and, thus, it is experimentally difficult to distinguish the appearance of the LOFF phase from other possibilities. Recently, both experimental attempts to reveal the FFLO phase and theoretical studies (see for, example, [103]) of its properties have been much intensified. It was shown that in low-dimensional superconductors the region of stability of the FFLO phase is much wider than in the 3D case. In partic-

ular, in Q1D $(TMTSF)_2PF_6$ superconductors the LOFF phase is stable at $Hp < H < 2.5Hp$ [101]. Since a number of quasi-2D organic superconductors have both quasi-2D and Q1D parts of the FS, we expect that the LOFF phase can exist in a broad range of magnetic fields. There are reports of first experimental evidence that the LOFF phase exists in (ET)-based superconductors [104]. Nevertheless, due to a lack of key-point experimental test and strong 2D fluctuations in high parallel magnetic field, all reported experimental observations of the LOFF phase are still questionable.

In the present work all these 3 kinds of effects are not considered because it is a somewhat different field. There is a large variety of compounds where these effects do not exist. However, even in the normal state there are still some open questions. The most important of them, in my opinion, are: the effects of magnetic field tilting (with respect to normal to the conducting planes) and the so-called "noncoherent" regime of interlayer magnetotransport in which the interlayer transfer integral is less than $\pi\hbar/\tau$ where τ is the electron relaxation time. In addition, a more accurate calculation of the electron self-energy is needed for a reliable quantitative description; it should take into account scattering on lattice imperfections of different types and, if possible, the electron-electron interaction.

Angle-dependent magnetoresistance oscillations

Due to the strong anisotropy, the magnetoresistance in ET-salts has strong dependence on the tilt angle of the magnetic field with respect to the conducting planes. Conductivity on both the 1D and 2D sheets of the FS shows this strong dependence. The resistance on the 1D sheets of the FS shows pronounced oscillations as a function of tilt angle of magnetic field, while on the quasi-2D sheets the beat frequency of the MQO depends strongly on this tilt angle. The existing theoretical models of the angular dependence of magnetic quantum oscillations are based on the quasi-classical approximation or on the assumption that interlayer hopping probability is much less than the cyclotron frequency. These approximations cover only narrow ranges of parameters and are not applicable in many interesting cases. For example, they are not applicable to describing the MQO when the interlayer transfer integral is comparable to the cyclotron energy, especially near the zeros of the main term of the interlayer transfer integral.

On the other hand, most experiments on MQO in ET-salts are performed in tilted magnetic field. A dHvA study based on the torque measurements can be run only in tilted field. Hence, without a reliable theoretical description of the angular dependence of MQO the quantitative comparison between theory and experiment is impossible. Moreover, the angular dependence of magnetoresistance oscillations can provide additional information about the electronic properties of compounds. Hence, this question is important both

for magnetization and conductivity oscillations. Actually, this question is already under study but this segment of research is not completed yet.

Electronic density of states in quasi-2D ET-salts

The problem is to propose an accurate calculation of the density of states in quasi-2D compounds (ET-salt or heterostructures) taking into account their layered structure, different scattering mechanisms and (if possible) electron-electron interactions.

The existing DoS calculations based on the point-like impurity approximation can not explain why the DoS oscillations are so smooth. This may be due to other scattering mechanisms, due to approximations used in the calculations or due to many-particle effects. It would be going beyond the accuracy to treat the oscillations of the Dingle temperature before clearing up this question. Nevertheless, the oscillations of the Dingle temperature are shown (in Sec. 4.2.3) to be important for a quantitative analysis of slow oscillations.

Another problem is to take into account the diagrams with the intersection of the impurity line and the vertex corrections in the calculation of conductivity in magnetic field. This may be important as the transfer integral becomes less than the cyclotron energy. But the complete solution of this problem is very complicated and comparable to the complete description of the integer quantum Hall effect. To avoid this obstacle the results are intended for the case of rather large transfer integral. Fortunately, slow oscillations and the beats exist in just this case.

Chapter 6

Summary

This Ph.D. thesis is devoted to the theory of magnetic quantum oscillations in quasi-two-dimensional (quasi-2D) compounds. This problems became important last decades because of interest in strongly anisotropic materials. These materials are quasi-two-dimensional organic metals and heterostructures, intercalated compounds and high-T_c superconductors. All these compounds are very promising for both physics and technology. The thesis contains many new results in the theory of quasi-2D de Haas-van Alphen (dHvA) and Shubnikov - de Haas (SdH) effects.

Chapter 1 is an introduction into the problem. This chapter contains a short review of the standard approaches to the theory of dHvA and SdH effects: the 3D Lifshitz-Kosevich formula, Shoenberg's formula and the simplest approach to the 3D SdH effect. The standard 3D theory of magnetic quantum oscillations turned out to be inappropriate in two- or quasi-two-dimensional compounds. The geometry of the 2D or quasi-2D Fermi surface (correspondingly, the cylinder and the warped cylinder along the Landau levels in momentum space) leads to qualitative differences with the 3D case. These differences are explained in detail (simply and with many pictures) in the first and second chapters. Two-dimensional Shoenberg's formula does not take into account the chemical potential oscillations, and is certainly not applicable to the quasi-2D case when the warping of the Fermi surface cylinder is comparable to the cyclotron energy.

In the second chapter a simple analysis of the behavior of the chemical potential and magnetization in 2D electron gas in magnetic field is presented. We discuss in detail the effects of temperature, spin-splitting, Landau level broadening, finite density of states between Landau levels (due to localized states or the open sheets of the Fermi surface) and finite k_z dispersion. For obviousness, this discussion is supported by many pictures. All these effects have a strong influence on the magnetization oscillations and its envelope.

In the third chapter we present a more general calculation of magnetization oscillations in two and quasi-two-dimensional cases.

In Sec. 3.2 an explicit relation between the oscillating density of electron states and magnetization is derived. This relation, in principle, allows a direct measurement of the shape of the Landau levels. This is of interest because no reliable theoretical calculation of the LL shape in 2D compounds exists despite many attempts to do this have been done. From the theoretical point of view, the density of electron states is an intermediate step in the calculation of physical observables (such as specific heat, magnetization, acoustic attenuation etc.). Therefore, a test of the theoretical model on this intermediate step would be of essential importance). The procedure of extracting of the density of states from the magnetization curve is discussed in Sec. 3.1.2. In Sec. 3.1.3 I propose an experimental test of the one-particle approximation (approximation where the electron-electron (more rigorously, quasi-particle) interactions are neglected; this approximation is traditionally used to describe the magnetic quantum oscillations). In Sec. 3.1.4 the envelopes of the magnetization oscillations are calculated at finite temperature and for two different shapes of the Landau levels. The envelope (i.e. the magnetic field dependence of the amplitude) of the magnetization oscillations is the most evident from the experiment and, hence, is of an essential interest also.

In Sec. 3.2 the general formula of magnetization oscillations in quasi-2D compounds is derived. This formula takes into account arbitrary temperature and LL broadening, oscillations of chemical potential at arbitrary electron reservoir arising from the open sheets of the Fermi surface in many organic metals, arbitrary spin-splitting and warping of the Fermi surface. This formula describes the magnetization oscillations at the conditions very close to those of real experiments. Therefore, this result is important. Additional analysis (starting from this formula) is done in different limiting cases. For example, at zero temperature and warping of the Fermi surface one can solve the equations for the chemical potential and, hence, write down simple explicit formulas for magnetization at different values of the electron reservoir that may be important for an analytical study of different effects, for example, the influence of the chemical potential oscillations on magnetotransport.

Chapter 4 is devoted to magnetotransport phenomena in quasi-2D metals. The difference between the 3D and 2D magnetotransport is drastic. Very many books and reviews have been written already on the two-dimensional transport phenomena in magnetic field. Nevertheless, the intermediate case of quasi-2D metals has not received any special attention. No theory of the quasi-2D magnetotransport existed, and even qualitatively new effects were not understood. Chapter 4 of this Ph.D. thesis presents a development of

such a theory. Two different approaches have been applied to this problem: the Boltzmann transport equation (section 4.1) and a more rigorous calculation using the Kubo formula (section 4.2). Two novel qualitative effects in quasi-2D magnetotransport (namely, the slow oscillations of conductivity and the phase-shift of the beats) are explained and studied. A detailed comparison of the obtained theoretical results with the experimental data is performed. This comparison proves beyond doubts the proposed theoretical model. In simple words, contrary to the 3D magnetotransport the magneto-oscillations of the quasi-2D conductivity are given by not only oscillations of the electron relaxation time but also of the mean electron velocity on the Fermi surface. This results in a phase shift of the beats of the conductivity and magnetization oscillations. Slow oscillations come from the entanglement of the oscillations of different quantities in the conductivity. These slow oscillations do not have the usual temperature damping factor. Their temperature dependence is described in the text. The slow oscillations can be used to (i) determine the role and the value of the long-range potential fluctuations in the sample; (ii) to estimate the chemical potential oscillations; (iii) to get an additional information about the tilt angle dependence of the transfer integral and electron spectrum in layered compounds.

Several open problems and prospects of the theory and applications of quasi-2D magnetic quantum oscillation phenomena are outlined in chapter 5. Some calculations and mathematical formulas that would obscure the simple picture if included in the main text, are moved to the Appendix.

Chapter 7

Some calculations and mathematical formulas

7.1 Transformation of sums over LLs to sums over harmonics

7.1.1 The Poisson summation formula

It is usually convenient to transform a sum over LLs to a sum over harmonics using the Poisson summation formula, [[22] Ch. 9].

In the range $n < x < n + 1$ we can write

$$f(x) = \sum_{s=-\infty}^{+\infty} e^{-2ixs} g_s$$

where

$$g_s = \int_n^{n+1} f(x') e^{2ix's} dx'.$$

This is just a Fourier series. Now we can write

$$f\left(n + \frac{1}{2}\right) = \sum_{s=-\infty}^{+\infty} e^{2\pi i s(n+1/2)} g_s = \sum_{s=-\infty}^{+\infty} e^{-i\pi s} g_s = \sum_{s=-\infty}^{+\infty} (-1)^s \int_n^{n+1} f(x) e^{2\pi i x s} dx.$$

Now summing this over all intervals of the variable x, we have

$$\sum_{n=0}^{\infty} f\left(n+\frac{1}{2}\right) = \int_0^{\infty} f(x)dx + \\ +2\sum_{s=1}^{\infty}(-1)^s \int_0^{+\infty} f(x)\cos(2\pi x s)dx. \qquad (7.1)$$

This mathematical trick of the transformation of the sum in energy space into the sum over harmonics is useful when the Fermi surface crosses many Landau levels, and magnetization smoothly oscillates with magnetic field. It was introduced into the theory of the dHvA by Landau.

7.1.2 Transformations of sums over LLs to sums over harmonics in the quasi-2D case

To transform sums over LL number into harmonic sums we apply the Poisson summation formula (7.1) that can be rewritten as

$$\sum_{n=n_0}^{\infty} f(n) = \sum_{k=-\infty}^{\infty} \int_a^{\infty} e^{2\pi i k n} f(n)\, dn\,, \quad \text{where } a \in (n_0-1; n_0).$$

This formula is valid for arbitrary function $f(n)$. The sum in (4.18) becomes

$$\begin{aligned}
\sum_n |v_z(\epsilon, n)| &= \sum_{n=0}^{\infty} \frac{d}{\hbar}\sqrt{4t^2 - \left(\epsilon - \hbar\omega_c\left(n+\frac{1}{2}\right)\right)^2} = \\
&= \frac{d}{\hbar}\hbar\omega_c \sum_{k=-\infty}^{\infty} \int_0^{\infty} dn\, \exp\left(2\pi i k\left(n-\frac{1}{2}\right)\right) \sqrt{\left(\frac{2t}{\hbar\omega_c}\right)^2 - \left(\frac{\epsilon}{\hbar\omega_c} - n\right)^2} \\
&= \frac{d}{\hbar}\hbar\omega_c \sum_{k=-\infty}^{\infty} (-1)^k \exp\left(\frac{2\pi i k\epsilon}{\hbar\omega_c}\right) \int_{-\infty}^{\infty} dx\, \exp\left(2\pi i k x\right) \sqrt{\left(\frac{2t}{\hbar\omega_c}\right)^2 - x^2} \\
&= \sum_{k=-\infty}^{\infty} \frac{dt}{\hbar k} (-1)^k \exp\left(\frac{2\pi i k\epsilon}{\hbar\omega_c}\right) J_1\left(\frac{4\pi k t}{\hbar\omega_c}\right). \qquad (7.2)
\end{aligned}$$

In a similar manner, we can also transform the sum

$$\frac{\pi}{N_{LL}}\rho_0(\epsilon) = \sum_{n=0}^{\infty} \frac{1}{\sqrt{4t^2 - \left(\epsilon - \hbar\omega_c\left(n+\frac{1}{2}\right)\right)^2}} = \qquad (7.3)$$

$$= \frac{1}{\hbar\omega_c}\sum_{k=-\infty}^{\infty}\int_0^{\infty}\frac{dn\,\exp\left(2\pi ik\left(n-\frac{1}{2}\right)\right)}{\sqrt{\left(\frac{2t}{\hbar\omega_c}\right)^2-\left(\frac{\epsilon}{\hbar\omega_c}-n\right)^2}} =$$

$$= \frac{1}{\hbar\omega_c}\sum_{k=-\infty}^{\infty}(-1)^k\exp\left(\frac{2\pi ik\epsilon}{\hbar\omega_c}\right)\int_{-\infty}^{\infty}\frac{dx\,\exp\left(2\pi ikx\right)}{\sqrt{\left(\frac{2t}{\hbar\omega_c}\right)^2-x^2}} =$$

$$= \frac{\pi}{\hbar\omega_c}\sum_{k=-\infty}^{\infty}(-1)^k\exp\left(\frac{2\pi ik\epsilon}{\hbar\omega_c}\right)J_0\left(\frac{4\pi kt}{\hbar\omega_c}\right) \tag{7.4}$$

7.2 Calculation of magnetization and its envelope in the quasi-2D case at weak warping

In this appendix we calculate magnetization and its envelope at finite warping of the Fermi surface. This warping $W = 4t$ is the width of the band to which each LL develops due to finite k_z dispersion. The calculation is performed at finite temperature but at sharp Landau levels. We consider warping to be smaller (not necessarily much smaller) than the energy level separation: $W < \Delta$. If spin-splitting is a multiple of the cyclotron energy $\hbar\omega_c$, the energy level separation $\Delta = \hbar\omega_c$ is just the Landau level separation. Otherwise, there are two different values of the energy level separation, Δ_1, Δ_2, $\Delta_1 + \Delta_2 = \hbar\omega_c$, in accordance with the value of the spin-splitting energy.

7.2.1 Chemical potential

In order to calculate magnetization we need first to obtain an expression for chemical potential $\mu(B)$. Let us write the number of particles as a sum over all Landau levels with the Fermi distribution function f_n:

$$N = \frac{ga}{2\pi\hbar}\sum_{n=0}^{\infty}\int_0^{\frac{2\pi\hbar}{a}} f_n dp_z \quad , \tag{7.5}$$

where g is the degeneracy of a LL, a is the lattice constant in the z direction (the 2D layer separation in heterostructures) and N is the number of particles in one layer. The chemical potential is situated between two LLs with energies $\hbar\omega_c(n_F - \frac{1}{2})$ and $\hbar\omega_c(n_F + \frac{1}{2})$ where $\omega_c = eB/m^*c$ is the cyclotron frequency. Since we assume $\hbar\omega_c \gg kT$, only these two Landau levels make contribution to thermodynamics. Thus, we can set $f_n = 1$ for all

$n < n_F - 1$ and $f_n = 0$ for all $n > n_F$:

$$N = (n_F - 1)g + \frac{ga}{2\pi\hbar}\int_0^{\frac{2\pi\hbar}{a}} (f_{n_F-1} + f_{n_F})dp_z \quad .$$

The energy of electron is given by $E = \hbar\omega_c(n + \frac{1}{2}) + E_z$, where n is the number of the LL and the term $E_z = \frac{W}{2}[1 - \cos(p_z a/\hbar)]$ gives the dependence of energy on the momentum along the z axis. For ideal two-dimensional case we have $W = 0$, and $W \neq 0$ takes into account warping of the Fermi surface. Later for convenience we shall use another expression for E_z :

$$E_z = \frac{W}{2}\cos\left(\frac{p_z a}{\hbar}\right). \tag{7.6}$$

The difference between expression (7.6) and the previous one consists in only a shift of the starting point of energy by a constant $W/2$ (which of course does not change any physical result) and a shift of the starting point of quasi-momentum p_z by $\pi\hbar/a$ (that makes no difference because of the subsequent integration over the full period of p_z). Substituting the expression for $f_n = \dfrac{1}{1 + \exp(\frac{E-\mu}{kT})}$ into Eq. (7.5) we find

$$\begin{aligned}\frac{N}{g} - (n_F - 1) &= \frac{1}{2\pi}\int_0^{2\pi} \frac{\mathrm{d}y}{1 + \exp(X_F - \alpha)\exp(\frac{W}{2kT}\cos y)} \\ &\quad + \frac{1}{2\pi}\int_0^{2\pi} \frac{\mathrm{d}y}{1 + \exp(X_F + \alpha)\exp(\frac{W}{2kT}\cos y)} \quad , \end{aligned} \tag{7.7}$$

where $y = p_z a/\hbar$, $X_F = \dfrac{\hbar\omega_c n_F - \mu}{kT}$, and $\alpha = \dfrac{\hbar\omega_c}{2kT}$. In order to calculate the integral we will use the condition

$$\exp\left(-\alpha + \frac{W}{2kT} \pm X_F\right) \ll 1 \tag{7.8}$$

which, as will be shown later, is equivalent to $\sqrt{\alpha} \gg 1$ and even for $W \sim \hbar\omega$ is usually met in experiments. Hence, one can expand (7.7) in small parameter (7.8) keeping only the first two terms:

$$\begin{aligned}\frac{N}{g} - (n_F - 1) &= \frac{1}{2\pi}\int_0^{2\pi}\left[1 - e^{X_F-\alpha}\exp\left(\frac{W\cos y}{2kT}\right) + e^{-X_F-\alpha}\exp\left(\frac{-W\cos y}{2kT}\right)\right]\mathrm{d}y = \\ &= 1 - e^{-\alpha}\cdot 2\sinh X_F \cdot \; I_0\left(\frac{W}{2kT}\right) \end{aligned} \tag{7.9}$$

where $I_0(W/2kT)$ is the modified Bessel function of argument $W/2kT$. The sign in the exponents $\exp(\pm\frac{W}{2kT}\cos y)$ in (7.9) makes no difference because

of the integration over symmetric values of $\cos y$ (and one can replace $\cos y$ by $-\cos y$ in the integrand). Now we have

$$\frac{N}{g} - n_F = \tilde{n} = -e^{-\alpha} \cdot 2 \sinh X_F \cdot I_0\left(\frac{W}{2kT}\right). \tag{7.10}$$

Later we use the notation $\tilde{n} = \frac{N}{g} - n_F$. Equation (7.10) can be easily solved with respect to chemical potential:

$$\sinh X_F = -\frac{\tilde{n}e^{\alpha}}{2I_0(\frac{W}{2kT})} \ , \Rightarrow \qquad \mu = \hbar\omega_c n_F + kT \operatorname{arsh}\left(\frac{\tilde{n}e^{\alpha}}{2I_0(\frac{W}{2kT})}\right). \tag{7.11}$$

Let us see the limiting cases of the obtained expression for μ. For this purpose we need the asymptotic behavior of the modified Bessel function:

$$I_0(x) = 1 + \frac{x^2}{4} + \cdots \quad , \quad x \ll 1 \tag{7.12}$$

$$I_0(x) = \exp(x) \cdot \sqrt{\frac{1}{2\pi x}} \ , \quad x \gg 1. \tag{7.13}$$

For $\frac{W}{2kT} \ll 1$, formula (7.11) coincides with the expression for chemical potential without warping of the Fermi surface [17]

$$\mu = \hbar\omega_c n_F - kT \ln\left(\frac{-\tilde{n}\cosh\alpha + \sqrt{1 + \tilde{n}^2 \sinh^2\alpha}}{1 + \tilde{n}}\right)$$

To show this we simplify this expression using $\tilde{n}e^{\alpha} \gg 1$:

$$\begin{aligned} \mu &= \hbar\omega_c n_F - kT \ln\left[\frac{-\tilde{n}\cosh\alpha + \tilde{n}\cosh\alpha \cdot \left(1 + \frac{1-\tilde{n}^2}{2\tilde{n}^2\cosh^2\alpha}\right)}{1 + \tilde{n}}\right] \\ &= \hbar\omega_c n_F - kT \ln\left(\frac{2\tilde{n}\cosh\alpha}{1 - \tilde{n}}\right) \simeq \hbar\omega_c n_F - kT \ln\left(\frac{\tilde{n}e^{\alpha}}{1 - \tilde{n}}\right). \end{aligned} \tag{7.14}$$

Taking into account identity $\operatorname{asinh} x = \ln(x + \sqrt{1 + x^2})$ and inequality $\tilde{n}e^{\alpha} \gg 1$ we can rewrite formula (7.11) in the form

$$\mu = \hbar\omega_c n_F - kT \ln(\tilde{n}e^{\alpha}).$$

In the limit $\tilde{n} \ll 1/\sqrt{\alpha}$, when formula (7.11) is valid, it then coincides with (7.14).

7.2.2 Magnetization

For calculating the thermodynamic potential we use its definition:

$$\Omega = -kT\frac{ga}{2\pi\hbar}\int_0^{\frac{2\pi\hbar}{a}}\sum_{n=0}^{\infty}\ln\left(1+e^{\frac{\mu-E_n(p_z)}{kT}}\right)\,\mathrm{d}p_z \tag{7.15}$$

The calculation of the sum and the integral is analogues to the procedure used for chemical potential.

Making the expansion over the same small parameter $\exp(-\alpha+\frac{W}{2kT}\pm X_F)\ll 1$ and separating the contribution from the last two LLs we obtain

$$\begin{aligned}\Omega &= g\sum_{n=0}^{n_F-2}(\hbar\omega_c(n+\frac{1}{2})-\mu)+\\ &+\frac{gkT}{2\pi}\int_0^{2\pi}\left[(X_F-\alpha+\frac{W}{2kT}\cos y)-e^{X_F-\alpha}\exp(\frac{W}{2kT}\cos y)\right]\mathrm{d}y\\ &+\frac{gkT}{2\pi}\int_0^{2\pi}\left[-e^{-X_F-\alpha}\exp(\frac{-W}{2kT}\cos y)\right]\mathrm{d}y\end{aligned}$$

After taking the integrals and the sum we finely obtain

$$\Omega = g\left[\frac{{n_F}^2}{2}\hbar\omega_c-\mu n_F\right]-gkT\;e^{-\alpha}\cdot 2\cosh X_F\cdot I_0\left(\frac{W}{2kT}\right).$$

It is easy to check that in the limit $\frac{W}{2kT}\ll 1$ and $\tilde{n}\ll 1$ this formula coincides with the expression for thermodynamic potential in the 2D case of ideally cylindric Fermi surface[17]

$$\Omega = g\left[\frac{{n_F}^2}{2}\hbar\omega_c-\mu n_F+\frac{1}{2}\hbar\omega_c-kT\ln\left(2\cosh X_F+2\cosh\alpha\right)\right]$$

(to check this equivalence one should use $\cosh X_F\simeq\frac{|\tilde{n}|e^{\alpha}}{2I_0(\frac{W}{2kT})}\ll\cosh\alpha$) .

Free energy:

$$\begin{aligned}F &= \Omega+\mu N=\\ &= g\left\{\frac{{n_F}^2}{2}\hbar\omega_c+\left(\frac{N}{g}-n_F\right)\mu-kT\;e^{-\alpha}\cdot 2\cosh X_F\cdot I_0\left(\frac{W}{2kT}\right)\right\}.\end{aligned}$$

Now we can calculate the magnetization,

$$M=-\frac{\partial F}{\partial B}=-\frac{\partial F}{\partial\omega_c}\frac{e}{m^*c}-\frac{\partial F}{\partial g}\frac{S}{\Phi_0}-\frac{\partial F}{\partial\mu}\frac{\partial\mu}{\partial B} \tag{7.16}$$

(where $S-$ is the area of the sample and Φ_0- is the magnetic flux quantum). Now one only has to take this derivative accurately. We won't describe this procedure in detail but write out some intermediate steps for making it easier to follow the calculations:

1.
$$\frac{\partial F}{\partial \omega_c} = g\hbar \left\{ \frac{{n_F}^2}{2} + e^{-\alpha} \cdot I_0\left(\frac{W}{2kT}\right) [\cosh X_F - 2n_F \sinh X_F] \right\}$$

2.
$$\frac{\partial F}{\partial g} = \hbar\omega_c \frac{{n_F}^2}{2} - \mu n_F - kT\ e^{-\alpha} \cdot 2\cosh X_F \cdot I_0\left(\frac{W}{2kT}\right) =$$
$$= -\hbar\omega_c \frac{{n_F}^2}{2} - n_F kT \cdot \operatorname{arsh}\left(\frac{\tilde{n}e^{\alpha}}{2I_0(\frac{W}{2kT})}\right) - kTe^{-\alpha} \cdot 2\cosh X_F \cdot I_0\left(\frac{W}{2kT}\right)$$

3.
$$\frac{\partial F}{\partial \mu} = g\left[\tilde{n} + e^{-\alpha} \cdot I_0\left(\frac{W}{2kT}\right) \cdot 2\sinh X_F\right] = 0 \quad (\text{ see } (7.10)\ )$$

Substituting this into (7.16) and taking into account $g\hbar\frac{e}{m^*c} = \hbar\omega_c\frac{S}{\Phi_0}$ we get

$$M = \frac{S}{\Phi_0}\hbar\omega_c \left\{ -n_F\tilde{n} + \frac{n_F}{2\alpha}\operatorname{arsh}\left(\frac{\tilde{n}e^{\alpha}}{2I_0(\frac{W}{2kT})}\right) + e^{-\alpha} \cdot I_0\left(\frac{W}{2kT}\right) \cdot \cosh X_F \cdot \left(-1 + \frac{1}{\alpha}\right) \right\} \tag{7.17}$$

This is the expression for magnetization with warped Fermi surface. The only restriction on the magnitude W of the warping is that it must not be greater than the energy difference between LLs.

Formula (7.17) is valid only in the narrow region

$$\tilde{n} \ll I_0\left(\frac{W}{2kT}\right) e^{\frac{-W}{2kT}} \simeq \min\left\{\sqrt{\frac{kT}{\pi W}}, 1\right\}, \tag{7.18}$$

where the condition (7.8), $\exp(-\alpha + \frac{W}{2kT} \pm X_F) \simeq \dfrac{\tilde{n}e^{\frac{W}{2kT}}}{I_0\left(\frac{W}{2kT}\right)} \ll 1$, is satisfied.

What we are interested in is the envelope of magnetization oscillations, i.e. the amplitude of these oscillations as a function of magnetic field, temperature and the size of warping, because experiments detect only this amplitude. To calculate this amplitude one only need to know the values of maxima and minima of magnetization oscillations. So if these extrema of magnetization get into these narrow regions of $\tilde{n}$ or B, then we can use formula (7.17) to calculate the envelope. As will be shown later, these extrema of $M(B)$ occur at $\tilde{n} \simeq \frac{1}{2\alpha}$, so that condition (7.18) is usually satisfied (this restriction for $W \sim \hbar\omega_c$ is equivalent to $\sqrt{\alpha} \gg 1$).

7.2.3 The magnetization envelope

Let us turn to calculating the envelope of $M(B)$. Since $|\sinh X_F| = \left|-\tilde{n}e^{\alpha}/2I_0(\frac{W}{2kT})\right| \gg 1$, we have $\cosh X_F \simeq |\sinh X_F| = |\tilde{n}|e^{\alpha}/2I_0(\frac{W}{2kT})$, and the expression for magnetization (7.17) can be replaced by

$$\begin{aligned} M &= \frac{S}{\Phi_0}\hbar\omega_c\left\{-\tilde{n}(n_F+1)+\frac{n_F}{2\alpha}\mathrm{arsh}\left(\frac{\tilde{n}e^{\alpha}}{2I_0(\frac{W}{2kT})}\right)\right\} = \\ &= \frac{SE_F}{\Phi_0}\left\{-\tilde{n}(1+\frac{1}{n_F})+\frac{1}{2\alpha}\mathrm{arsh}\left(\frac{\tilde{n}e^{\alpha}}{2I_0(\frac{W}{2kT})}\right)\right\} \end{aligned} \tag{7.19}$$

where E_F is the Fermi energy of electrons without magnetic field. In order to find the amplitude of magnetization oscillations one has to differentiate (7.19) with respect to B. Taking into account that $n_F(B) = const$ for each interval of B where the extrema occur, we find

$$\frac{\partial M}{\partial B} \approx \frac{\hbar\omega_c}{B}\frac{gn_F}{B}\left\{n_F+\frac{3}{2}-\frac{n_F}{2\alpha}\frac{1}{|\tilde{n}|}\right\} = 0 \quad , \qquad \Rightarrow$$

$$\tilde{n}_{ex} = \pm\frac{1}{2\alpha}\frac{n_F}{n_F+3/2}. \tag{7.20}$$

The values B_{ex} of magnetic field at which magnetization M has extrema are given by

$$B_{ex} = B^*\left(1 \pm \frac{1}{2\alpha(n_F+3/2)}\right). \tag{7.21}$$

To obtain the envelope of magnetization one should substitute extreme values of $\tilde{n}_{ex}$ into (7.19) :

$$M_{\pm} = \pm\frac{SE_F}{2\Phi_0}\left\{\frac{1}{\alpha}\mathrm{arsh}\left(\frac{e^{\alpha}}{4\alpha I_0(\frac{W}{2kT})}\frac{n_F}{n_F+3/2}\right)-\frac{1}{\alpha}\frac{n_F+1}{n_F+3/2}\right\}. \tag{7.22}$$

All the above calculations were made for spinless electrons. To generalize them one should substitute all $\hbar\omega_c$ in the resulting formula by the real distances between energy levels; this takes into account the spin splitting. These distances will depend periodically on magnetic field, and this period in the energy scale is equal to the LL separation. If the spin-orbit interaction is weak compared to the cyclotron energy, the spin up states add one level between each two LLs with spin down no matter what the ratio of spin splitting energy to the distance between LLs is (we assume that g-factor of electrons is independent of magnetic field). In special cases, when the spin

splitting energy is just n-times the distance between LLs (with the precision of the temperature or the LL broadening), formula (7.22) acquires only a factor 2, because the effect of spin on magnetization oscillations in this case is only to double the degeneracy of the LLs. Then we get formula (2.19) for the envelope of magnetization oscillations.

7.3 The absence of slow oscillations in magnetization

The first harmonic of the oscillating part of magnetization is given by (3.59)(from [38], formula 6)

$$\tilde{M}(B) = \frac{2N_{LL}\varepsilon_F}{\pi B} \sin\left(\frac{2\pi\left(\varepsilon_F + \tilde{\mu}(B)\right)}{\hbar\omega_c}\right) J_0\left(\frac{4\pi t}{\hbar\omega_c}\right) R_T R_S R_D(\varepsilon_F). \quad (7.23)$$

where the oscillating part of the chemical potential is given by (3.57) (from [38], formula 5)

$$\tilde{\mu}(B) = \frac{\hbar\omega_c}{\pi(1+n_R(\varepsilon_F))} \times \sin\left(\frac{2\pi\left(\varepsilon_F + \tilde{\mu}(B)\right)}{\hbar\omega_c}\right) J_0\left(\frac{4\pi t}{\hbar\omega_c}\right) R_T R_S R_D. \quad (7.24)$$

The entanglement of magnetization oscillations (7.23) with the oscillations of the Dingle factor (4.22) produces an additional term

$$\propto \sin\left(\frac{2\pi\varepsilon_F}{\hbar\omega_c}\right) J_0\left(\frac{4\pi t}{\hbar\omega_c}\right) \times \cos\left(\frac{2\pi\varepsilon_F}{\hbar\omega_c}\right) J_0\left(\frac{4\pi t}{\hbar\omega_c}\right)$$

$$= \frac{1}{2}\sin\left(\frac{4\pi\varepsilon_F}{\hbar\omega_c}\right) J_0^2\left(\frac{4\pi t}{\hbar\omega_c}\right)$$

which give rise to the second harmonic but makes zero contribution to the slow oscillations of magnetization.

The entanglement with the oscillations of the chemical potential (7.24) produces the term

$$\propto \sin\left(\frac{2\pi\left(\varepsilon_F + \tilde{\mu}(B)\right)}{\hbar\omega_c}\right) - \sin\left(\frac{2\pi\,\varepsilon_F}{\hbar\omega_c}\right)$$

$$= \sin\left(\frac{2\pi\varepsilon_F}{\hbar\omega_c}\right)\left[\cos\left(\frac{2\pi\tilde{\mu}(B)}{\hbar\omega_c}\right) - 1\right] + \cos\left(\frac{2\pi\varepsilon_F}{\hbar\omega_c}\right) \sin\left(\frac{2\pi\varepsilon_F}{\hbar\omega_c}\right) J_0\left(\frac{4\pi t}{\hbar\omega_c}\right) \frac{2R_T R_D}{1+n_R}$$

which also contribute only to the second harmonics (or higher harmonics) but not to slow oscillations.

Bibliography

[1] Shoenberg D. "Magnetic oscillations in metals", Cambridge University Press, 1984

[2] D. Schoenberg – Proc. Roy. Soc. A, v.170, p.341 (1939)

[3] W.J. de Haas, P.M. van Alfphen – Leiden Commun. A, v. 212, p. 215 (1930) ; Proc. Amsterdam Acad. Sci., v. 33, p. 1106 (1930)

[4] L.M.Lifshitz and A.M.Kosevich, Zh. Eksp. Teor. Fiz. **29,** 730 (1956).

[5] L. D. Landau Z. Phys. **64**, 629 (1930).

[6] I.M.Lifshitz and A.M.Kosevich, Zh.Eksp.Teor.Fiz.**29** ,730(1956) [Sov.Phys.JETP **2**,636(1956)].

[7] R. Peierls, Z. Phys. **81**, 186 (1933);

[8] A.A. Abrikosov, *Fundamentals of the theory of metals*, North-Holland, 1988

[9] L. Onsager, Phil. Mag. **43**, p. 1006 (1952)

[10] E.N. Adams, T.D. Holstein, J. Phys. a. Chem. Solids, v. 10, p. 254 (1959); A.A. Abrikosov, Zh. Ex. Teor. Fiz. **56**, p. 1391 (1969)

[11] J.P. Eisenstein, H.L. Störmer, V. Narayanamurti, A.Y. Cho, A.C. Gossard and C.W.Tu, Phys. Rev. Lett.**55**, 875 (1985);

[12] W. Joss, J.M. van Ruitenbeek, I.D. Vagner, F. Jost, F. Rachdi and S. Roth, Synth. Met., **34**, 381 (1989).

[13] R.S. Markiewicz, M. Meskoob and B. Maheswaran, Phys. Rev. B **36** (1987) 7859; B. Maheswaran and R.S. Markiewicz, Phys.Rev.B **39**, 1946 (1989);

[14] J. Wosnitza et al. Phys. Rev. B**45**, 3018 (1992).

[15] I.D. Vagner, T. Maniv and E. Ehrenfreund, Phys. Rev. Lett. **51** 1700 (1983); I.D. Vagner and T. Maniv, Phys. Rev. B**32**, 8398 (1985).

[16] D. Shoenberg, J. Low Temp. Phys. **56** 417 (1984)

[17] K.Jauregui, V.I.Marchenko, I.D.Vagner, Phys. Rev. B **41**, Rapid Comm., 12922 (1990)

[18] D. Hofstadter, Phys. Rev. B **14**, 2239 (1976); M. Ya. Azbel', Sov. Phys. JETP **19**, 634 (1964).

[19] Ju. H. Kim and I. D. Vagner Phys. Rev. B. **48** 16564 (1994).

[20] L. D. Landau and E. M. Lifshitz, Statistical Physics, 2nd ed. (Pergamon Press, Oxford, England, 1969).

[21] R.Peierls, *Surprises in Theoretical Physics*, Princeton Univ. Press, Princeton, 1979

[22] J. M. Ziman, *Principles of the Theory of Solids*, (Cambridge, Univ. Press, 1972).

[23] S. A. J. Wiegers, M. Specht, L. P. Levy et al. , Phys. Rev. Lett. **79**, p. 3238 (1997)

[24] N. Harrison, A. House, I. Deckers et al. , Phys. Rev. B **52**, 5584 (1995).

[25] P. S. Sandhu, G. J. Athas, J. S. Brooks et al. , Surf. Sci. **361-362**, 913 (1996).

[26] V. N. Laukhin, A. Audouard, H. Rakoto et al. , Physica B **211**, 282 (1995)

[27] K. Jauregui, W. Joss, V. I. Marchenko, and I. D. Vagner, (in *High Magnetic Fields in Semiconductor Physics* III, edited by H.K.V.Lotsch, Springer Series in Solid-State Sciences 101, Springer-Verlag, Berlin, 1992), p. 668.

[28] N. Toyota, E. W. Fenton, T. Sasaki and M. Tachiki, Solid State Commun. **72**, 859 (1989)

[29] J. Singleton, F. L. Pratt, M. Doporto et al., Phys. Rev. Lett. **68**, 2500 (1992)

[30] T. Sasaki and N. Toyota, Phys. Rev. B **49**, p. 10120 (1994)

[31] N.E.Alekseevskii and V.I.Nizhanovskii, Zh. Eksp. Teor. Fiz. **88,** 1771 (1985).

[32] V.M. Gvozdikov, Fiz. Tverd. Tela **26**, p. 2574 (1984) [Sov. Phys. Solid State **26** (9), p. 1560 (1984)]

[33] K. Jauregui, V.I. Marchenko, I.D. Vagner, Phys. Rev. B **41,**, 12922 (1990).

[34] N. Harrison et al., Phys. Rev. B **54**, 9977 (1996).

[35] P. Grigoriev, I. Vagner, JETP Letters **69** (2), p.145 (1999)

[36] M.A. Itskovsky, T. Maniv, I.D. Vagner, Phys. Rev. B **61**, 14616 (2000)

[37] T. Champel and V.P. Mineev, Phil. Magazine B **81**, 55 (2001) or cond-mat/0006156.

[38] P. Grigoriev, Zh. Eksp. Teor. Fiz. **119**(6), 1257 (2001) [JETP **92**, 1090 (2001)] .

[39] T. Champel, Phys. Rev. B 64, 054407 (2001)

[40] J-Y Fortin, J. Bellissard, M. Gusmao and T. Ziman, Phys. Rev. B **57** p. 1484 (1998).

[41] M.Ya. Azbel, Phys. Rev. B **33**, 8844 (1986)

[42] J. Wosnitza, E. Balthes, N. Harrison et al., Phys. Rev. B **61**, 7383 (2000)

[43] F.A.Meyer, A.G.M. Jansen, W.Joss et al, Europhys. Lett. **32**, p. 681 (1995)

[44] J-Y Fortin, T.Ziman, Phys. Rev. Lett. **80**, p. 3117 (1998)

[45] M.A.Itskovsky, S. Askenazy, T. Maniv et al. , Phys. Rev. B **58,** p. 13347 (1998)

[46] "*Standard Mathematical Tables and Formulae*", CRC Press, 1996

[47] R. Peierls, Z. Phys. **81**, 186 (1933)

[48] J. H. Condon, Phys. Rev. **45**, 526 (1966)

[49] R.B. Dingle, Proc. Roy. Soc. **A211,** 517 (1952)

[50] Yu. A. Bychkov, Zh. Exp. Theor. Phys. **39,** 1401 (1960), [Sov. Phys. JETP **12,** 977 (1961)]

[51] T.Ando and Y.Uemura, Journal of the Physical Society of Japan **36**, p. 959 (1974)

[52] K.B.Efetov, V.G.Marikhin, Phys. Rev. B **40**, p. 12126 (1989) and references therein

[53] T.Maniv, I.Vagner, Phys. Rev. B **38,** 6301 (1988)

[54] X.C. Xie, Q.P. Li and S. Das Sarma, Phys. Rev. B **42,** 7132 (1990)

[55] P. Grigoriev, I. Vagner, cond-mat /0009409

[56] J. Wosnitza, G.W. Crabtree, H.H. Wang et al., Phys. Rev. Lett. **67**, 263 (1991)

[57] S. Hill, Phys. Rev. B **55,** 4931 (1997)

[58] N. Harrison, R. Bogaerts, J. Singleton et al., Phys. Rev. B 54, 9977 (1996)

[59] T. Ishiguro, K. Yamaji and G. Saito, *Organic Superconductors*, 2nd Edition, Springer-Verlag, Berlin, 1998.

[60] J. Wosnitza, *Fermi Surfaces of Low-Dimensional Organic Metals and Superconductors* (Springer-Verlag, Berlin, 1996); M.V. Kartsovnik and V.N. Laukhin, J. Phys. I France **6**, 1753 (1996); J. Singleton, Rep. Prog. Phys. **63**, 1111 (2000).

[61] W. Kang, G. Montambaux, J. R. Cooper, D. Jerome, P. Batail and C. Lenoir, Phys. Rev. Lett. **62**, 2559 (1989).

[62] V.N. Laukhin, A. Audouard, H. Rakoto et al., Physica B **211**, 282 (1995).

[63] A.E.Datars and J.E.Sipe, Phys. Rev. B **51**, 4312 (1995)

[64] P. Moses and R.H. McKenzie, Phys. Rev. B **60**, 7998 (1999)

[65] V.M. Gvozdikov, Fiz. Nizk. Temp. **27** (9/10), p. 956 (2001) [Sov. J. Low Temp. Phys. **27**(9/10) (2001)].

[66] P.D. Grigoriev, M.V. Kartsovnik, W. Biberacher, N.D. Kushch, P. Wyder, Phys. Rev. B **65**, 60403(R) (2002).

[67] N.S. Averkiev, L.E. Golub, S.A. Tarasenko and M. Willander, J. of Phys. Cond. Matter **13**, 2517 (2001).

[68] A.P. Mackenzie, S.R. Julian, A.J. Diver et al., Phys. Rev. Lett. **76**, 3786 (1996); C. Bergemann, S.R. Julian, A.P. Mackenzie, S. NishiZaki and Y. Maeno, Phys. Rev. Lett. **84**, 2662 (2000).

[69] H. Weiss, M. V. Kartsovnik, W. Biberacher, E. Balthes, A.G.M. Jansen, and N.D. Kushch, Phys. Rev. B **60**, R16259 (1999).

[70] M.Schiller, W.Schmidt, E.Balthes et al., Europhys. Lett. **51**, 82 (2000).

[71] J.M. Williams, H.H. Wang, M.A. Beno et al., Inorg. Chem. **23**, 3839 (1984).

[72] An observation of slow oscillations of the resistivity resembling strongly the SdH effect have lead to a suggestion of an additional, very small FS pockets in this compound [73]. However, the recent analysis [75] have shown that such oscillations may originate from the strongly anisotropic character of the main FS cylinder and do not necessarily invoke additional pockets.

[73] M.V. Kartsovnik, P.A. Kononovich,V.N. Laukhin and I.F. Schegolev, , Pis'ma Zh. Eksp. Teor. Fiz. **48**, 498 (1988) [Sov. Phys. JETP Lett. **48**, 541 (1988)]; M.V. Kartsovnik, P.A.Kononovich, V.N.Laukhin, S.I.Pesotskii and I.F.Schegolev, Zh. Eksp. Teor. Fiz. **97**, 1305 (1990) [Sov. Phys. JETP **70**, 735 (1990)]; M.V. Kartsovnik, V.N.Laukhin, S.I.Pesotskii, I.F.Schegolev and V.M.Yakovenko, J. Phys. I France **2**, 89 (1992).

[74] M.V. Kartsovnik, P.D. Grigoriev, W. Biberacher, N.D. Kushch, P. Wyder, Phys. Rev. Lett. **89**, 126802 (2002).

[75] P.D. Grigoriev, submitted for publication (cond-mat/0204270).

[76] J. Wosnitza, G.W. Crabtree, K.D. Carlson, H.H. Wang and J.M. Williams, Physica B **194-196**, 2007 (1994); J. Wosnitza, G. Goll, D. Beckmann, S. Wanka, D. Schweitzer and W. Strunz, J. Phys. I France **6**, 1597 (1996).

[77] G. Mahan, *Many-Particle Physics*, 2nd ed. (Plenum Press, New York, 1990).

[78] For the fit shown on Fig. 4.4 only the data corresponding to the nodes with $N = 3$ to 5 were used. The phase shift for $N = 6$ was disregarded due to the very large error bar.

[79] M. Kartsovnik, V. Laukhin, V. Nizhankovskii and A. Ignat'ev, Pis'ma Zh. Eksp. Teor. Fiz. **47**, 302 (1988) [Sov. Phys. JETP Lett. **47**, 363 (1988)]; M. Kartsovnik, P. Kononovich, V. Laukhin and I. Schegolev, Pis'ma Zh. Eksp. Teor. Fiz. **48**, 498 (1988) [Sov. Phys. JETP Lett. **48**, 541 (1988)]; M. Kartsovnik, V. Laukhin and S. Pesotskii, Fiz. Nizk. Temp. **18**, 22 (1992) [Sov. J. Low Temp. Phys. **18** 13 (1992)].

[80] M. Kartsovnik, P. Kononovich, V. Laukhin, S. Pesotskii and I.F.Schegolev, Pis'ma Zh. Eksp. Teor. Fiz. **49**, 453 (1989) [Sov. Phys. JETP Lett. **49**, 519 (1989)].

[81] T. Terashima, S. Uji, H. Aoki, M. Tamura, M. Kinoshita and M. Tokumoto, Solid State Commun. **91**, 595 (1994).

[82] E. Ohmichi, H. Ito, T. Ishiguro, G. Saito and T. Komatsu, Phys. Rev. B **57**, 7481 (1998).

[83] B. Narymbetov, N. Kushch, L. Zorina, S. Khasanov, R. Shibaeva, T. Togonidze, A. Kovalev, M. Kartsovnik, L. Buravov, E. Yagubskii, E. Canadell, A. Kobayashi and H. Kobayashi, Eur. Phys. J. B **5**, 179 (1998); Togonidze, M. Kartsovnik, J. Perenboom, N. Kushch and H. Kobayashi, Physica B **294-295** 435 (2001).

[84] L. Balicas, J. Brooks, K. Storr, D. Graf, S. Uji, H. Shinagawa, E. Ojima, H. Fujiwara, H. Kobayashi, A. Kobayashi and M. Tokumoto, cond-mat/0008287 (2000).

[85] In the real layered compounds the impurity distribution may have periodic modulation in the direction perpendicular to the layers and with period equal to the interlayer distance. However, in Born approximation this modulation leads only to a constant factor in (4.24) that renormalizes the Dingle temperature.

[86] This fact has an evident physical meaning. The matrix element of the electron scattering by a point-like impurity U is the same for all transitions that do not change the electron energy. Hence, the scattering rate $1/\tau(\epsilon) = -2\mathrm{Im}\Sigma^R/\hbar$ is proportional to the number of states to which an electron may scatter, that is, to the density of states at a given energy.

[87] P.D. Grigoriev, M.V. Kartsovnik, W. Biberacher and P. Wyder, cond-mat/0108352 (2001) (unpublished).

[88] This fact can be understood in a different way: slow oscillations originate from local electron motion and are not sensitive to global variations of the position of the chemical potential with respect to the bottom of the conducting band.

[89] Yamaji K., J. Phys. Soc. Jpn. **58**, 1520 (1989)

[90] Yasunari Kurihara, J. Phys. Soc. Jpn. **61**, 975 (1992)

[91] P. Grigoriev et al., to be published

[92] N. Harrison, L. Balicas, J.S. Brooks, M. Tokumoto, Phys. Rev. B **62**, 14212 (2000)

[93] N. Harriso, Phys. Rev. Lett. **83**, 1395 (1999)

[94] F.A. Meyer et al., Europhys. Lett. 32,681(1995); E.Steep, et al., Physica B 259-261, 1079(1999); J.Wosnitza, et al. PRL 86, 508 (2001)

[95] J.Y. Fortin, T. Ziman, Phys. Rev. Lett. 80, 3117 (1998)

[96] Ju H. Kim, S. Y. Han and J. S. Brooks, Phys. Rev. B **60**, 3213 (1999)

[97] L. P. Gor'kov and A. G. Lebed, J. Phys. (Paris) Lett., vol. **45**, p. L-433 (1984); D. Zanchi et al., Phys. Rev. B, vol. 53 , p. 1240 (1996); A. G. Lebed, JETP Lett. vol. 72, p. 141 (2000).

[98] D. Andres, et al., Phys. Rev. B (Rapid Commun.), vol. **64**, p. 161104 (2001)

[99] A.G.Lebed and K.Yamaji, Phys. Rev. Lett. vol. **80**, p. 2697 (1998)

[100] I. J. Lee, M. J. Naughton, G. M. Danner, and P. M. Chaikin, Phys. Rev. Lett., vol. 78, p. 3555 (1997); I. J Lee, P. M. Chaikin, M. J. Naughton, Phys. Rev. B, vol. 62, p. R14669(2000)

[101] H. Shimahara, J. Phys, Soc. Jpn, vol. 66, 541 (1997); A.G. Lebed, Phys.Rev. B vol. 59, p. R721 (1999)

[102] P. Fulde and R. A. Ferrell, Phys. Rev. , vol. 135, p. A550 (1964); A. I. Larkin and Yu. N. Ovchinnikov, Sov. Phys. JETP, vol. 20, p. 762 (1965)

[103] A. I. Buzdin and J. P. Brison, Europhys. Lett., vol. 35, p. 707 (1996)

[104] J. Singleton et al., J. Phys.: Cond. Mat., vol. 12, p. L641 (2000)

[105] N. Harrison, Phys. Rev. Lett. **83**, 1395 (1999).

CURRICULUM VITAE

ADDRESS

L. D. Landau Institute for Theoretical Physics,
142432, Chernogolovka, Moscow region, Russia
Tel: (7)-095-137-32-44; Fax: (7)-095-938-20-77.
E-Mail: pashag@itp.ac.ru

or Grenoble High Magnetic Field Laboratory, MPI-FKF and CNRS,
BP 166, F-38042 Grenoble Cedex 09, France

EDUCATION

September 2002 Defense of the present Ph. D. thesis at the University of Konstanz (sehr gut).

June 2001 First Ph. D. degree at L.D. Landau Institute for Theoretical Physics. Title: *Quasi-two-dimensional electron gas on the helium surface*, (in Russian).

1998-2001 L. D. Landau Institute for Theoretical Physics,
study for Ph.D.

1997- 2002 Practice in the Grenoble High Magnetic Field Laboratory, MPI & CNRS, Grenoble,France

1992-1998 Study at Moscow Institute of Physics and Technology,
Received Master's Degree in Theoretical Physics
(with highest honors: the excellent grades ¿ 95%).

1982-1992 High School,
Received the highest honor (the "gold" medal for all grades are excellent)

REFERENCES

1. Prof. A. M. Dyugaev, leading researcher, L. D. Landau Institute for Theoretical Physics, Russian Academy of Science, 117940, Kosygin Str. 2, Moscow, Russia; Tel: (7)-095-137-32-44; Fax: (7)-095-938-20-77

2. Prof. I. Vagner, head of Theory Group, Grenoble High Magnetic Field Laboratory, MPI&CNRS, 166X, F-48042, Grenoble, Cedex 9, *FRANCE; Tel: +33-4-76-88-11-27; Fax: +33-4-76-85-56-10; E-Mail: vagner@labs.polycnrs-gre.fr*

3. Prof. P. Wyder, director, Grenoble High Magnetic Field Laboratory, MPI&CNRS, 166X, F-48042, Grenoble, Cedex 9, FRANCE; tel: +33-4-76-88-56-00; Fax: +33-4-76-85-56-10

MAIN PUBLICATIONS (in historical order)

1. P.D.Grigoriev, "Bound states of an electron on the helium surface in the impurity potential", JETP Lett., Vol.66, page 630-636, Nov. (1997)

2. P.D.Grigoriev, A.M.Dyugaev, "Negative ions of big size Ca^- and Ba^- inside helium and on its surface", JETP, v. 115, iss. 3, p.1 (1999)

3. P.D.Grigoriev, I.D.Vagner "De Haas - van Alphen effect in quasi-two-dimensional materials", JETP Letters, vol 69, iss. 2, p.139 (1999)

4. P. Grigoriev, I. Vagner, "The de Haas - van Alphen effect in two-dimensional metals", cond-mat/0009409 (2000)

5. A. M. Dyugaev, P. D. Grigoriev, and Yu. N. Ovchinnikov, "Properties of a classical electron gas at the surface of condenced media", JETP **90**, p.1089 (2000)

6. P. D. Grigoriev, "The influence of the chemical potential oscillations on the de Haas - van Alphen effect in quasi-two-dimensional compounds", JETP, vol. 92, p.1090-1094 (2001) (or cond-mat/0102177)

7. P. D. Grigoriev, A. M. Dyugaev, "Theory of the resonant properties of electrons localized on the surface of liquid helium", JETP **93**, p.103-110 (2001)

8. P.D. Grigoriev, M.V. Kartsovnik, W. Biberacher, N.D. Kushch, P. Wyder, "Anomalous beating phase of the oscillating interlayer magnetoresistance in layered metals", Phys. Rev. B **65**, 60403(R) (2002)

9. M.V. Kartsovnik, P.D. Grigoriev, W. Biberacher, N.D. Kushch, P. Wyder, "Slow oscillations of magnetoresistance in quasi-two-dimensional metals", Phys. Rev. Lett. **89**, 126802 (2002)

10. P.D. Grigoriev, "Theory of the Shubnikov-de Haas effect in quasi-two-dimensional metals", submitted to Phys. Rev. B (cond-mat/0204270) (2002)

Zusammenfassung

Magnetische Quantenoszillationen (MQO) werden seit vielen Jahrzehnten als mächtiges Werkzeug zum Studium der Geometrie der Fermifläche und anderer elektronischer Eigenschaften verschiedener Metalle benutzt. Diese Oszillationen zeigen in stark anisotropischen, quasi-zweidimensionalen Systemen im Vergleich zu solchen in herkömmlichen dreidimensionalen (3D) Systemen viele neuartige Eigenschaften. Die Standard-Lifshitz-Kosevich-Formel, die herkömmlich für dreidimensionale Systeme benutzt wird, erklärt die an zweidimensionalen (2D) oder quasi-2D-Systemen beobachteten neuen Effekte noch nicht einmal qualitativ. In dieser Dissertation wird eine detaillierte theoretische Studie der MQO in zweidimensionalen (2D) und quasi-2D Metallen vorgestellt.

Der erste Teil der Dissertation ist dem de Haas-van Alphen Effekt im 2D und quasi-2D Fall gewidmet. In Kapitel 2 wird der Einfluß verschiedener Faktoren (die die Berechnungen verkomplizieren, aber in realen Experimenten vorhanden sind) auf einfache Weise studiert. In Kapitel 3 wird eine allgemeine Formel für Magnetisierungsoszillationen unter Berücksichtigung beliebiger Parameter (diese Formel berücksichtigt Oszillationen des chemischen Potentials bei beliebigem Elektronenreservoir, beliebiger Spinaufspaltung und Krümmung der Fermifläche, beliebiger Temperatur und Verbreiterung der Landau-Energieniveaus) hergeleitet, die quantitative Vergleiche zwischen Theorie und Experiment erlaubt. Zusätzlich wird eine Methode zur direkten Ableitung der Elektronenzustandsdichte aus der experimentell bestimmten Magnetisierungskurve als Funktion des magnetischen Feldes vorgeschlagen. Eine solche Methode wäre von wesentlichem Nutzen, weil das Problem der Form der Landau-Energieniveaus sowohl in Heterostrukturen wie auch in stark anisotropischen organischen Metallen nach wie vor ungelöst ist. Schließlich wird eine mögliche Methode zum Test der Ein-Teilchen-Näherung ebenfalls vorgeschlagen.

Der zweite Teil der Dissertation ist einer Theorie der Magnetowiderstandsozillationen in quasi-2D Metallen gewidmet, wobei eine solche Theorie zum ersten Mal entwickelt wird (Kapitel 4). Diese Theorie erklärt zwei qualitativ neue Effekte, namentlich die Phasenverschiebung der Schwe-

bung und die langsamen Oszillationen der Leitfähigkeit in quasi-2D organischen Verbindungen. Es wird theoretisch gezeigt, daß diese beiden Effekte eine allgemeine Eigenschaft des quasi-2D Falles sind und daß sie in Erscheinung treten, wenn die Krümmung der Fermifläche mit der Zyklotronfrequenz vergleichbar wird. Die Phasenverschiebung der Schwebung kann erklärt und abgeschätzt werden, wenn man nicht nur die Oszillationen der Elektronenrelaxationszeit als Funktion des Magnetfeldes berücksichtigt (in der Standard-3D-Theorie wird nur dieser Beitrag zum Shubnikov-de Haas-Effekt berücksichtigt), sondern außerdem Oszillationen der Elektronengeschwindigkeit an der Fermifläche. Die Schwebung der Elektronengeschwindigkeitsoszillationen ist im Vergleich zu der Schwebung der Elektronenrelaxationszeitoszillationen um $\pi/2$ phasenverschoben und die Gesamtphase der Schwebung der Shubnikov-de Haas- Oszillationen wird durch das Verhältnis der Oszillationsamplituden dieser beiden beitragenden Größen bestimmt.

Die langsamen Oszillationen des quasi-2D Magnetowiderstandes sind ebenfalls abhängig von der Schwebung der schnellen Oszillationen und die Frequenz der langsamen Oszillationen ist zweimal so groß wie Schwebungsfrequenz. Langsame Oszillationen werden durch eine Interferenz von schnellen Oszillationen verschiedener Eigenschaften verursacht, die zum Magnetowiderstand beitragen. Die Magnetisierung zeigt keine langsamen Oszillationen. Langsame Oszillationen entstehen aus recht verschiedenen Ursachen im Vergleich zu Shubnikov-de Haas Oszillationen. Anders als die schnellen Shubnikov-Oszillationen zeigen die langsamen Oszillationen keine Temperaturdämpfung und können bei wesentlich höheren Temperaturen beobachtet werden.

Nur kurzreichweitige Streuung an Verunreinigungen trägt zum Dingle-Faktor der langsamen Oszillationen bei. Dieser Umstand gestattet die Trennung des Beitrages der kurzreichweitigen Verunreinigungen vonn demjenigen der makroskopischen Probeninhomogenitäten und anderen langreichweiten Imperfektionen der Probe.

Ein detaillierter Vergleich zwischen den gewonnenen theoretischen Ergebnissen mit Experimenten wird durchgeführt. Dieser Vergleich beweist unzweifelhaft die vorgeschlagene theoretische Beschreibung. Er liefert außerdem zusätzliche Informationen über die untersuchten Verbindungen. So ergibt beispielsweise der Vergleich der Dingle-Auftragung der langsamen Magnetowiderstandsoszillationen mit derjenigen der schnellen Shubnikov-de Haas-Oszillationen, daß die kurzreichweitigen Streuzentren nur etwa ein Drittel zu der gesamten Dingle-Temperatur der untersuchten Probe des organischen Metalls β-(BEDT-TTF)$_2$IBr$_2$ beitragen.

Zusammenfassend wird in der vorliegenden Arbeit eine zuverlässige Theorie der Magnetoquantenoszillationen in verschiedenen Gesichtspunkten und Einzelheiten entwickelt. Diese Theorie kann auf reale Experimente ange-

wandt werden und macht mehrere neue, wichtige Vorhersagen über Magnetowiderstandsoszillationen.

Lebenslauf

Name: Pavel Dmitrievich Grigoriev

Geburtsdatum: 10/07/1975

Geburtsort: Samara (Rußland)

Schule : 1982 - 1992

Studium: 1992-1998.

Diplom: Juni 1998

1998-2001 Doktorarbeit am Landau Institut für TheoretishePhysik, Chernogolovka, Russia. (Prof. A. Dyugaev).
Doktorprüfung Juni 2001
Dissertationstitel: *Quasi-two-dimensional electron gas on the helium surface*, (in Russian).

1999-2002 Praktikum und Doktorarbeit am MPI für Fëstkörperforschung, Hochfeldmagnetlabor Grenoble (Prof. P. Wyder)
Doktorprüfung (sehr gut) September 2002
Dissertationstitel: *Magnetische Quantenoszillationen in quasi-zweidimensionalen Metallen*